STUDY OF CROSS-LINKED POLYMER GEL SYSTEMS FOR POTENTIAL USE AS LOSS PREVENTION AGENTS

BY

MOHAMMAD DANISH HASHMAT

A Thesis Presented to the

DEANSHIP OF GRADUATE STUDIES

KING FAHD UNIVERSITY OF PETROLEUM & MINERALS

DHAHRAN, SAUDI ARABIA

In Partial Fulfillment of the
Requirements for the Degree of

MASTER OF SCIENCE

In

PETROLEUM ENGINEERING

December, 2014

KING FAHD UNIVERSITY OF PETROLEUM & MINERALS

DHAHRAN- 31261, SAUDI ARABIA

DEANSHIP OF GRADUATE STUDIES

This thesis, written by **MOHAMMAD DANISH HASHMAT** under the direction his thesis advisor and approved by his thesis committee, has been presented and accepted by the Dean of Graduate Studies, in partial fulfillment of the requirements for the degree of **MASTER OF SCIENCE IN PETROLEUM ENGINEERING.**

Dr. Abdullah S. Sultan
(Advisor)

Dr. Ibnelwaleed Ali Hussein
(Member)

Dr. Abdullah S. Sultan
Department Chairman

Dr. Mohammed Enamul Hossain
(Member)

Dr. Salam A. Zummo
Dean of Graduate Studies

Dr. Syed M. Shakil Hussain
(Member)

20/5/15
Date

Dr. Mohamed Mahmoud
(Member)

© MOHAMMAD DANISH HASHMAT

2014

Dedicated to my parents, guardians, teachers, friends and siblings

ACKNOWLEDGMENTS

All praises belong to Almighty Allah, the Eternal and the Absolute. Salutations on the Last and Final Messenger of Allah (Peace Be Upon Him).

For the duration and completion of my thesis and degree I owe my gratitude to the King Fahd University of Petroleum & Minerals, the Petroleum Engineering Department and the Centre of Petroleum & Minerals for giving me this opportunity and providing full scholarship.

I am thankful to my Advisor, my thesis committee and my teachers for all of their guidance and support. I would also like to acknowledge Dr. Saif, Mr. AbdusSamad, Dr. Shahzad Kamal and Dr. Khalid El-karsani for their immense help with my thesis and other non-academic matters. Thanks are due to Dr. Asroof for his help in the synthesis part of this work.

My humble heartfelt gratitude is due towards my parents, guardians and siblings for their constant prayers and encouragements. I am grateful to all my friends specially Mansoor Alam, Saad Mehmood, Zaeem Khan, Osama Yusuf, Mobeen Murtaza, Sarmad, Abdulhaleem, Musab, Abdullah and Mustafa. I feel blessed to have them as a part of my life, I thank them all.

TABLE OF CONTENTS

ACKNOWLEDGMENTS ..... **V**

TABLE OF CONTENTS ..... **VI**

LIST OF TABLES ..... **IX**

LIST OF FIGURES ..... **X**

LIST OF ABBREVIATIONS ..... **XIII**

ABSTRACT ..... **XIV**

ARABIC ABSTRACT ..... **XVII**

CHAPTER 1 INTRODUCTION **1**

1.1 Statement of Problem **2**

1.2 Objectives **3**

CHAPTER 2 LITERATURE REVIEW **4**

2.1 Polyacrylamide as LCM **4**

2.1.1 Inorganically Crosslinked Polymer Gels **5**

2.1.2 Organically Crosslinked Gels **8**

2.2 Thermoviscosifying polymer (TVP) **13**

2.3 Clay **17**

CHAPTER 3 METHODOLOGY **19**

3.1 Rheology **19**

3.2 Rheometer **20**

3.3 Rheology Tests....21
3.3.1 Oscillating Amplitude Test....21
3.3.2 Oscillating Frequency Test....21
3.3.3 Flow Sweep Test....21
3.3.4 Flow Temperature Ramp....22
3.3.5 Oscillation Temperature Ramp....22
CHAPTER 4 RESULTS AND DISCUSSION....24
4.1 Polyacrylamide....24
4.1.1 Optimum polymer/crosslinker concentration identification....25
4.1.2 Thermal Stability....28
4.1.3 Polymer Rheology....30
4.1.4 Gel Rheology....39
4.2 TVP....46
4.2.1 Rheology....46
4.2.2 TVP Interaction with PEI and Clay....51
4.2.3 Salinity Effect....58
4.3 Polymer Interaction with Clay....63
4.3.1 Alcomer130/ATP system....63
4.3.2 Alcomer130/15A system....75
4.3.3 Interaction with Calcium bentonite....77
CHAPTER 5 DIFFERENTIAL SCANNING CALORIMETRY....82
5.1 Experiment Procedure....83
5.2 Results....84
CHAPTER 6 SEE THROUGH SETUP....89

6.1 Core Characterization 91
6.1.1 Porosity Determination 91
6.1.2 Permeability Determination 96
6.2 Core Properties 99
6.3 Experiment Procedure 101
6.4 Commercial LCM 101
6.5 Polyacrylamide/Phenol Formaldehyde (PAM/PF) 110
6.6 HPAM/PEI (3/1.2) and A130/PEI (2/1.2) see through results 117
CHAPTER 7 CONCLUSION AND RECOMMENDATION 122
REFERENCES 126
VITAE 133

LIST OF TABLES

Table 1 Gel ageing scheme 42

Table 2 system composition..... 52

Table 3 Brine composition..... 59

Table 4 System composition..... 59

Table 5 Avrami parameters for HPAM/PEI 87

Table 6 Avrami parameters for A130/PEI 88

Table 7 Core properties..... 99

Table 8 Rheological properties of the Mud/LCM systems at r.t.p..... 109

LIST OF FIGURES

Figure 1 Crosslinking reactions taking place by the complexation of carboxylate groups on the polymer chains by Cr species. (Dona et al., 1997)..... 7
Figure 2 Chemical structures of the (a) PAtBA, (b) PAM, and (c) PHPA (Al-Muntasheri et al., 2009)..... 12
Figure 3 Gelation mechanism between PAM and PEI (Reddy et al., 2003; Al-Muntasheri et al., 2006)..... 12
Figure 4 Molecular structures of the thermoviscosifying polymer (TVP) and HPAM (Chen et al., 2012)..... 15
Figure 5 Comparison of viscosifying behavior upon increased temperature for TVP andHPAM in synthetic brine (Cp = 0.2 wt %, TDS = 32868 mg/L, $[Ca^{2+}]$ + $[Mg^{2+}]$ = 873 mg/L, fixed shear rate= 10 s-1, heating rate: 2 ^{o}C/ min) (Chen et al., 2012)..... 15
Figure 6 Viscoelastic properties plotted as a function of temperature for TVP and HPAMsolutions in synthetic brine (Cp = 0.2 wt%, TDS = 32868 mg/L, $[Ca^{2+}]$ + $[Mg^{2+}]$ = 873 mg/L, f = 1 Hz, heating rate: 2^{o}C/ min) (Chen et al., 2012)..... 16
Figure 7 TA Instruments Rheometer with concentric cylinder geometry 23
Figure 8 HPAM 3wt% solution (left), Alcomer130 2wt% (right)..... 27
Figure 9 Crosslinked samples in vials at room temperature; HPAM/PEI (3/0.6), 3(/1), (3/1.2) and A130/PEI (2/0.6), (2/1), (2/1.2) [left to right]..... 29
Figure 10 Gels aged at 100^{o}C for 28 days; HPAM/PEI (3/0.6), 3(/1), (3/1.2) and A130/PEI (2/0.6), (2/1), (2/1.2) [left to right]..... 29
Figure 11 Oscillation Amplitude test for HPAM (3 wt%)..... 32
Figure 12 Flow sweep profile of HPAM (3 wt%) 32
Figure 13 Frequency sweep profile of HPAM (3 wt%)..... 33
Figure 14 Flow temperature ramp of HPAM (3 wt%)..... 33
Figure 15 Oscillation temperature ramp of HPAM (3 wt%) 34
Figure 16 Oscillation Amplitude test for Alcomer130 (2 wt%) 36
Figure 17 Flow sweep profile of Alcomer130 (2 wt%)..... 36
Figure 18 Frequency sweep profile of Alcomer130 (2 wt%) 37
Figure 19 Flow temperature ramp of Alcomer130 (2 wt%) 37
Figure 20 Oscillation temperature ramp of Alcomer130 (2 wt%)..... 38
Figure 21 HPAM/PEI gels storage modulus comparison..... 43
Figure 22 A130/PEI gels storage modulus comparison..... 44
Figure 23 HPAM/PEI (3/1.2) G' improvement with time (left) and with temperature (right)..... 45
Figure 24 A130/PEI (3/1.2) G' improvement with time (left) and with temperature (right)..... 45
Figure 25 K20 (0.75 wt%) homogenous solution obtained after 2-3 hours of stirring..... 48
Figure 26 Amplitude oscillation test for K20 (0.75 wt%) 48
Figure 27 Flow sweep test of K20 (0.75 wt%) at 25^{o}C 49
Figure 28 Frequency sweep test for K20 (0.75 wt%) 49
Figure 29 Flow temperature ramp test of K20 (0.75 wt%)..... 50

Figure 30 Oscillation temperature ramp of K20 (0.75 wt%) 50
Figure 31 K20/15A (0.75/0.1) system (left) and K20/PEI (0.75/0.1) system (right) 52
Figure 32 Flow sweep comparison chart of the K20 systems 54
Figure 33 Frequency sweep comparison of K20 (0.75 wt%) and K20/PEI (0.75/0.1)..... 54
Figure 34 Frequency sweep comparison of K20 (0.75 wt%) and K20/15A (0.75/0.1).... 55
Figure 35 Frequency sweep comparison of all the three systems..... 55
Figure 36 Flow temperature ramp test comparison of the three systems 57
Figure 37 Oscillation temperature ramp comparison of all the systems..... 57
Figure 38 K20 (0.75 wt%) solution in sea water and formation water after preparation . 60
Figure 39 Flow temperature ramp test comparison of K20 (0.75wt %) at different salinity 62
Figure 40 Flow temperature ramp comparison b/w K20(0.2 wt%) and K20(0.75 wt%) . 62
Figure 41 ATP/A130 (0.1/0.75) homogenous solution obtained after one day stirring ... 65
Figure 42 A130/ ATP (0.75/0.1) after one day of stirring. ATP aggregates are visible in the system. 65
Figure 43 A130/ATP (0.75/0.1) system after 4 days of stirring 66
Figure 44 Flow sweep profile comparison 68
Figure 45 Frequency sweep profile comparison..... 68
Figure 46 Flow temperature ramp comparison..... 70
Figure 47 Oscillation temperature ramp profile comparison..... 70
Figure 48 ATP/A130 (0.3/0.75) after 3 days 73
Figure 49 ATP/A130 (0.3/0.75) after 5 days (left) ATP deposits are visible on the stir bar (right)..... 73
Figure 50 Flow sweep profile comparison 74
Figure 51 Frequency sweep profile comparison..... 74
Figure 52 A130/15A (0.75/0.1) system after 2 days..... 76
Figure 53 Frequency sweep profile comparison of A130/15A..... 76
Figure 54 Ca-bent/A130 (0.1/0.75) system 78
Figure 55 Flow sweep profile of Ca-bent/A130 (0.1/0.75) vs Alcomer130 (0.75) 78
Figure 56 Frequency sweep profile of Ca-bent/A130 (0.1/0.75) vs Alcomer130 (0.75) . 79
Figure 57 Flow Temperature Ramp profile of Ca-bent/A130 (0.1/0.75) vs Alcomer130 (0.75). 79
Figure 58 Ca-bent/HPAM (0.1/0.75) before (left) and after (right) HPAM addition..... 81
Figure 59 Frequency sweep profile of Ca-bent/HPAM(0.1/0.75) vs HPAM(0.75 wt%). 81
Figure 60 Fractional gelation profiles for HPAM/PEI 86
Figure 61 Avrami plot HPAM/PEI..... 86
Figure 62 Fractional gelation profiles for A130/PEI..... 87
Figure 63 Avrami plot A130/PEI..... 88
Figure 64 Schematic Diagram of the see through setup 90
Figure 65 See through setup 90
Figure 66 the synthetic see through core 94
Figure 67 Different glass beads sizes (sizes from left to right: 0.5 mm, 3 mm and 6 mm) 94
Figure 68 Schematic diagram of the porosity determination setup 95
Figure 69 Porosity determination setup..... 95
Figure 70 Schematic diagram of the permeability determination setup 97

Figure 71 Permeability determination setup 97
Figure 72 Transducer calibration 100
Figure 73 Representation of Darcy law 100
Figure 74 DrilEzy (left), SoluSeal (middle) and Stoploss (right) 105
Figure 75 PV profile of DrilEzy 105
Figure 76 YP profile of DrilEzy 106
Figure 77 PV profile of SoluSeal 106
Figure 78 YP profile of SoluSeal 107
Figure 79 Gel strength profile comparison of SoluSeal 1wt% and 8wt% Mud/LCM system 107
Figure 80 PV profile of Stoploss 108
Figure 81 YP profile of Stoploss 108
Figure 82 Flow performance of the LCMs 109
Figure 83 PAM/PF gel 113
Figure 84 k1 after PAM/PF gel injection (left) and after mud injection (right) 114
Figure 85 Upstream end of the core after unpacking (left), depth of penetration of the gel [1.6 cm] (right) 114
Figure 86 PAM/PF migration in k2 (left) PAM/PF gel encased in glass beads after unpacking (right) 114
Figure 87 PAM/PF saturated k3 core compromised by mud flow at 33psi ΔP 115
Figure 88 PAM/PF performance w.r.t to core type 115
Figure 89 PAM/PF performance in relation to time and effective penetration in k1 116
Figure 90 k3 core saturated with HPAM/PEI (3/1.2) 120
Figure 91 Mud breakthrough in the HPAM/PEI (3/1.2) saturated k3 core 120
Figure 92 A130/PEI (2/1.2) saturated k1 core, maximum penetration of 7.1 cm 120
Figure 93 HPAM/PEI (3/1.2) and A130/PEI (2/1.2) performance w.r.t permeability 121
Figure 94 Schematic diagram of the proposed HPHT flow loop 125

LIST OF ABBREVIATIONS

LCM	:	Loss Circulation Material
TVP	:	Thermo-viscosifying polymer
LVR	:	Linear Viscoelastic Range
FW	:	Formation Water
SW	:	Sea Water
PAM	:	Polyacrylamide
HPAM	:	Hydrolyzed Polyacrylamide
PEI	:	Polyethylneimmine
ATP	:	Attapulgite
TDS	:	Total Dissolved Solute
HPHT	:	High Pressure High Temperature
PV	:	Plastic Viscosity
YP	:	Yield Point
wt%	:	Weight Percent
WBM	:	Water Based Mud
∆P	:	Pressure Difference
PF	**:**	Phenol Formaldehyde

ABSTRACT

Full Name : Mohammad Danish Hashmat

Thesis Title : Study of Cross-linked Polymer Gel Systems for potential use as Loss Prevention Agents

Major Field : Petroleum Engineering

Date of Degree : December 2014

At the core of any drilling operation lies the drilling fluid. This vital fluid is circulated through the drill string into the wellbore during drilling of an oil or gas well. The drilling fluid serves the basic function of removing the drill cuttings and maintaining the borehole hydrostatic pressure. During the drilling operation whenever weak, fractured, unconsolidated or low pressured zones are encountered, there is an appreciable loss of this drilling fluid. This fluid loss or loss circulation is a major drilling problem as it results in not only drilling fluid loss and drilling operation interruption but it also adds up to the total drilling cost of the operation.

In order to counter this problem and to ensure a smooth operation, Loss Circulation Materials (LCMs) are used. Various LCMs have been designed and are being used in the industry. With better understanding of loss inducing zones and advancements in material sciences, new LCMs are appearing in the limelight.

Amongst the various loss prevention techniques; one is the use of cross-linking polymers that would enter the thief zone, form a strong gel and seal the loss inducing formation. This LCM should be strong enough to withstand the hydrostatic pressure and be thermally stable as per the formation conditions.

In this work various polymer based gel forming systems were studied for their possible use as a loss preventive and sealing agent. This work highlights the rheological studies conducted in the laboratory to study the strength and stability of the LCMs for their potential use in overcoming the loss circulation problem.

In this thesis, gels of polyacrylamide based polymers and polyethylenimine were prepared and studied. At optimum concentrations stable gels were obtained. The gels composed of the highest polymer/crosslinker concentration proved to be strong and stable in relation to time and temperature. This was reflected in both the rheology and differential scanning calorimetric tests. HPAM/PEI (3/1.2) and A130/PEI (2/1.2) were the two systems that gave the best results. At 100% solution to gel conversion was attained for the systems in nearly three and a half hours of total ageing time at 100^{o}C isothermal condition. Both systems when aged at 100^{o}C for 24 hours showed an almost 400% increase in gel strength than that of the base polymer at the angular frequency of 10 rad/s. Ageing at 120^{o}C for 1 day resulted in greater enhancement. The HPAM/PEI (3/1.2) system experienced a 2935% increase in its storage modulus value, while the A130/PEI (2/1.2) system showed a 603% increase in relation to that of the respective base polymers. The gelants at this concentration were tested in a see through flow setup and were found to be able to prevent mud losses till the pressure difference of 150 psi across a 300 D porous media. Gel of polyacrylamide and phenol-formaldehyde was synthesized and its performance was also studied in the flow setup with reference to permeability and time. It was found to be effective under certain conditions.

In this work, the interaction of polymers with clays was also studied and interesting results were obtained. This work also includes the study of the behavior of a

polyacrylamide based thermoviscosifying polymer and its interaction with crosslinkers. The thermoviscosifying property of this polymer was found to be dependent on salinity and polymer concentration.

ARABIC ABSTRACT

ملخص الرسالة

الاسم الكامل: محمد دانش حشمت

عنوان الرسالة: دراسة أنظمة البوليمرات المترابطة ولإمكانية أستخدامها كمواد منع فقدان موائع الحفر

التخصص: هندسة البترول

تاريخ الدرجة العلمية: ديسمبر ٢٠١٤

في صميم أي عملية حفر لأبار النفط والغاز تبرز أهمية موائع الحفر. ويتم تدوير هذا المائع الحيوي عبر أنابيب الحفر ورأس الحفارة داخل البئر ومن ثم عبر الفراغ الحلقي بين أنابيب الحفر والبئر أثناء حفر أبار النفط والغاز. مائع الحفر يخدم الوظيفة الأساسية لإزالة فتات الصخور الناتج من عميلة الحفر والمحافظة علي الضغط الهيدروليكي داخل البئر. أثناء عملية الحفر كلما ظهرت طبقات هشه، تحتوي علي شقوق، أو غير صلبه أو ذات ضغط منخفض ، هنالك عبر تلك الطبقات يحدث فقدان ملموس في موائع الحفر. هذه الخسارة أو فقدان موائع الحفر المهمة تمثل أحدي مشاكل الحفر الأساسية، ليس فقط الخسارة الناتجه عن فقدان كميات من موائع الحفر وأنقطاع الحفر لفترات طويلة ولكن أيضا وتمثل تكاليف أضافية الى تكلفة عمليةالحفر الإجمالية.

من أجل مواجهة هذه المشكلة وضمان إستقرار عملية الحفر ، تستخدم مواد لمنع فقدان موائع الحفر. وقد تم تصميم وإستخدام أنواع مختلفه منها في هذه الصناعة. والآن مع فهم أفضل لعوامل فقدان الموائع في الطبقات والتطور في علم المواد, نتيجة لهذا التطور ظهرت مواد جديدة لمنع فقدان الموائع زات فعالية في نطاقات وظروف حفر أكبر. بين مختلف التقنيات المستخدمة لمنع فقدان الموائع, يتم إستخدام البوليمرات المترابطة التي يتم أدخالها للطبقة التي تتعرض لفقدان الموائع. ، ومن ثم تقوم علي تشكيل مادة هلامية قوية وأغلاق هذه الطبقات. وينبغي أن تكون هذه المواد قوية بما يكفي لتحمل الضغط الهيدروستاتيكي وأن تكون مستقرة حراريا وفقا للشروط تكوينها.

في هذا البحث تم دراسة عدة انظمة مكونة من البوليمر التي تكون هذه المواد الهلامية, من حيث أمكانية التشكيل واستخدامها كمادة تمنع فقدان موائع الحفر وإحكام أغلاق الطبقات المعرضة للفقدان. في هذا العمل تم تسليط الضوء على الدراسات علي الخواص الجريانية التي أجريت في المعمل لدراسة قوة واستقرار هذه المواد لتقييم أمكانية أستخدامها للتغلب علي مشاكل قدان دورة مائع الحفر.

في الهذا البحث جل ناتج من تفاعل بولي اكريلي ماید و بولي اثيلين امين تم تحضيره ودراسته . جل ذوثباتية تم التحصل عليه عند التركيز المناسب. الجل الناتج من اعلى تركيز لالبوليمر والرابط البوليمري وجد انها تكون جل ذو قوة وثباتية مع الوقت و الحرارة. هذه المشاهدة تم التحصل عليها من كلى اختباري خواص المواد الحركية و المسح التفاضلي الكالوري. الخليطان (2/1.2) A130/PEI و (3/1.2) HPAM/PEI حققا افضل النتائج. 100% من الخليط تحول الي جل عند مضي ثلاث ساعات و نصف من الزمن الكلي الذي ياخذه الجل ليتكون عند درجة حرارة ثابته (100^oC). كلى الخليطان عند ما درسا عند 100^oC لمدة 24 ساعة تم التحصل على 400% زيادة في قوة الجل اكثر من الذي تم ملاحظته بنسبة لنظام البوليمر الاساسي عند تردد زاوي (10راد/ثانية). تحسن ملحوظ تم التحصل عليه عند تكوين الجل عند 120^oC لمدة يوم. الخليط (3/1.2) HPAM/PEI اظهرزيادة بمقدار 2935%

في قيمة معامل التخزين ، بينما A130/PEI (2/1.2) اظهر 603% مقارنة بالبوليمر الاساسي. الجلاتينات عند هذا التركيز تم اختبارها في جهاز لدراسة الجريان حيث وجد ان الخليط قادر على منع فقدان مائع الحفر حتى فرق ضغط 150psiعبر الوسط الصخري 300D. جل البولي اكريلي ماید و الفينول فرومالدهايد تم تحضيره و دراسة اداءه من خلال النفاذية و الوقت باستخدام جهاز دراسة الجريان. قد وجد انه فعال عند توفرظروف محددة.

في هذه الدراسة تم التحقيق في تفاعل البوليمرات مع الكلي. هذه البحث يشمل دراسة سلوك البولي اكريلي ماید المبني على اللزوجة الحرارية للبوليمر و تفاعله مع الرابط البوليمري. خاصية ا للزوجة الحرارية لهذا البوليمر وجد انها تعتمد على الملوحة وتركيز البوليمر.

CHAPTER 1

INTRODUCTION

During drilling of oil and gas wells, drilling fluids are circulated through the drill bit into the wellbore for removing the drill cuttings. It also maintains a predetermined hydrostatic pressure to balance the formation pressure and can be re-circulated into the well, since it is expensive. When low pressure subterranean zones are encountered while drilling, there is an appreciable loss of this drilling fluid. Bugbee (1953) defined lost circulation as the loss of substantial part or entire volume of the drilling fluid through the borehole into the vuggy, cavernous, fractured and highly porous formations.

Lost circulation problem is common and frequent in on-shore and offshore fields whenever the formations are weak, fractured or unconsolidated. Drilling for oil and gas in deep water encounters further challenges brought about by various reasons like gas kicks, blowouts, presence of unconsolidated sand formations, shallow gas, gas hydrate, lost circulation, sea floor washout and borehole erosion (Amanullah and Boyle, 2006). These problems are hazardous and also cause significant increase in the drilling cost. This has presented one of the greatest problems to the petroleum industry.

Cavernous, vugular formations, unconsolidated zones, high permeable zones and naturally or artificial fractured formations are mainly responsible for loss circulation of drilling fluids. Depending upon the intensity of loss, the loss circulation treatment is designed. If the severity of loss of drilling fluids is between 1 bbl/hr and 10 bbl/hr then it

is known as seepage loss. If the losses exceeds 10 bbl/hr but is less than 50 bbl/hr it is defined as partial loss. The loss is said to be complete loss when there is around 500 bbl/hr losses (Marinescu et al., 2007).

The lost circulation problem can be reduced by introducing LCMs into the wellbore to seal the zones. LCMs are classified according to their properties and applications. They are classified into three categories: bridging agents, gelling agents and cementing agents. LCMs can be flakes, fibers, sized marble, nut plug, cotton seeds, sized mica, water-soluble polymers, crosslinking agents etc. (Ghassemzadeh, 2009).

A lost circulation material is mixed with the drilling fluid and sent downhole. Once it encounters a loss zone, owing to triggering mechanisms it is activated. The LCM consisting of polymers expands in the presence of water due to electrostatic repulsion between charge sites on the co-polymers (Zusatz, 2004) and seals the fracture.

1.1 Statement of Problem

Due to the development of technology various types of LCMs are being designed to suit different requirements downhole to combat the lost circulation problems. The main objective of each lost circulation additive is to control or reduce loss of drilling fluid downhole.

Different blends of LCM materials, gel systems, nano particles and specially designed muds have shown to improve the formation stability and mitigation of loss of circulation in some cases. However, the elimination or control of loss of circulation in fractured and cavernous formations is one of the drilling challenges faced by the oil and gas industry.

This highlights the need of development of out-of-box test facilities and LCM materials composed of gels, chemicals, polymers, expandable or a hybrid LCM combining two or more of the convention and non-conventional LCM materials in alleviating the current as well as future loss of circulation problems along with other associated drilling hazards.

While the loss of circulation itself is a big drilling hazard, there are several associated problems which can increase the total drilling cost dramatically. The elimination of a single casing string by mitigating loss of circulation problem could save millions of dollars/well. Other problems such as well control problem, lost wellheads, rig instability, equipment instability, blowouts, requirement of unplanned casing string, etc. that are allied with loss of circulation problem could save billions of dollars per year. A better designed and developed LCM will eliminate or at least mitigate the loss of circulation problem for uninterrupted drilling operation.

Hence the goal of this thesis is to investigate the use of cross-linked polymer gels as possible candidates for LCM that would get the job done and save drilling time and cost.

1.2 Objectives

1. To study the rheological properties of cross-linked polymers
2. To study the thermal properties of cross-linked polymers
3. To study the effect of permeability on loss performance of the cross-linked polymer samples

CHAPTER 2

LITERATURE REVIEW

Various cross-linked polymer gels are being used in different fields for different purposes. In the petroleum industry, cross-linked polymer gels systems have seen great usage in water shut off operations. They have been used to completely block the permeable regions of the water producing zones in both fractures (Alqam et al., 2001) and matrix (Vasquez et al., 2003). They therefore hold a great potential in handling loss circulation issues. Most of these gel systems are based on polyacrylamides (PAM) which has an added advantage of being inexpensive.

2.1 Polyacrylamide as LCM

Partially hydrolyzed Polyacrylamide (PHPAM) is often used to identify the copolymer acrylamides/ acrylate. The end product of a PHPAM is formed by acrylamides/ acrylate copolymerization. During copolymerization, the two monomers are linked together in a random fashion and form a linear, carbon-carbon backbone. The resulting copolymer has carboxyl groups and amide groups randomly distributed along its backbone. Due to the presence of Carbon-Carbon linkage in the polyacrylamide, it has decent thermal stability and is resistant to bacteria (Ukachukwua et al., 2010).

For a given well candidate, several factors, including reservoir temperature, lithology, and salinity of the formation water, affects the selection of the required polymer-gel

treatment. Depending upon the crosslinker used, gelling systems can be classified into two categories—inorganically and organically crosslinked gels.

2.1.1 Inorganically Crosslinked Polymer Gels

Inorganically crosslinked gels rely mainly on the ionic interaction between the trivalent cation (such as Cr^{3+} and Al^{3+}) and the carboxylate groups on the partially hydrolyzed polyacrylamide (Prud'homme et al., 1983; Lockhart, 1994; te Nijenhuis et al., 2003; Sydansk, 1990). Chromium(III) cross-linked HPAM is the most commonly used inorganic water shutoff polymer gel. The crosslinking reactions in these gel systems take place by the complexation of Cr(III) oligomers with carboxylate groups on the polymer chains, as shown in Figure 1.

Low cost and easy availability of acrylamide polymer and Chromium (III) acetate crosslinker makes this gel system a cost effective solution for water shutoff applications. Such inorganically crosslinked polymer gels, because of coordination bonding are believed to be unstable at high temperatures (Al-Muntasheri et al., 2007). Although Cr(III)-carboxylate/acrylamide-polymer gels have been reported to be stable at temperatures up to 148.9°C (300°F) in Berea cores under pressure drops of 68.95 bars (1,000 psi) (Sydansk and Southwell, 2000), they exhibited other detrimental issues such as 'Syneresis' and toxicity.

The Chromium (III) crosslinked polymer gels are known to form weak gels at low polymer concentrations and exhibit syneresis, which is expulsion of water due to excessive crosslinking at higher crosslinker concentration (Sydansk, 2003). Such gel systems also lose water to the formation while forming a dehydrated cake on the

formation surface (this is termed as ‘leakoff’). There are also concerns associated with injection of Chromium (III) based polymer gels because of its short gelation time. Other than operational limitations, inorganically crosslinked polymer gels with metallic ions are considered a health and an environmental concern in some regulatory environments.

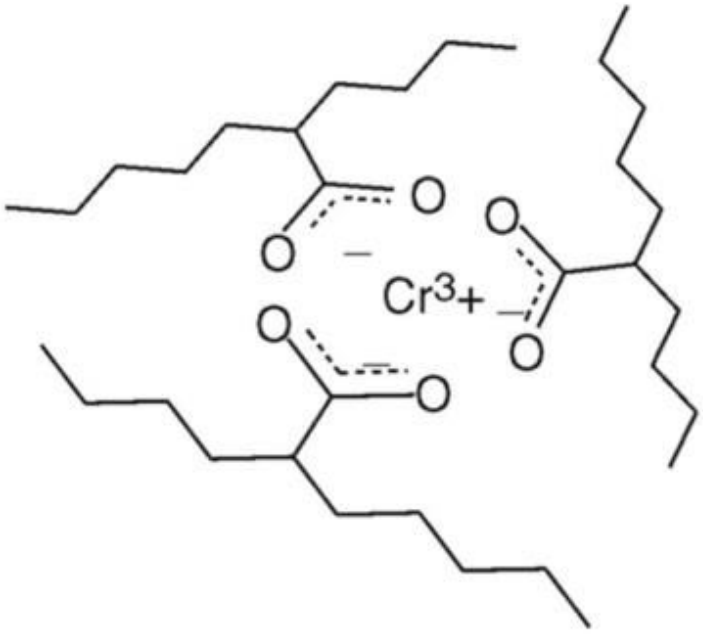

Figure 1 Crosslinking reactions taking place by the complexation of carboxylate groups on the polymer chains by Cr species. (Dona et al., 1997)

2.1.2 Organically Crosslinked Gels

Gels attained as a result of organic crosslinkers were reported to be stable over a wide range of temperature because the crosslinking is carried out via covalent bonding (Moradi-Araghi, 1991; Albonico et al., 1994; Hardy et al, 1999). A typical example of an organically crosslinked gel is the polyacrylamide-phenol/formaldehyde system, which has been reported to be stable at 121^{o}C for 13.3 years (Moradi-Araghi, 1993). However, its toxicity has limited its broad use in the field. Chemical alternatives for the phenol/formaldehyde system were also reported by (Moradi-Araghi, 1994; Dovan et al., 1997). These compounds include o-or p-aminobenzoic acid, m-aminophenol, aspirin, furfuryl alcohol, methyl p-hydroxybenzoate, phenyl acetate, phenyl salicylate, salicylamide and salicylic acid as phenol alternatives. The only suitable compound identified in their study, which could be used in place of formaldehyde and produce stable gels, is hexamethylenetetramine (HMTA), a precursor of formaldehyde. HMTA thermally hydrolyzes to formaldehyde and ammonia at elevated temperatures which will go on to crosslink with acrylamide containing polymers and phenol or its replacements.

Thermally stable covalently bonded systems are suitable for high temperature applications; long-term stability however cannot always be guaranteed. Literature reports highlight the importance of using a thermally stable polymer to produce thermally stable gels. Polyacrylamide-based polymers are known to hydrolyze at high temperatures causing gel syneresis (Moradi-Araghi, 2000), especially in brines with high contents of Mg^{2+} and Ca^{2+}, where polymer precipitation may also occur (Moradi-Araghi and Doe, 1987). Therefore, more thermally stable monomers are copolymerized with the acrylamide polymer to minimize excessive hydrolysis and enhance its thermal stability

(Moradi-Araghi and Doe, 1987). Omer and Sultan (2013) have studied the thermal stability of HPAM (0.95 wt%) in the presence of Ca^{2+}, Mn^{2+} and Mg^{2+} ions (0.05 wt%). The thermal stability of pure HPAM was till 70^{o}C, but in the presence of counterions it reduced.

PEI is reported in literature to form thermally stable gels with polyacrylamide-based copolymers. For example, copolymers of polyacrylamide tert-butyl acrylate (PAtBA) (Morgan et al., 1998), mixtures of acrylamide and acrylamido-2-methylpropane sulfonic acid (AMPSA) (Vasquez et al., 2003), mixtures of acrylamide, AMPSA and N,N-dimethyl acrylamide (Vasquez et al., 2005) can be crosslinked with PEI through covalent bonding. These PEI crosslinked systems have also been extensively examined in porous media (Hardy et al., 1998; Alqam et al., 2001; Zitha et al., 2002; Vasquez et al., 2003, 2005). PEI has been found to be a less toxic crosslinker and has been approved by USFDA for food contact (Reddy et al., 2003).

It has been reported that PEI can form gels with HPAM at room temperature (Allison and Purkaple, 1988). A study by Al-Muntasheri et al. (2008) has indicated the possibility of crosslinking a simple PAM with PEI at high temperatures. The gelation kinetics of the PAtBA and PAM crosslinked with PEI has been studied in detail at temperatures ranging from 80 to 140^{o}C (Al-Muntasheri et al., 2007, 2008). Figure 2 shows the molecular formulas of PAtBA, PAM, and PHPA.

According to literature the crosslinking reaction between PAM and PEI can be explained as a transamidation reaction (Al-Muntasheri et al., 2007). It is a nucleophilic substitution reaction in which nucleophilic imine nitrogen on PEI replaces the amide group on PAM.

Reaction between PAM and PEI leads to the formation of a covalent bond between the two, providing the gel system with a higher temperature stability than the polymer gels formed with metal ion crosslinkers (Al-Muntasheri at al., 2007). Figure 3 illustrates the above mentioned gelation mechanism and shows how the imine group in PEI attacks the amide group in HPAM to from a covalent bond and thereby form a gel. Gel based on PAM and PEI has also been investigated at temperatures as high as 140°C (Al-Muntasheri et al., 2006).

Gel system based on the crosslinking of polyacrylamide/tert-butyl acrylate (PAtBA) copolymer with polyethyleneimine (PEI) has been reported to be stable at temperatures up to 160^{o}C (Morgan et al., 1998; Hardy et al., 1998). It was first applied in a carbonate reservoir at nearly 130^{o}C and in sandstone reservoirs at 75^{o}C and 82^{o}C (Hardy et al., 1999; Polo et al., 2004).

The performance of the PAM/PEI gel system was examined in porous media (Al-muntasheri et al., 2007). The displacement of this gel system was visualized with Computed Tomography (CT) in sandstone cores. A permeability reduction of more than 94% was realized indicating the possibility of using this system in water shut-off treatments and loss zone treatments. Bulk testing of this system was also conducted over a wide range of concentrations of PAM and PEI at 100^{o}C (212^{o}F) for three weeks. Visual observations revealed the formation of thermally stable gels. These gels were rigid and non-flowing at PAM concentrations of 7 and 9 wt%.

Gakhar et al. (2012) tested HPAM/PEI gelant samples based on both research and commercial grade PEI for viscosity variation under variable shear rate at room

temperature and at 150°F using a Fann–35 Viscometer. It was found from the study that viscosity of all the gelant samples decreased with increased shear rate, both at room temperature and at 150°F. This behavior confirmed the shear thinning nature of HPAM/PEI gels.

Manganese for the first time was used in the preparation of PAM-PEI gel system (Omer and Sultan, 2013). Among the various metal ions used, it was observed that manganese results in very little viscosity drop.

The gel system based on an acrylamide-based base polymer and PEI as the crosslinker employs both polymers as liquid concentrates in water. They are mixed in water at the desired polymer ratios and concentrations dictated by formation temperatures; salt and gelation retarder are added as necessary. To counter a loss zone this polymer mix will then be pumped into the formation matrix around the wellbore where the crosslinking reaction would take place. On the formation of a rigid and stable gel, this system will hold the capacity to prevent losses.

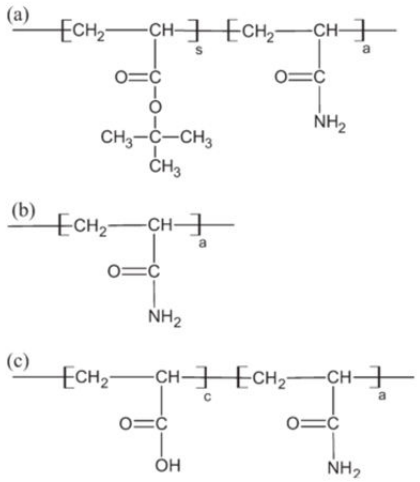

Figure 2 Chemical structures of the (a) PAtBA, (b) PAM, and (c) PHPA (Al-Muntasheri et al., 2009)

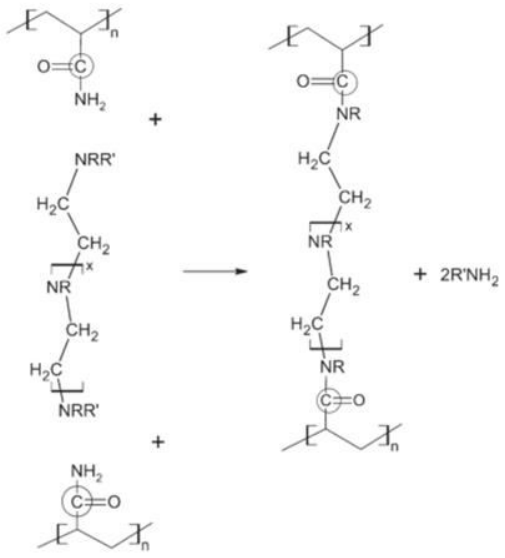

Figure 3 Gelation mechanism between PAM and PEI (Reddy et al., 2003; Al-Muntasheri et al., 2006)

2.2 Thermoviscosifying polymer (TVP)

Partially hydrolyzed polyacrylamide is also used in polymer flooding process, it is used to thicken the injected water to mobilize capillary trapped water-flooded oil in the secondary stage, and thus improve the sweep efficiency to increase the oil recovery factor (Chelaru et al., 1998; Zhong et al., 2009; Hou J, 2007; Kulicke et al., 1982). Under a hostile environment, the efficiency loss of the HPAM aqueous solution at elevated temperature becomes more serious as more amide groups undergo extensive hydrolysis into carboxylic units (Leung et al., 1987; Yang, 1999; Sabhapondit et al., 2003), and the hydrolyzed products precipitate when contacted with the commonly present divalent cations, such as Ca^{2+} and Mg^{2+}, in oil reservoir brines or hard water. In addition, the interaction of metal ions in the oilfield brines largely shields the mutual repulsion from the carboxylic groups along the HPAM skeleton, leading to the polymer coils to collapse, decreasing the hydrodynamic volume and ultimately lowering the solution viscosity (Kheradmand et al., 1988; Francois et al., 1997).

To obviate the limitations of HPAM, (Hourdet et al., 1994) proposed the concept of ‘‘thermoviscosifying polymer’’ (TVP). In these polymer systems, some ‘‘blocks’’ or ‘‘grafts’’, mainly poly (N-isopropylacrylamide) (PNIPAM) and polyethylene-oxide (PEO), with the character of lower critical solution temperature (LCST), were incorporated onto the hydrosoluble skeleton. When the temperature is increased, water becomes a poor solvent for the thermosensitive blocks, rendering them to self-aggregate with thermoassociative polymers. Above a critical associative temperature (T_{ass}), physical

junctions of the network are formed, giving rise to a viscosity enhancement macroscopically.

Chen et al. (2012) had synthesized a TVP by the copolymerization of acrylamide with their newly developed thermosensitive comonomer (MPAD) based on N-(1,1-dimethyl-3- oxobutyl)-acrylamide (DAAM) (Wang et al., 2010) Figure 4. They then studied it in comparison with traditional partially hydrolyzed polyacrylamide (HPAM) in synthetic brine regarding their rheological behaviors and core flooding experiments under certain reservoir conditions (85^{o}C, and total salinity of 32,868 mg/L, [Ca^{2+}] + [Mg^{2+}]: 873 mg/L). It was found that with increasing temperature, both apparent viscosity and elastic modulus of the TVP polymer solution increased, while those of the HPAM solutions decreased Figure 5 & Figure 6. Such a difference is attributed to their microstructures formed in aqueous solution, which were observed by cryogenic transmission electron microscopy.

TVPs can thus be a good candidate for use as a crosslinking gel system for loss circulation problem because of their resistance to salinity and viscosity buildup with temperature. Temperature can also serve as a triggering mechanism for such a LCM system. To the best of our knowledge TVPs have not been used for loss circulation prevention but they do look promising and that needs to be studied.

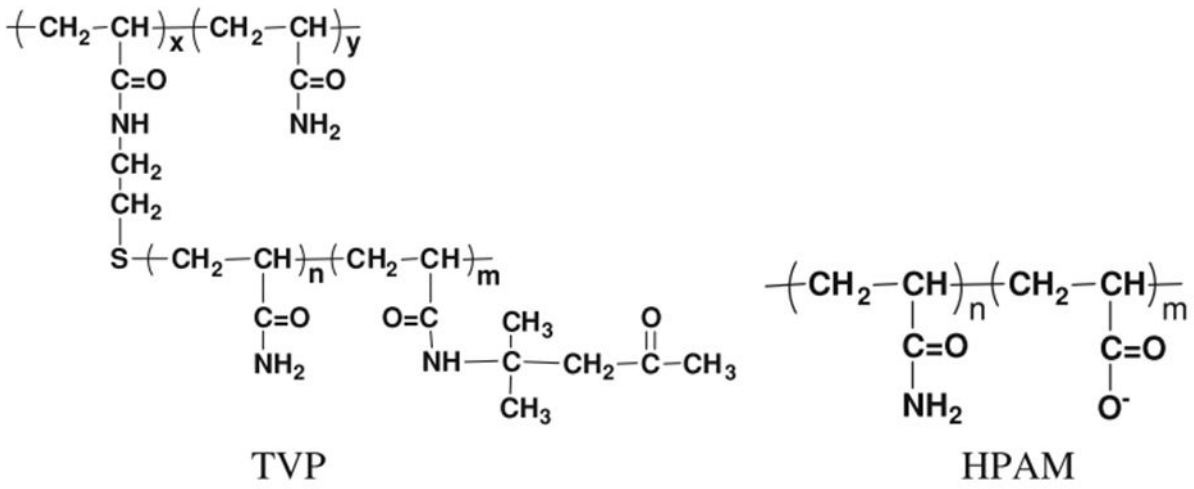

Figure 4 Molecular structures of the thermoviscosifying polymer (TVP) and HPAM (Chen et al., 2012)

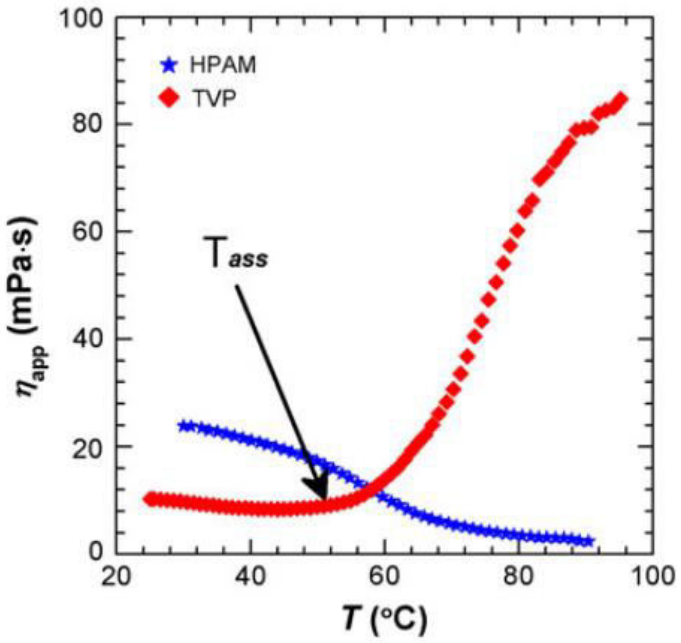

Figure 5 Comparison of viscosifying behavior upon increased temperature for TVP and HPAM in synthetic brine (Cp = 0.2 wt %, TDS = 32868 mg/L, $[Ca^{2+}] + [Mg^{2+}]$ = 873 mg/L, fixed shear rate= 10 s-1, heating rate: 2 ^{o}C/ min) (Chen et al., 2012)

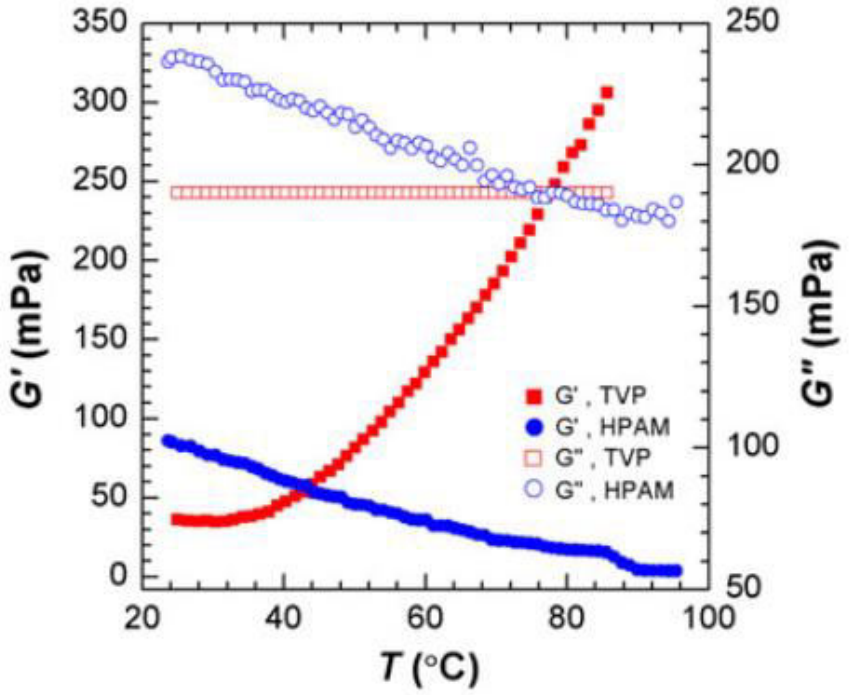

Figure 6 Viscoelastic properties plotted as a function of temperature for TVP and HPAM solutions in synthetic brine (Cp = 0.2 wt%, TDS = 32868 mg/L, $[Ca^{2+}] + [Mg^{2+}]$ = 873 mg/L, f = 1 Hz, heating rate: 2°C/ min) (Chen et al., 2012)

2.3 Clay

Clay is a large family of complex minerals containing the elements magnesium, aluminum, silicon and oxygen (magnesium, aluminum silicates) combined in a sheet-like structure. They are used in many industries for various purposes. In the petroleum industry clays are a basic component of the drilling fluid.

Polymer/clay composite hydrogel have been studied to improve the properties of hydrogel, such as mechanical strength, swelling and deswelling properties. For example, Messersmith and Znidarsich (1997) had prepared stimuli-responsive hydrogel/clay composites by the polymerization of aqueous suspension composed of N-isopropylacrylamide, N,N'-methylene bisacrylamide and Na-montmorillonite. Wu et al. (2000 and 2001) have reported the preparation of starch-graft-polyacrylamide/clay and poly (acrylic acid)/mica composites with striking capability of water absorption by grafting the monomers on the inorganic clay/mica. Zhang et al. (2005) had synthesized nano-composite hydrogel with high thermal stability and swelling ratio by grafting acrylic acid on the organophilic montmorillonite.

Bai et al. (2007) had synthesized polymer-clay composite gels from an acrylamide monomer, (N,N'-methylenebisacrylamide), crosslinker (N,N'-methylenebisacrylamide), initiator (peroxyl- disulfate), and bentonite clay. The swelling ratio could be controlled from a few to 100 times its original volume in formation water and could resist temperatures up to 120 ºC (248 ºF). This has been the most commonly used Preformed Particle Gel (PPG) in China since 2009.

Yuanqing Xiang et al. (2012) had developed a series of new poly (HEMA–PEGMA–MAA)/attapulgite nano-composite hydrogels by free radical polymerization. As the content of attapulgite increased, the tensile strength, effective cross-link chain density and glass transition temperature increased, while the deswelling rate of the system decreased.

Clays could hence be tested as a component of a cross-linked polymer gel system. They could serve in the capacity of a viscosifying agent, a swelling agent or an additional crosslinker.

CHAPTER 3

METHODOLOGY

3.1 Rheology

Rheology is the science of the deformation and flow of matter. In rheology studies determining viscosity and complex moduli is essential in understanding the behavior of the polymeric LCM. Viscosity is basically the resistance of a fluid to flow but this definition is too simplified as instead of just one absolute value, viscosity is a set of data at different stress, strain and other conditions for non-Newtonian fluids. Therefore, the study of the complete viscosity profile of a polymeric system is essential.

Polymers and their solutions are viscoelastic in nature. For a crosslinked polymer system that might act as a potential LCM, study of its complex moduli is necessary. Complex moduli is composed of two parameters; Storage modulus (G') and Loss modulus (G"). G' exhibits the elasticity of a material or how solid-like that material is. It is the ability of the material to store energy. Elastic materials deform instantly as shear is applied. G" on the other hand is a measure of how viscous or liquid like a material is. It is the ability of the material to dissipate energy. Viscous materials have a lag in deformation as shear is applied. Since PAM and its associative polymers are viscoelastic materials their behavior lies within the purely elastic and purely viscous spectrum. Oscillatory or dynamic rheology tests are performed via rheometer to obtain the complex moduli. For a polymer\crosslinker system, pre and post dynamic tests can help identify the

improvement (if any) on the system, the formation and transition of the sol-gel system and the changes in its properties.

Oscillatory rheology experiments require the knowledge of the Linear Viscoelastic Region (LVR). Viscoelasticity is a time-dependent property in which a material under stress produces both a viscous and an elastic response. A viscoelastic material will exhibit viscous flow under constant stress, but a portion of mechanical energy is conserved and recovered after stress is released. For polymer solutions, viscoelastic properties are usually measured as responses to an instantaneously applied or removed constant stress or strain or a dynamic stress or strain (Hackley and Ferraris, 2001). LVR therefore is a region where stress and strain magnitudes are linearly related and the material behavior is time dependent.

3.2 Rheometer

In order to judge the effectiveness of the crosslinked polymer gel systems as an LCM, rheological properties need to be studied. For this study all the rheology has been conducted using the Discovery Hybrid Rheometer with a Peltier Concentric 40 mm diameter cylinder arrangement from TA Instruments. The peltier concentric cylinder system consists of a jacket, an inner cylinder, and a rotor. This arrangement is used for fluids having viscosity from low to medium Range. Figure 7 is the schematic representation of the concentric cylinder. The operation of the system and plotting of the experimental results was done using TRIOS software.

The concentric cylinder geometry cannot be however used for a solid gel; concentric cylinder geometry can only be used if the polymer\crosslinker system is in a flowing

condition. For a solid gel, parallel plate or cone and plate geometry of the rheometer can be used for its rheology studies.

3.3 Rheology Tests

3.3.1 Oscillating Amplitude Test

This test is conducted to determine the LVR. It is the region in a material where stress & strain are related linearly; i.e. where modulus is independent of the stress or the strain used. All subsequent oscillation tests require the amplitude or strain percentage that lies within the LVR. This test was conducted at the temperature of 25^{o}C, a shear rate of 10(1/s) was used and the oscillation strain % over a range of 0.01 to 1000 has been explored.

3.3.2 Oscillating Frequency Test

Also called the frequency sweep test, the main objective of this test is to study the effect of angular velocity on complex modulus and dynamic viscosity at constant strain within the linear viscoelastic region. Complex moduli have been studied over the range of 0.1-250 (rad/s) angular frequency at a specific temperature, shear rate was kept at 10(1/s), maximum strain % obtained from the oscillation amplitude test was used as an input parameter.

3.3.3 Flow Sweep Test

This test is conducted to study the effect of shear rate on the viscosity of the material. Viscosity profile of the polymer systems was studied for the shear rate of 0.001 to 1000 (1/s). The results of this test will help in determining whether a material is shear thinning or shear thickening. For a LCM system based on polymers, this test is very essential. Not

only will the flow sweep test present the viscosity profile; it also is an approximate representation, at a small time scale, of the polymeric LCM through the drill string. It is because the fluid would experience low shear rates near the surface drill stem and maximum shear rates at the drill bit nozzles. Since PAM is shear thinning in nature, its viscosity would decrease at the bit nozzle and it would flow with relative ease and penetrate the thief zone. Shear rates in highly permeable and porous zones are low; there PAM would start experiencing an increase in its viscosity.

3.3.4 Flow Temperature Ramp

This test is primarily used to study the thermal stability of the fluid or the polymer system with respect to temperature variation at regular intervals. The temperature was varied from 25-90^{o}C at 10(1/s) shear rate. This test would show the effect of temperature on viscosity at a particular shear rate i.e whether the viscosity increases with temperature (as expected from a TVP) or whether it decreases with temperature increase.

3.3.5 Oscillation Temperature Ramp

Oscillation temperature ramp is a dynamic rheology test that is used to study the effect of temperature on the complex moduli of a material. Like the flow temperature ramp the temperature range for this test would be 25-90^{o}C at 10(1/s) shear rate with the angular frequency of 10 (rad/s) and strain % value obtained from the oscillation amplitude test.

Figure 7 TA Instruments Rheometer with concentric cylinder geometry

CHAPTER 4

RESULTS AND DISCUSSION

4.1 Polyacrylamide

There are different grades of PAM and PAM derivatives that are commercially available. These vary owing to differences in molecular weight, degree of hydrolysis, charge and type of co-monomer.

For this study two different, high molecular weight, polymers from different vendors were used. The HPAM used goes by the generic name of Flopaam 3330S. Flopaam 3330S is a polyacrylamide in the form of white powder obtained from SNF Floerger. It is an anionic PAM with 25-30% degree of hydrolysis, having a molecular weight of 8 million Dalton.

The second PAM based polymer used for this study has the commercial name Alcomer130. It is an anionic polyacrylamide based copolymer, acquired from BASF. It is used as a viscosifier in water based muds. Its molecular weight is rated as ultra-high. Flopaam 3330S is rated as medium to high and its molecular weight is 8 million Da. Alcomer130 being ultra-high have to be more than 8 million Da, atmost by 1 to 5 million Da.

4.1.1 Optimum polymer/crosslinker concentration identification

Identification of an optimum polymer and crosslinker concentration is essential because a rigid and stable gel is dependent on this parameter. If the concentration is too low the gel formed might not be strong and the gelation process would span over a long time period. If the concentration is too high then this may result in syneresis and gel shrinkage.

For the base polymer the maximum wt% that could be achieved was firstly identified. This is because higher wt% means availability of more crosslinking sites for the crosslinker. For this purpose different wt% solutions of these polymers were prepared in distilled water. The procedure for the preparation of such polymer solution is to weigh the required quantity of the polymer slowly and gently add the polymer in the vessel containing the specified amount of water, while the water is being stirred at high rpm. The stirring speed should be high enough to generate a vortex in the solvent medium without causing any spillage. To prepare a 100 ml solution about 500 rpm stirring speed is enough. This was achieved by stirring the water in a beaker using a magnetic stirrer and stirring plate, in this case distilled water was used. The polymer was slowly added to the stirring distilled water and left for few hours. The solution is ready once homogeneity is obtained. The mixing time is dependent on the molecular weight and the concentration of the polymer, higher the values; higher would be the mixing time.

The maximum polymer concentration is that concentration which would result in a homogenous and flow-able solution when mixed in water, adding any further amount of solute content after that would result in precipitation. Furthermore, in such solution where the solute content is higher than that required to attain the maximum polymer concentration, the agitation caused by the magnetic stirrer is not felt in the entire solution.

Only the medium near the magnetic stirrer gets agitated while the rest of the region remains unaffected.

For 3330S and Alcomer130 the maximum concentrations were found out to be 3wt% and 2wt% respectively, Figure 8 shows the prepared polymer solutions. The effect of concentration was studied by using three crosslinker concentrations, 0.6, 1 and 1.2 wt%s. The crosslinker used in this study is PEI. PEI is obtained in the form of a 33wt% active solution from Halliburton.

After the polymer solution was prepared, PEI was added it to drop by drop while the solution was being stirred using a magnetic plate and stirrer. In order to ensure proper mixing the solution was stirred for 20 minutes.

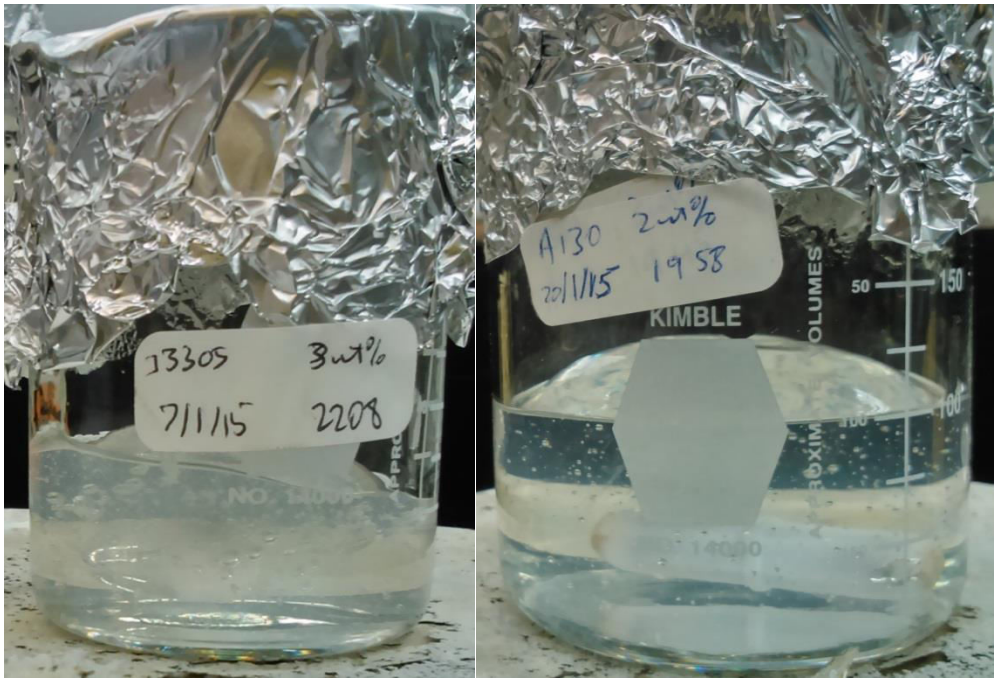

Figure 8 HPAM 3wt% solution (left), Alcomer130 2wt% (right)

4.1.2 Thermal Stability

Determining thermal stability of a gel is essential because polymer hydrolysis at high temperature can result in gel syneresis, which means water expulsion and significant reduction of gel volume. A thermally stable gel will be unaffected by syneresis and may show signs of minor gel shrinkage.

A total of six samples were prepared, three for each polymer, with varying PEI concentration; HPAM/PEI (3/0.6), (3/1) and (3/1.2) for HPAM and A130/PEI (2/0.6), (2/1) and (2/1.2) for Alcomer130. After preparation, these samples were placed inside air tight glass vials and placed in an oven at 100^{o}C in order to study their thermal stability. Figure 9 shows the samples placed in vials at room temperature. The HPAM/PEI samples are translucent and off-white in appearance while that of the A130/PEI samples are of a lighter whitish color tone. The samples were heated at 100^{o}C and periodically checked for signs of gelation and instability if any. After an hour of ageing, signs of gelation became apparent. The samples were aged for 28 days and were found to be thermally stable. With reference to the bottle-test gel strength codes developed by R. Sydansk (Sydansk., 1990), the gels formed could be regarded as I level gels. According to the code description, code I gels are non-flowing rigid gels that show no surface deformation upon inversion. The Sydansk gel code ranges from code A to J, where higher the alphabet the more rigid is the gel. Figure 10 shows the aged gels in an inverted position; the gels are rigid and exhibit no surface deformation. The top parts of the HPAM/PEI gels have turned orange in color while the rest of the gel is opaque white. A130/PEI gels display a similar appearance. The top part of the gels is bright yellow and the rest of the gels are white.

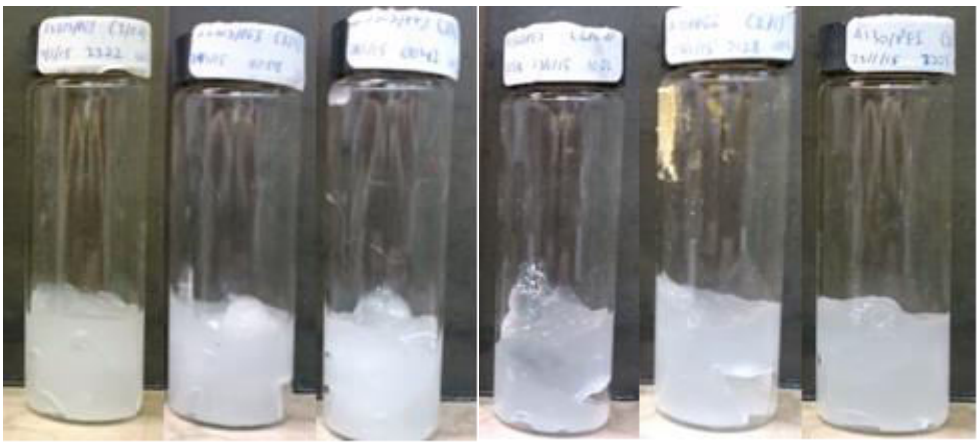

Figure 9 Crosslinked samples in vials at room temperature; HPAM/PEI (3/0.6), 3(/1), (3/1.2) and A130/PEI (2/0.6), (2/1), (2/1.2) [left to right]

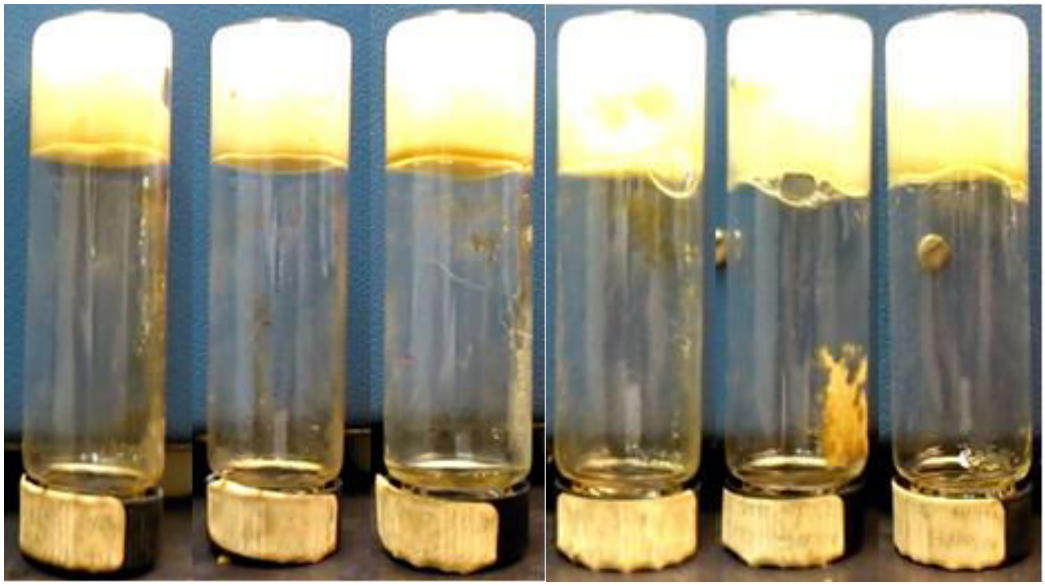

Figure 10 Gels aged at 100^{o}C for 28 days; HPAM/PEI (3/0.6), 3(/1), (3/1.2) and A130/PEI (2/0.6), (2/1), (2/1.2) [left to right]

4.1.3 Polymer Rheology

4.1.3.1 HPAM

3wt% HPAM solution was prepared following the procedure discussed earlier. Rheological studies were carried on this sample using the Discovery Hybrid rheometer. Amplitude oscillation test was run on the solution to determine the LVR for the base polymer. From the graph in Figure 11 the 25% strain value is the maximum strain value till which the polymer remains viscoelastic. This value was taken as an input parameter for the dynamic rheology tests.

HPAM is a shear sensitive polymer and its viscosity decreases with increasing shear, (Zaitoun et al., 2012). Figure 12 illustrates this behavior for the HPAM sample. The flow sweep test shows that the viscosity at the shear rate of 0.01 (1/s) was 622 Pa.s (622,000 cp) that reduced to 0.1945 Pa.s (194.5 cp) at 1000 (1/s) shear rate. This means that on exiting the drill bit nozzle, HPAM would have low viscosity and will be more flow-able than its static state.

Frequency sweep test was conducted on the sample using 25% oscillation strain value, Figure 13. The angular frequency was varied from 0.1 to 250 rad/s. With increasing angular frequency the solution gets more elastic as can be seen by the increasing separation between the storage and loss modulus curves. This behavior is reflective of the high molecular weight of this polymer.

The flow temperature test conducted on HPAM (3 wt%) solution showed that at fixed shear rate HPAM exhibits viscosity decreasing behavior with temperature increase, as

illustrated in Figure 14. At 10 (1/s) shear rate the viscosity of HPAM (3 wt%) is 10 Pa.s at 26^{o}C, this gets reduced to about 1.4 times at 90^{o}C.

Figure 15 highlights the result of the oscillation temperature ramp test. The results showed that there was a gradual decrease in the storage modulus profile of HPAM at a fixed oscillation strain % and shear rate while the loss modulus profile was pretty much uniform, this behavior is attributed to the viscosity decrease of HPAM with temperature.

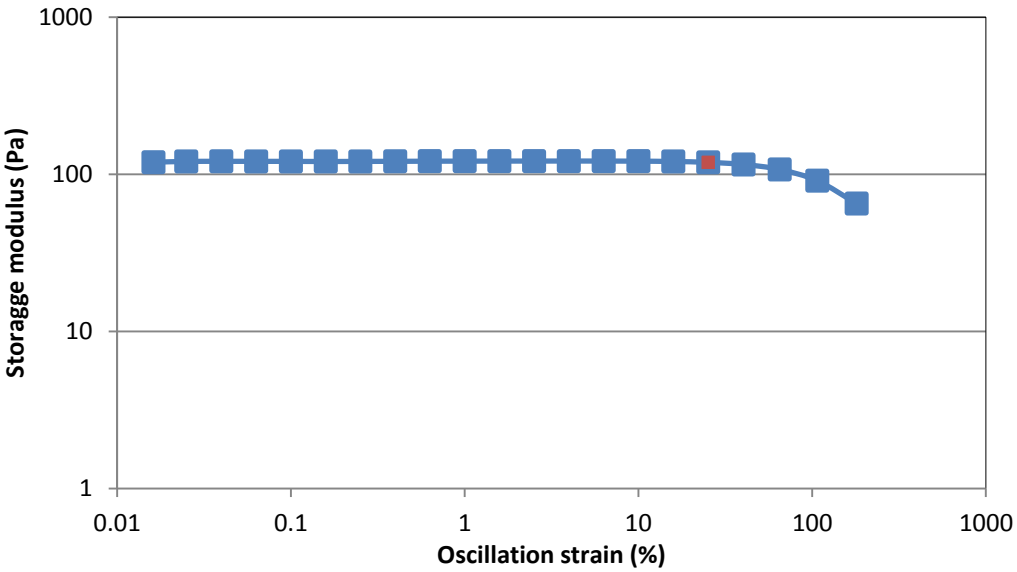

Figure 11 Oscillation Amplitude test for HPAM (3 wt%)

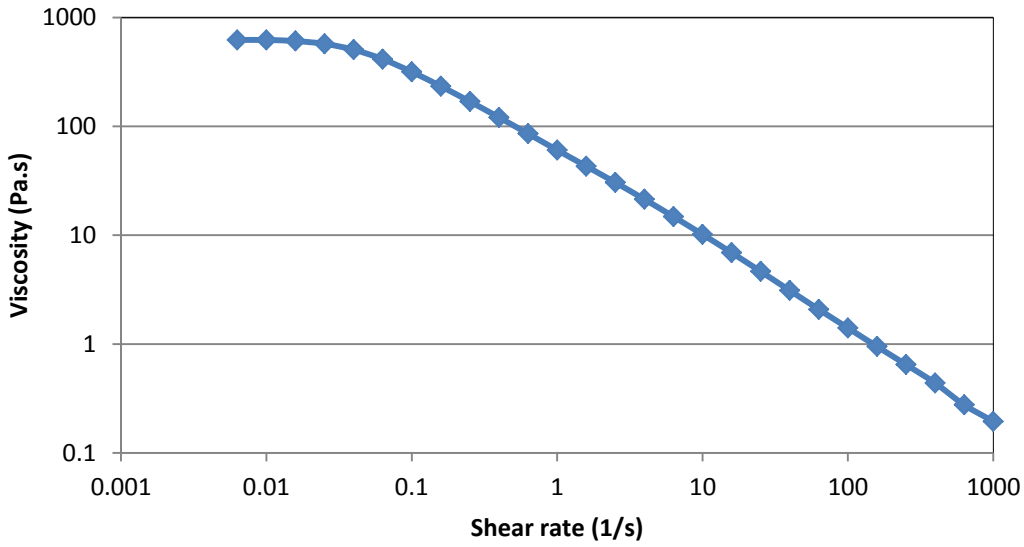

Figure 12 Flow sweep profile of HPAM (3 wt%)

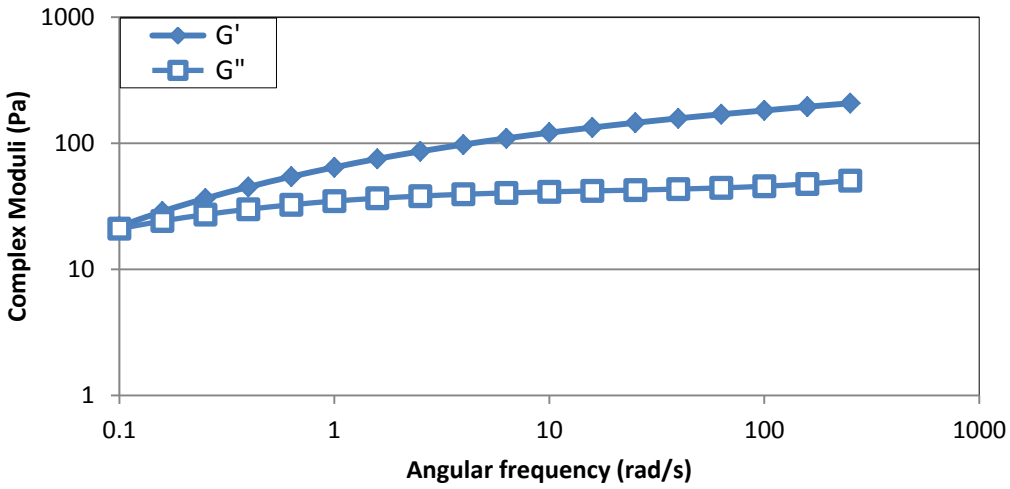

Figure 13 Frequency sweep profile of HPAM (3 wt%)

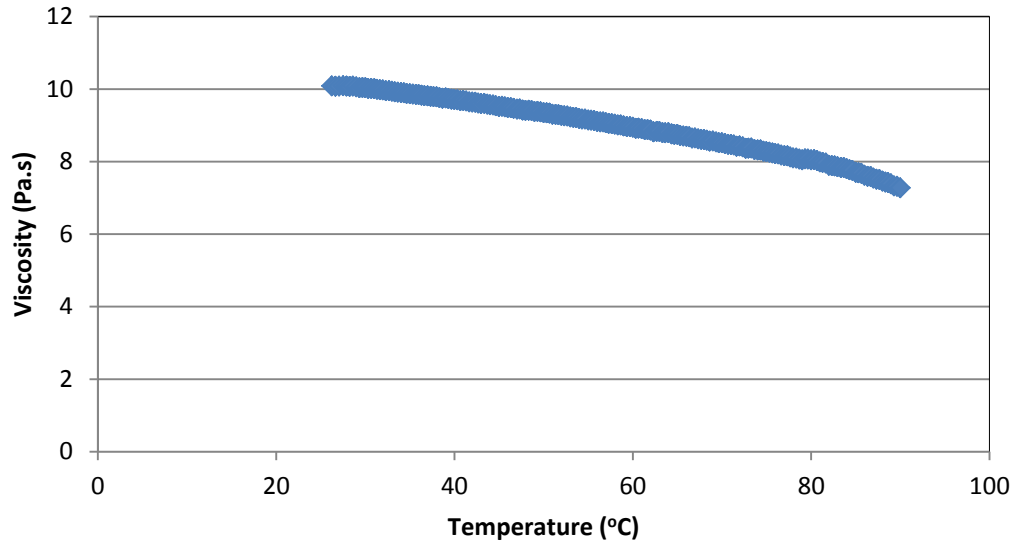

Figure 14 Flow temperature ramp of HPAM (3 wt%)

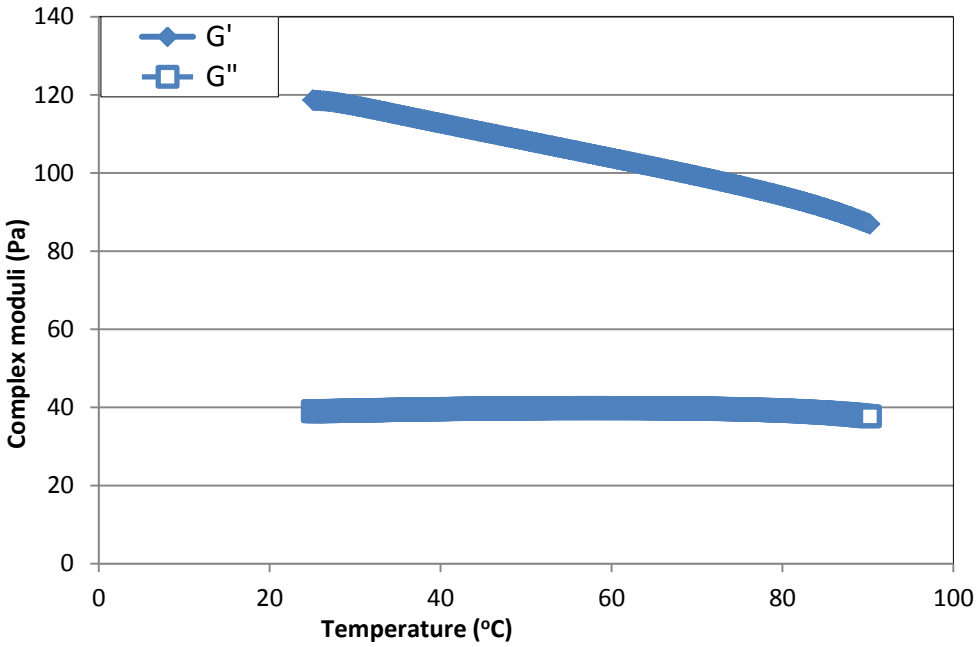

Figure 15 Oscillation temperature ramp of HPAM (3 wt%)

4.1.3.2 Alcomer130

For Alcomer130 (2 wt%) 25% strain value was the max strain % obtained for LVR, as can be seen from the polymer's oscillation amplitude profile in Figure 16. The curve dips downwards after 25% strain value, indicating the end of the LVR for this polymer solution.

Viscosity profile of Alcomer130 (2 wt%) at 25^{o}C showed that just like HPAM, this acrylamide based copolymer is shear sensitive and shear thinning in nature, as can be observed in Figure 17. The flow sweep test shows that at the shear rate of 0.01 (rad/s) the viscosity of the solution was 1561 Pa.s (1,561,000 cp) which got reduced to 0.1325 Pa.s (132.5 cp) at the shear rate of 1000 (1/s).

The frequency sweep results of Alcomer130 (2 wt%) are illustrated in Figure 18. The complex moduli have greater separation than the HPAM polymer; it is only due to that fact that Alcomer130 is a polymer having very high molecular weight.

Flow temperature ramp profile of Alcomer130 (2 wt%) can be seen in Figure 19. The polymer showed thermo-thinning behavior for a fixed shear rate like HPAM but the viscosity decrease for Alcomer130 with temperature was not gradual. The viscosity steadily decreased from 25^{o}C (6.48 Pa.s) to 50^{o}C (6.33 Pa.s) but from 50^{o}C (6.33 Pa.s) to 90^{o}C (4.49 Pa.s) the rate of decline in viscosity increased.

The oscillation temperature ramp graph showed that complex moduli of Alcomer130 (2 wt%) are affected by the temperature variation. The storage modulus decreased while the loss modulus increased with an increase in temperature, this can be observed in Figure 20.

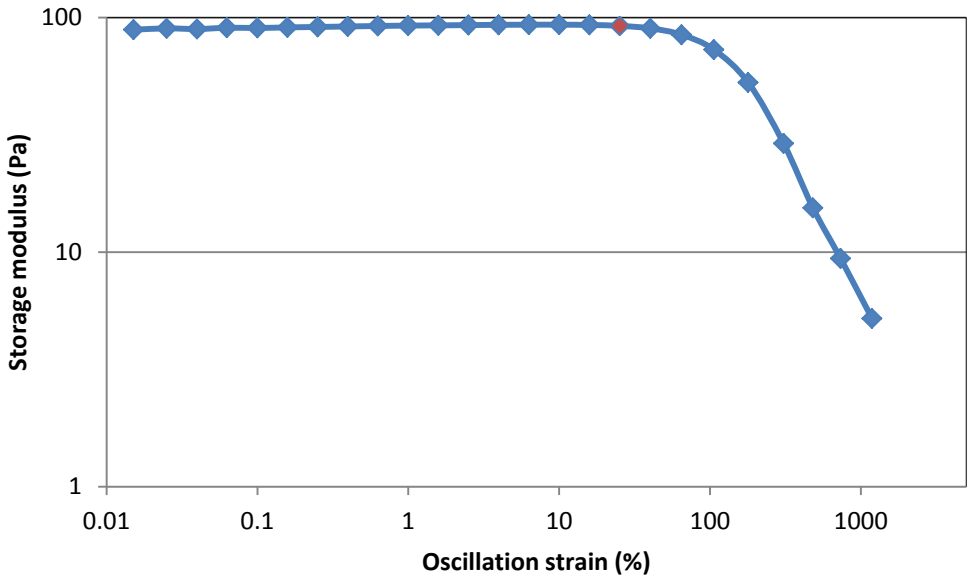

Figure 16 Oscillation Amplitude test for Alcomer130 (2 wt%)

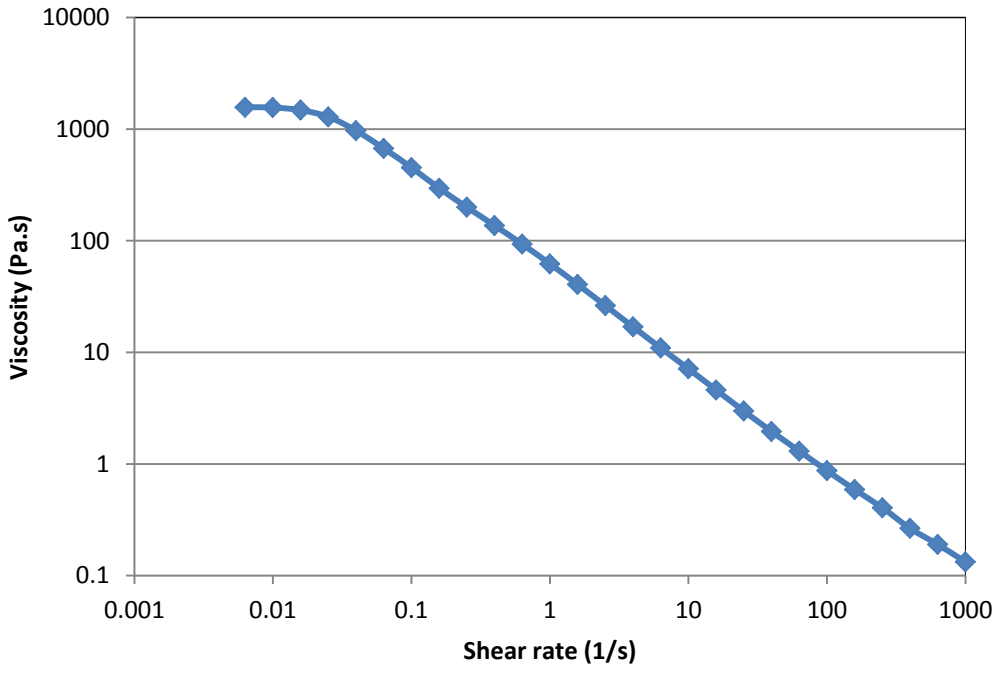

Figure 17 Flow sweep profile of Alcomer130 (2 wt%)

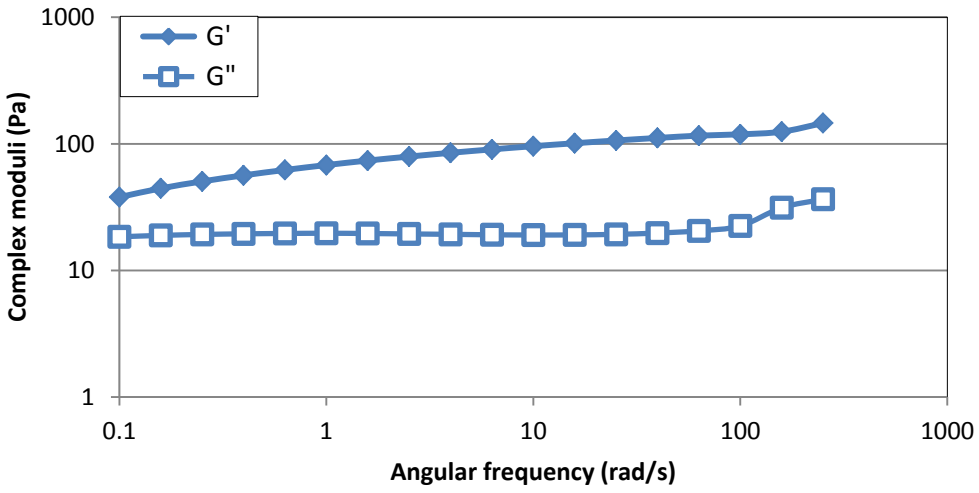

Figure 18 Frequency sweep profile of Alcomer130 (2 wt%)

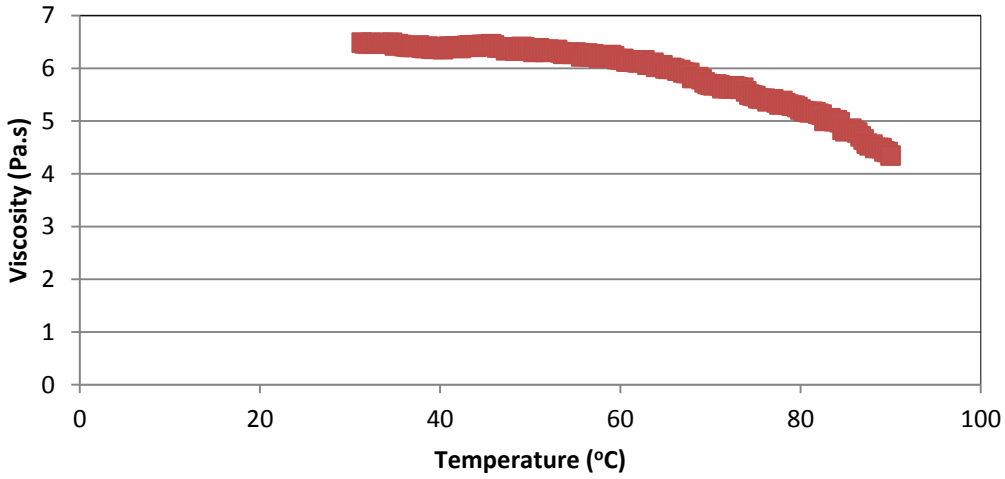

Figure 19 Flow temperature ramp of Alcomer130 (2 wt%)

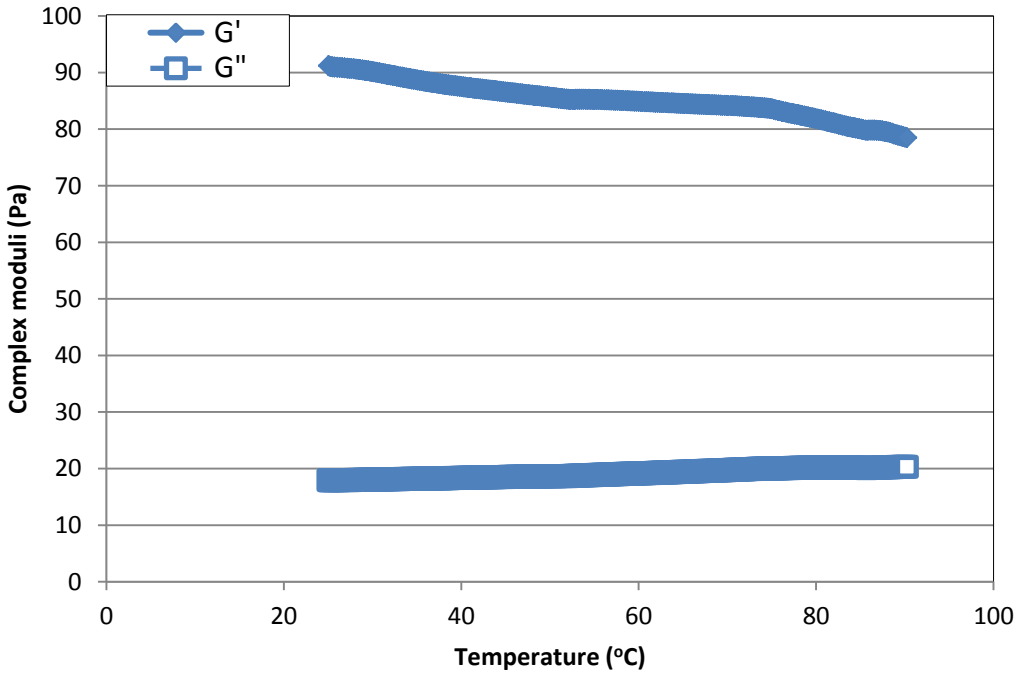

Figure 20 Oscillation temperature ramp of Alcomer130 (2 wt%)

4.1.4 Gel Rheology

After mixing the polymer and crosslinker for 20 minutes the samples were placed in vials and aged in an oven. Rheology of the aged samples was then conducted to study the effect of crosslinker concentration, time and temperature on the properties of the gel.

HPAM/PEI (3/0.6) and (3/1) samples were aged at 100^{o}C for 1 day. For the case of HPAM/PEI (3/1.2) four samples were prepared to be aged at different temperature and time conditions; those being aged at 100^{o}C for 6hrs and 1 day and for the same time duration at 120^{o}C. The same scheme was followed for A130/PEI samples. This scheme is summarized in Table 1. All the gels exhibited Sydansk code I characteristics after ageing.

Rheology of the aged gels was performed on the Discovery hybrid rheometer, using the cone and plate geometry. The aged gel is carefully taken out from the vial and placed at the center of the peltier plate. The cone is then lowered till the closure gap of the geometry and any gel component that spills over from the geometry is cut off using a knife. To study the rheology of the gels, oscillation amplitude and oscillation sweep tests were performed.

The maximum limit of the LVR of almost all of the gels lied between 10% and 15% oscillation strain value. These values are less than that of the base polymers' because of the gels being more rigid in nature. Two samples gave the highest G' values and they were the ones with the highest crosslinker concentration and were aged at the highest temperature for the longest time. These samples are HPAM/PEI (3/1.2) and A130/PEI (2/1.2) aged at 120^{o}C for 1 day; their maximum strain value was 1% and 2.5% respectively.

Figure 21 and Figure 22 summarizes the storage modulus comparison of the gels for HPAM/PEI and A130/PEI respectively. The gel strength is purely dependent on the crosslinker concentration, ageing time and heating temperature. An increasing trend in G' is apparent with respect to these parameters in both the HPAM/PEI and A130/PEI cases. At the angular frequency of 10 rad/s HPAM alone had the storage modulus of 121 Pa, with 0.6 and 1 wt% PEI at 100^{o}C the G' became 272 Pa and 289 Pa respectively, an almost two fold increase, after 1 day of ageing. For the same condition 1.2 wt% PEI gave a fourfold increase, the value for this concentration at 10 rad/s is 475 Pa. HPAM/PEI (3/1.2) aged at 120^{o}C for 1 day at 10 rad/s showed the G' value of 3564 Pa, an almost 29 times higher value than that of the base polymer. Here high crosslinker concentration and static heating at high temperature greatly enhanced the gel strength of the system.

The G' value of 2wt% Alcomer130 solution obtained at 10 rad/s is 95.8 Pa. For the case of 0.6 and 1 wt% PEI, a G' improvement of 1.2 times was obtained for the samples aged at 100^{o}C for 1 day. The sample with 1.2 wt% PEI under the same conditions gave an improvement of 4 times. A130/PEI (2/1.2) sample aged at 120^{o}C for 1 day gave the G' value of 578 Pa at the angular frequency of 10 rad/s. This increment is six fold when compared to that of the base polymer. Gel strength was enhanced with respect to time and temperature but not exactly in the same manner as that of HPAM/PEI gels.

Figure 23 and Figure 24 highlights the extent of G' improvement of HPAM/PEI (3/1.2) and A130/PEI (2/1.2) gels respectively, in relation to time and temperature. At 100^{o}C the HPAM/PEI (3/1.2) experienced a strength enhancement by a factor of 2.5 when it was aged for 24 hours with respect to it being aged for 6 hrs. At 120^{o}C this G' enhancement was by a factor of 9.7. When the gel strength improvement was compared in relation to

ageing time, it was observed that the gel that had aged for 6 hours at 120^{o}C improved the G' profile 1.8 times than when the sample was aged at 100^{o}C for the same amount of time. The improvement for the 24 hours duration at 120^{o}C was 7.3 times than that at 100^{o}C. For HPAM/PEI gels time and temperature collectively increased the gel characteristics.

A130/PEI (2/1.2) at 100^{o}C exhibit a triple G' improvement with respect to time, however at 120^{o}C the G' improvement is by a factor of 2.2 in relation to sample ageing time. Although the G' values are higher at 120^{o}C, both for 6 hours and 24 hours aged samples in comparison to the samples aged for the same duration at 100^{o}C, the degree of strength improvement is less than that at 100^{o}C. A similar trend was observed for A130/PEI (2/1.2) gels in relation to temperature. The difference between G' values at 120^{o}C and 100^{o}C aged at 6 hours is by a factor of 2 while that for a 24 hours ageing period is 1.5. This means that the degree of gel strength enhancement as a function of time and temperature gets reduced for A130/PEI gels.

Table 1 Gel ageing scheme

HPAM/PEI	A130/PEI	Temperature (^{o}C)	Time (hr)
3/0.6	2/0.6	100	24
3/1	2/1	100	24
3/1.2	2/1.2	100	6
3/1.2	2/1.2	100	24
3/1.2	2/1.2	120	6
3/1.2	2/1.2	120	24

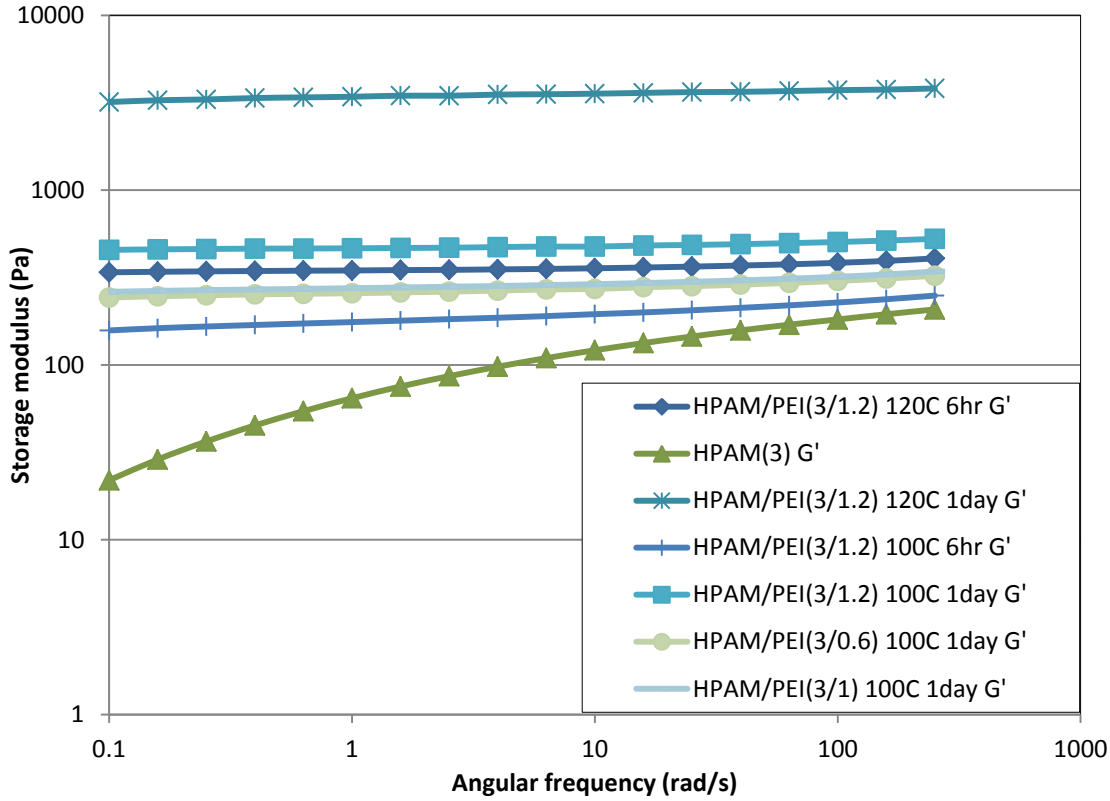

Figure 21 HPAM/PEI gels storage modulus comparison

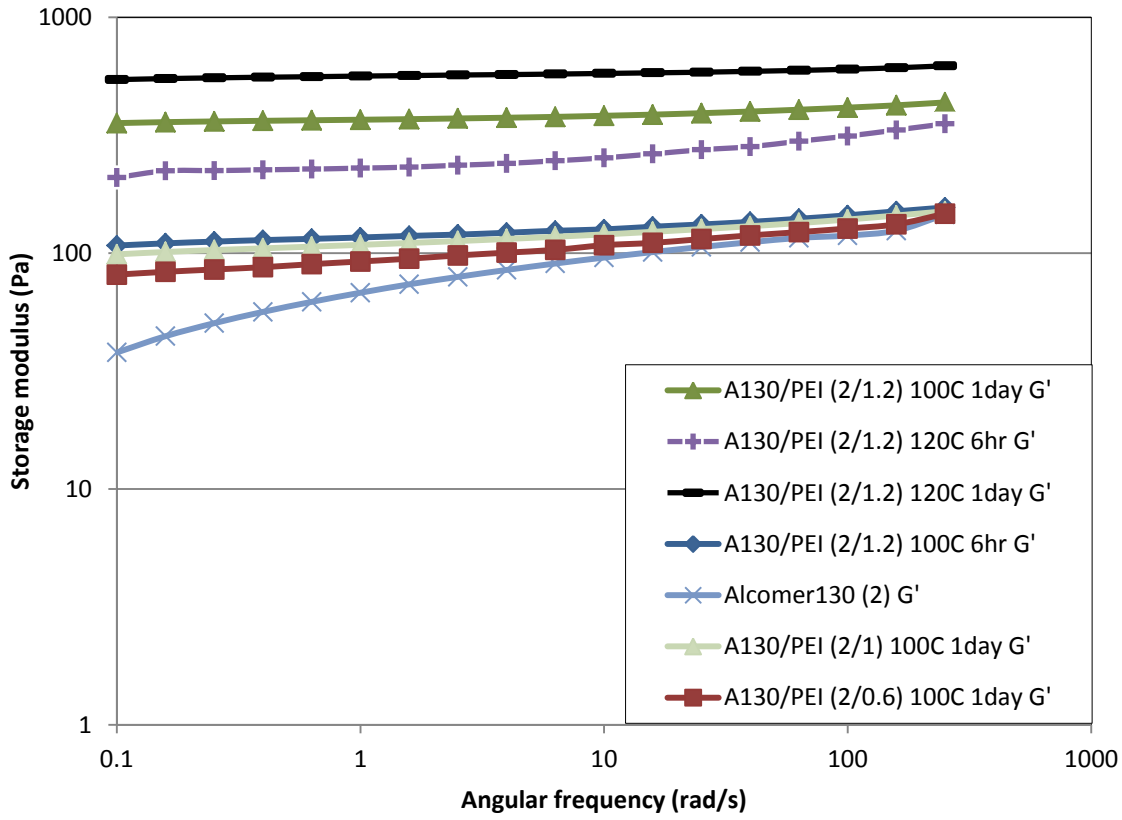

Figure 22 A130/PEI gels storage modulus comparison

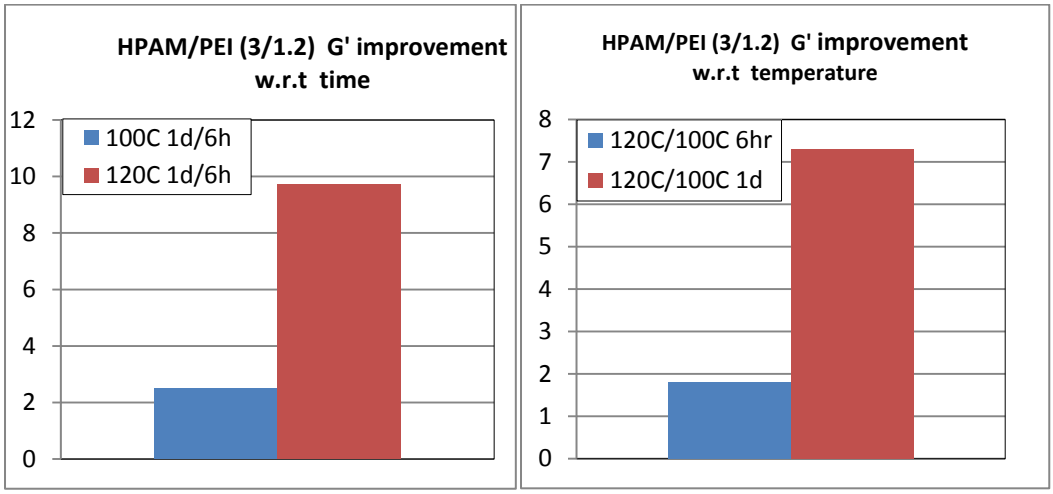

Figure 23 HPAM/PEI (3/1.2) G' improvement with time (left) and with temperature (right)

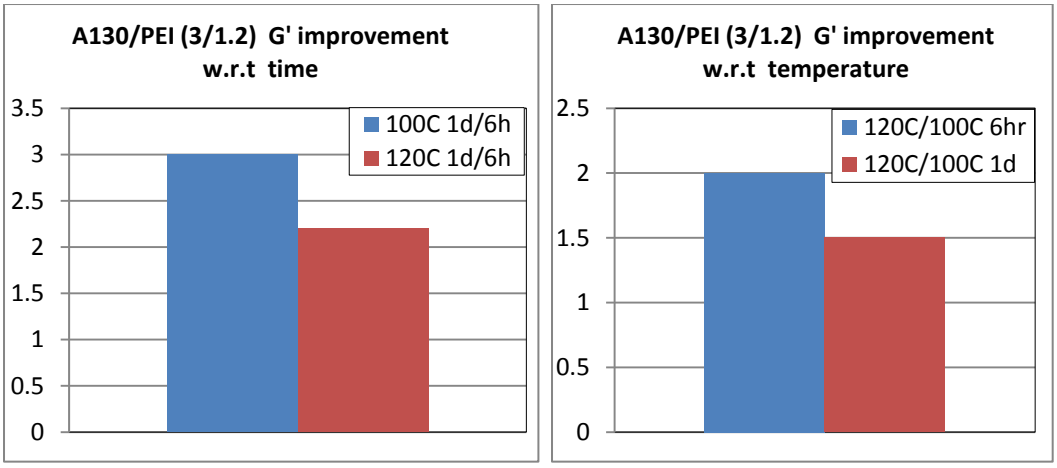

Figure 24 A130/PEI (3/1.2) G' improvement with time (left) and with temperature (right)

4.2 TVP

The TVP used in this study is generically named K20. K20 is a low molecular weight TVP based on PAM, having acrylate group it is believed to crosslink with the immine group in PEI in a manner similar to PAM. The molecular weight of K20 is 7870 Da with a degree of hydrolysis of 3% and the thermosensitive monomer content of 5%. A TVP is unique in a way that it undergoes viscosity enhancement with temperature at certain conditions.

4.2.1 Rheology

A 0.75 wt% of K20 solution was prepared using deionized water and its rheology was studied using the rheometer. K20 solute was gradually added to the stirring deionized water; in a manner similar to the preparation of a PAM solution. After 2-3 hours of stirring the solution was ready. The preparation time was less because K20 has a low molecular weight. Figure 25 shows the homogenous solution after preparation.

Rheology studies of K20 (0.75 wt%) were started off with the amplitude sweep test. It showed that a value of 25% of oscillation strain % as the maximum strain % value for the LVR, Figure 26.

Figure 27 shows that like PAM, TVP is shear thinning in nature. 0.75 wt% of K20 has a viscosity of 0.151 Pa.s (151 cp) at the shear rate of 1 1/s this gets reduced to 0.02 Pa.s (20 cp) at 1000 1/s.

Frequency sweep results are expressed in Figure 28, the test shows that G" overshadows the G' over most of the tested frequency range and it is true because K20 has a small

molecular weight and at this concentration the solution is not viscous. At high frequency the solution becomes more elastic as after 100 rad/s the elastic complex modulus of K20 surpasses the viscous complex modulus.

The result of the flow temperature ramp, Figure 29, test showed that the viscosity of K20 reduced with temperature. Since it is a TVP, its viscosity was expected to rise with temperature but a converse of this theory happened. What it meant was that the thermoviscosifying property of such polymer might be dependent upon certain other conditions as well, which needs to be investigated.

Figure 30 presents the oscillation temperature ramp test result of K20 (0.75 wt%). The results showed that under the testing conditions and parameters, the complex moduli of K20 were inversely related to temperature.

Figure 25 K20 (0.75 wt%) homogenous solution obtained after 2-3 hours of stirring

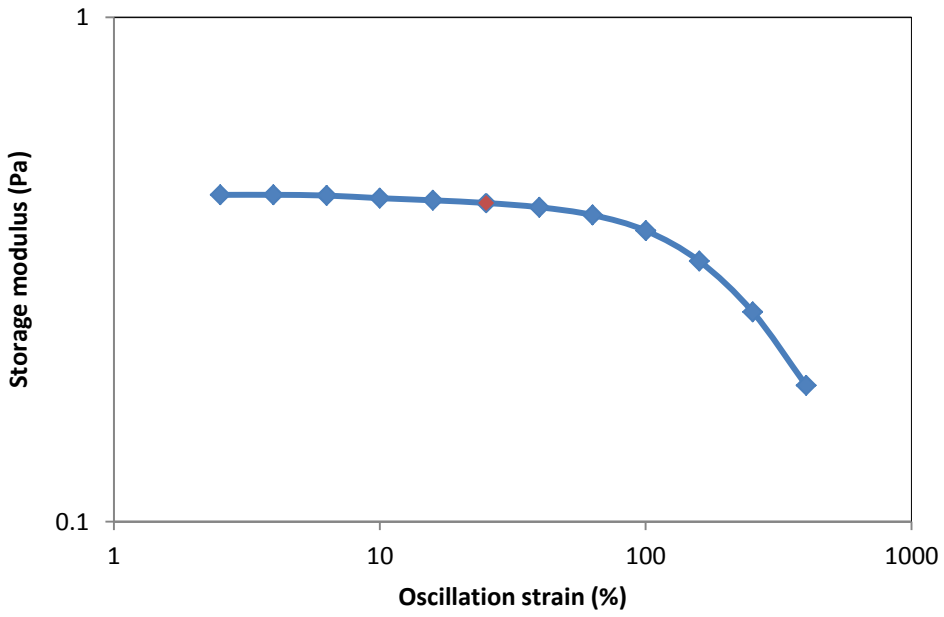

Figure 26 Amplitude oscillation test for K20 (0.75 wt%)

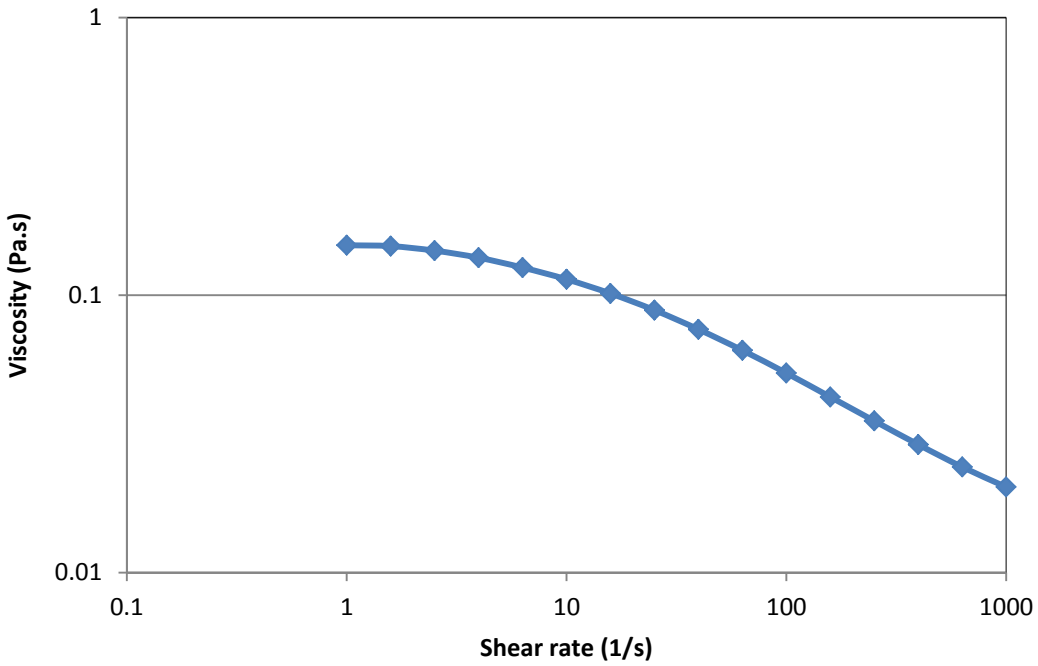

Figure 27 Flow sweep test of K20 (0.75 wt%) at 25°C

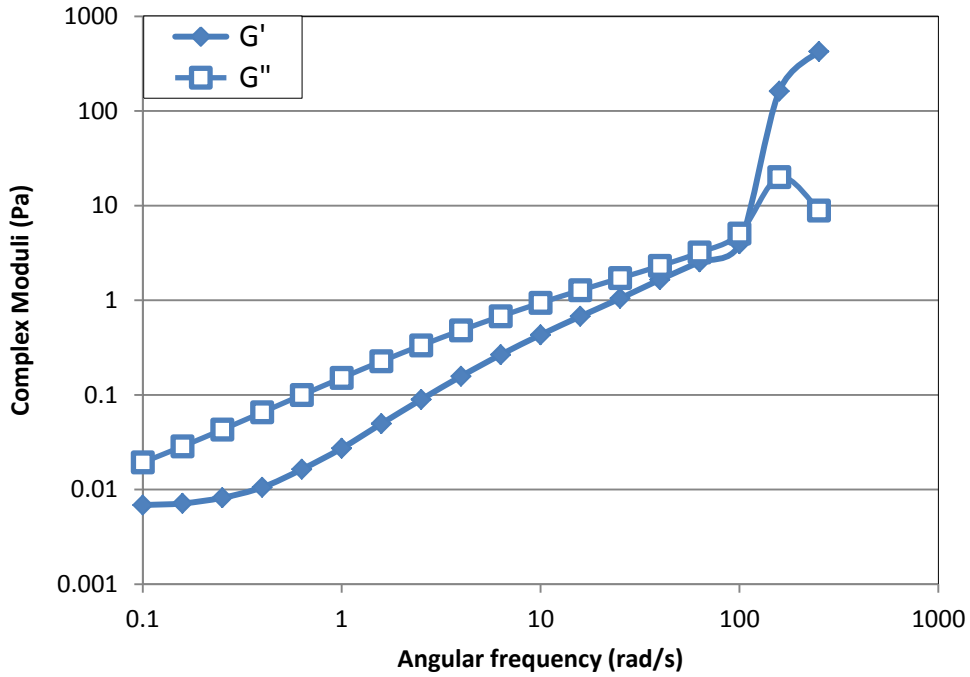

Figure 28 Frequency sweep test for K20 (0.75 wt%)

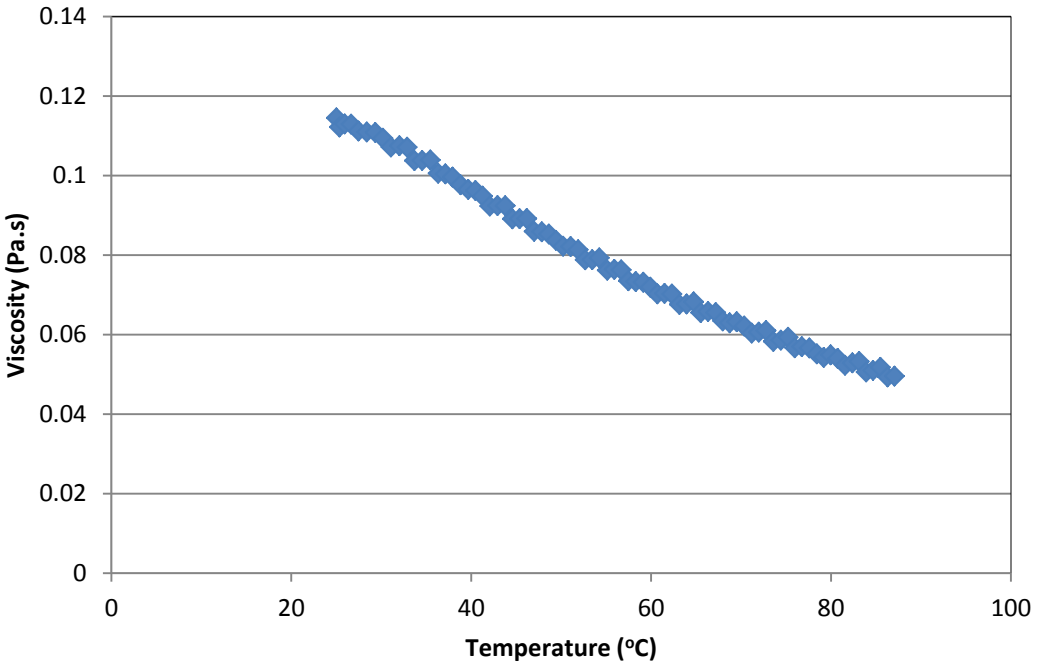

Figure 29 Flow temperature ramp test of K20 (0.75 wt%)

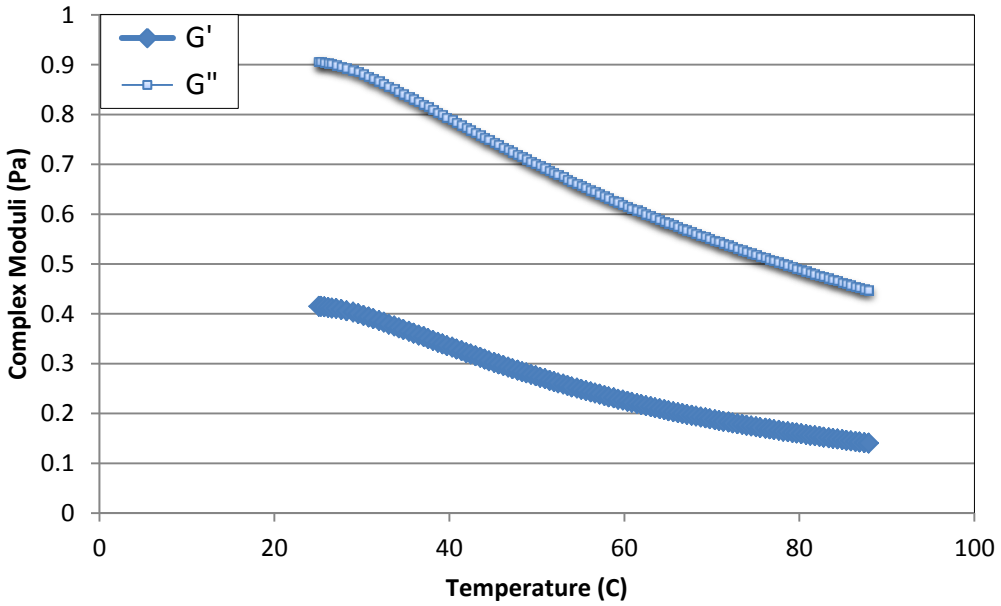

Figure 30 Oscillation temperature ramp of K20 (0.75 wt%)

4.2.2 TVP Interaction with PEI and Clay

To investigate the interaction of K20 with PEI and clay two separate solutions were prepared in deionized water. The clay used in this case is generically called 15A, which is a functionalized nano-clay. Once a uniform solution of the base polymer was obtained the potential cross-linkers were added to the solution and stirred for a sufficient amount of time before studying their rheology. The compositions are mentioned in Table 2. After the addition of 15A to K20 a uniform solution was obtained after about 10 minutes. The solution was left for stirring for 1 day before conducting rheology tests. Same as the 15A system, a homogenous system with PEI was attained after 10 minutes of mixing; the solution remained the same even after it was left for stirring for 1 day. 15A deposits were visible on the base of the beaker after the K20/15A (0.75/0.1) system was taken out for rheology study and some deposits were found on the stir bar. This meant that the interaction b\w the TVP and the nano-clays were minimal. Figure 31 shows both the systems after preparation. From the transparent solution of K20 both systems had turned a different shade of milky white.

Both the K20 systems containing 15A and PEI respectively were then tested in the rheometer and their results were compared with that of the base polymer alone.

Table 2 system composition

Base polymer	Cross-linker
K20 (0.75 wt%)	PEI (0.1 wt%)
K20 (0.75 wt%)	15A (0.1 wt%)

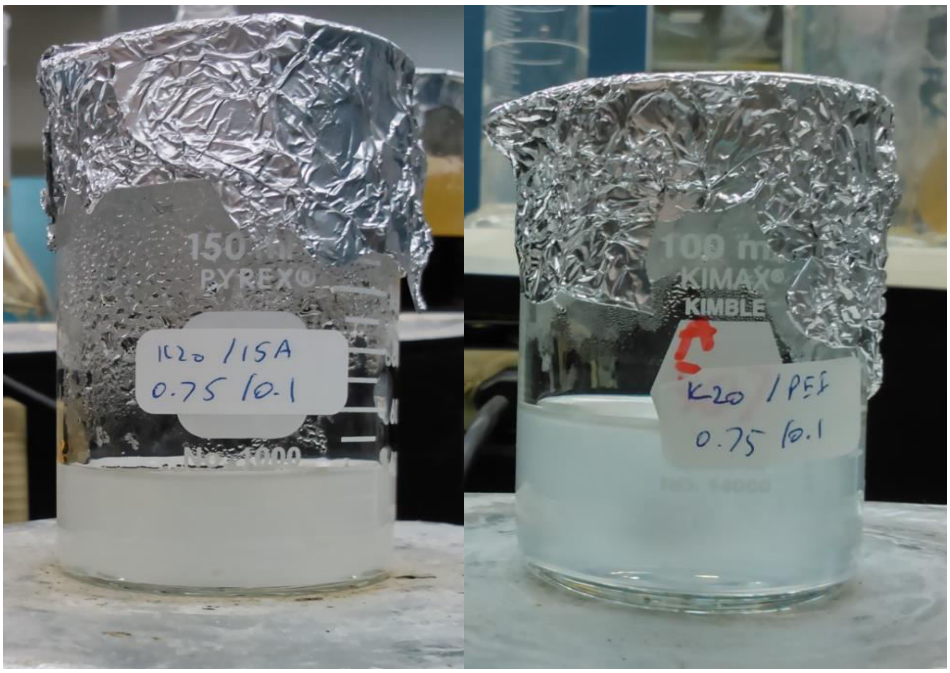

Figure 31 K20/15A (0.75/0.1) system (left) and K20/PEI (0.75/0.1) system (right)

In Figure 32 the flow sweep comparison indicates that both systems gave low viscosity profiles than that of the base polymer, at higher frequencies though the difference is not significant. K20/PEI (0.75/0.1) system gave the lowest viscosity profile of the three. PEI it seems did not interact and boost the system property as it was expected to do.

Interesting results were obtained with the frequency sweep tests which are summarized in Figure 33, Figure 34 and Figure 35. Addition of PEI had no incremental effect on the complex moduli of the base polymer. Not only were the elastic and viscous properties of the K20/PEI system less than that of the base polymer, even the storage modulus was not dominant than the loss modulus at higher frequencies. G' of the K20/PEI system passed the G" at 158 rad\s but the G" soon caught up to it.

For the system with 15A the complex moduli were less than the base polymer's at low frequencies. After 30 rad/s the K20/15A shifted more towards the elastic spectrum and it's G' values went higher than the base polymer. This improvement in G' existed till 150 rad/s after which the G' of both K20 and K20/15A became the same. This clearly indicated that interaction and property improvement of K20 with the nano-clay are limited to a certain degree under the tested conditions.

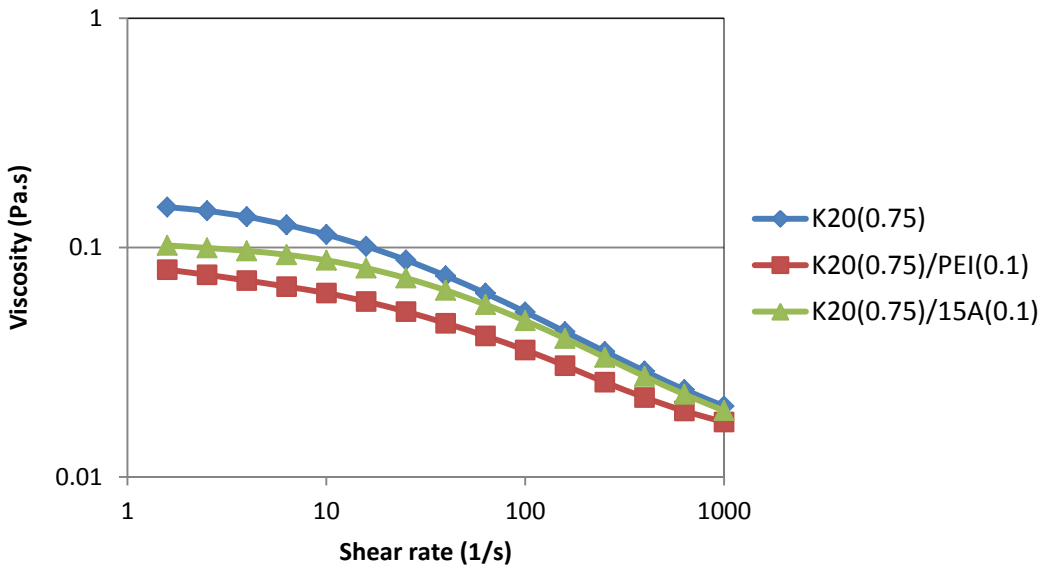

Figure 32 Flow sweep comparison chart of the K20 systems

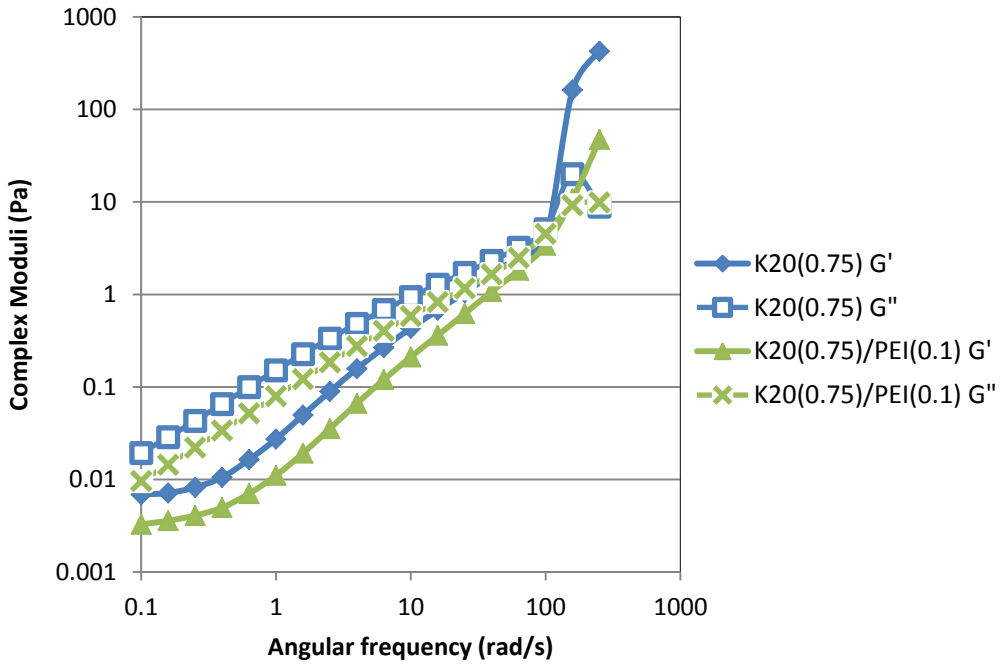

Figure 33 Frequency sweep comparison of K20 (0.75 wt%) and K20/PEI (0.75/0.1)

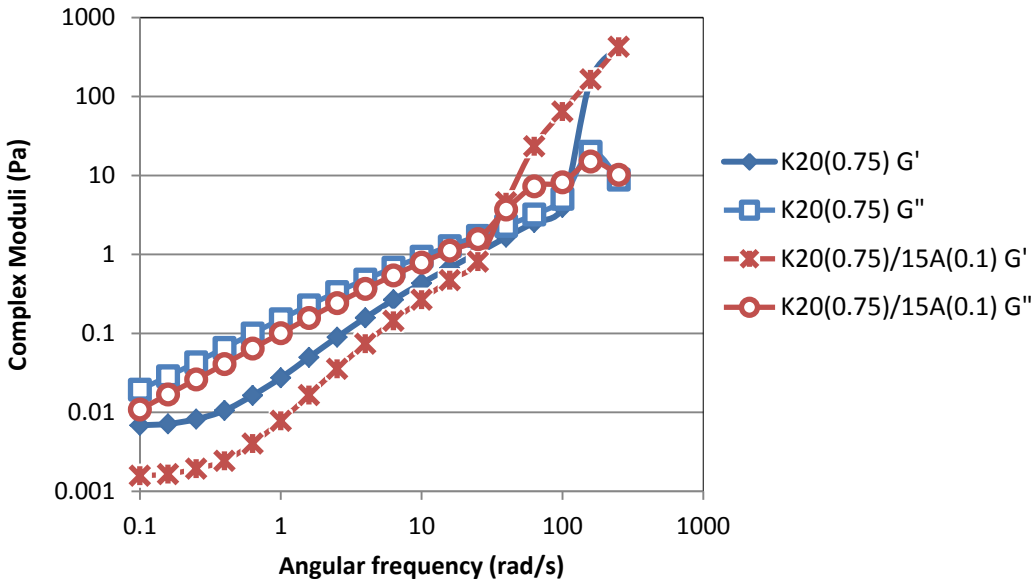

Figure 34 Frequency sweep comparison of K20 (0.75 wt%) and K20/15A (0.75/0.1)

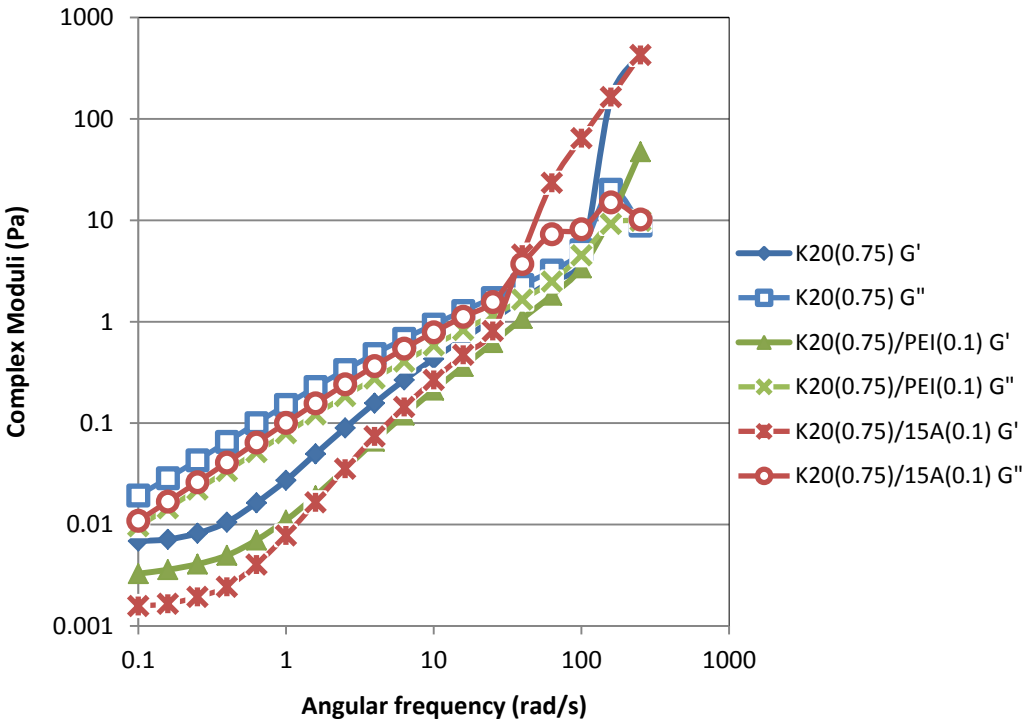

Figure 35 Frequency sweep comparison of all the three systems

Results of the flow temperature ramp test, Figure 36, showed that like the base polymer the other two systems followed the same decreasing viscosity trend. Since thermo-thickening effect was not obtained with the base polymer, this effect was also absent from the other two systems.

Figure 37 highlights the oscillation temperature ramp result comparison of the three systems at the shear rate of 10(1/s). Both K20/PEI and K20/15A have low complex moduli than the base polymer as is evident from the frequency sweep test also. G" of K20/15A follows exactly the same trend as that of K20. At this shear condition K20/PEI has the lowest energy dissipation capacity then the rest.

At higher temperature the rate of decrease of G' of both the K20/PEI and K20/15A systems change and the two curves gradually converge at temperatures above 80^{o}C. This means that at high temperatures energy storage ability of both these systems, having different additives and experiencing the same shear rate were the same.

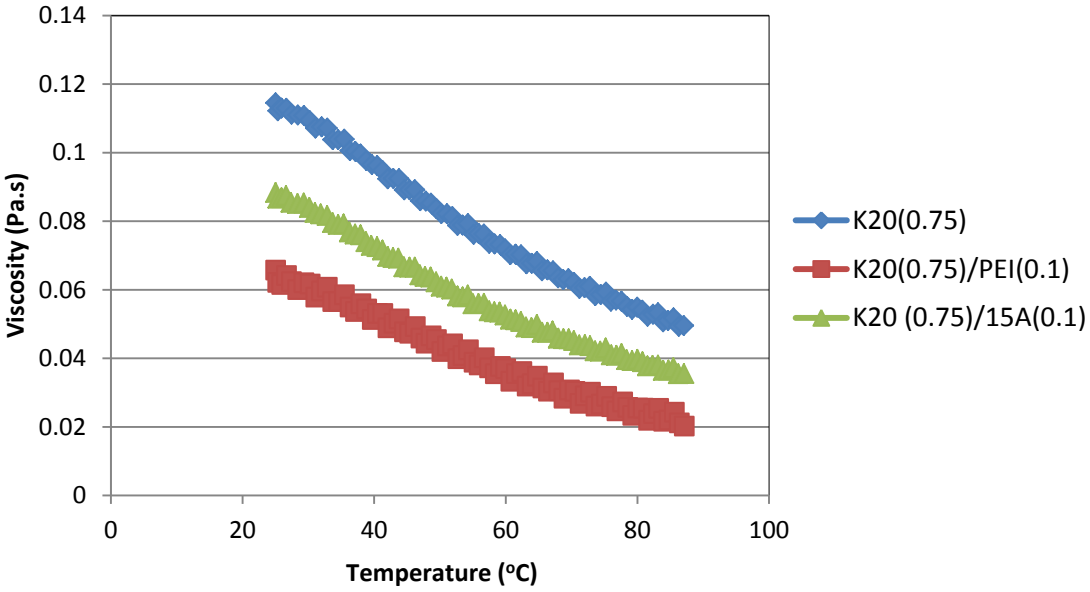

Figure 36 Flow temperature ramp test comparison of the three systems

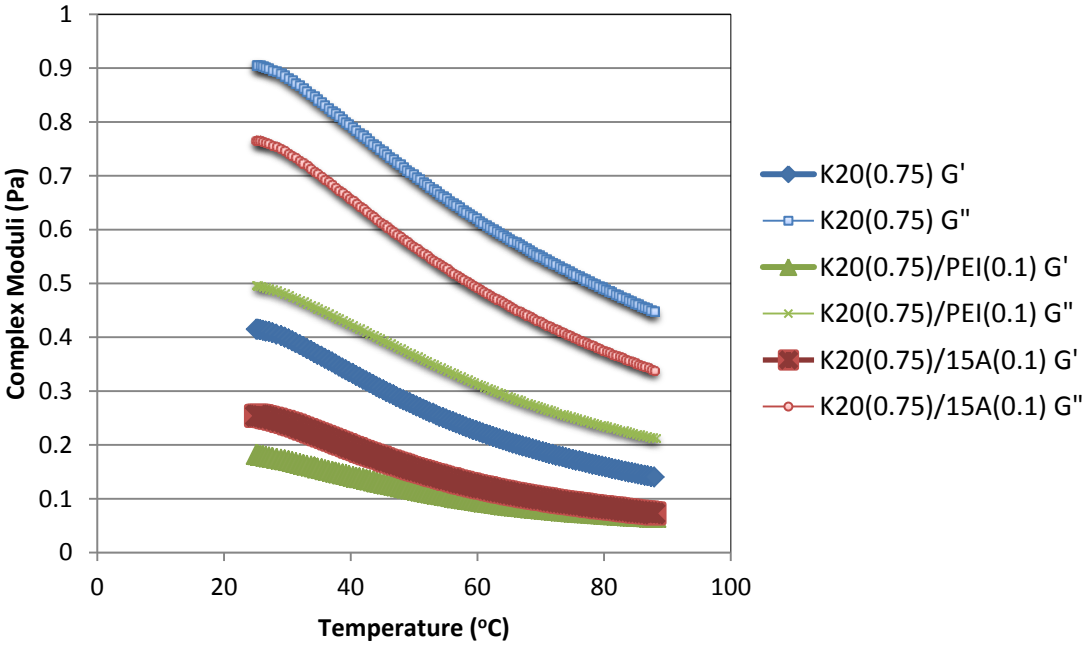

Figure 37 Oscillation temperature ramp comparison of all the systems

4.2.3 Salinity Effect

Since the TVP did not show any thermoviscosifying property, it implied that there were other factors due to which the thermo-thickening effect would become apparent. Those factors could be polymer wt% and salinity. The effect of these parameters were studied and compared.

In the work by Chen et al. (2012) the similar TVP showed increase in temperature after 60^{o}C. The polymer weight used in that work was 0.2 % under a highly saline environment. These factors were looked into in studying the effect of salinity, 0.2 wt% and 0.75 wt% solutions of K20 were prepared in different saline environments. Table 3 shows the brine composition used for the saline environment and Table 4 summarizes the system compositions at different salinity that were studied. Figure 38 shows the K20 (0.75 wt%) solutions in seawater and formation water.

Table 3 Brine composition

Ions	Formation Water (FW)	Seawater (SW)
Sodium	59,491	18,300
Calcium	19,040	650
Magnesium	2,439	2,110
Sulfate	350	4,290
Chloride	132,060	32,200
Carbonate	0	0
Bicarbonate	354	120
TDS	**213,734**	**57,670**

Table 4 System composition

K20 concentration	Salinity
0.2	SW
0.2	FW
0.75	SW 50%
0.75	SW
0.75	FW

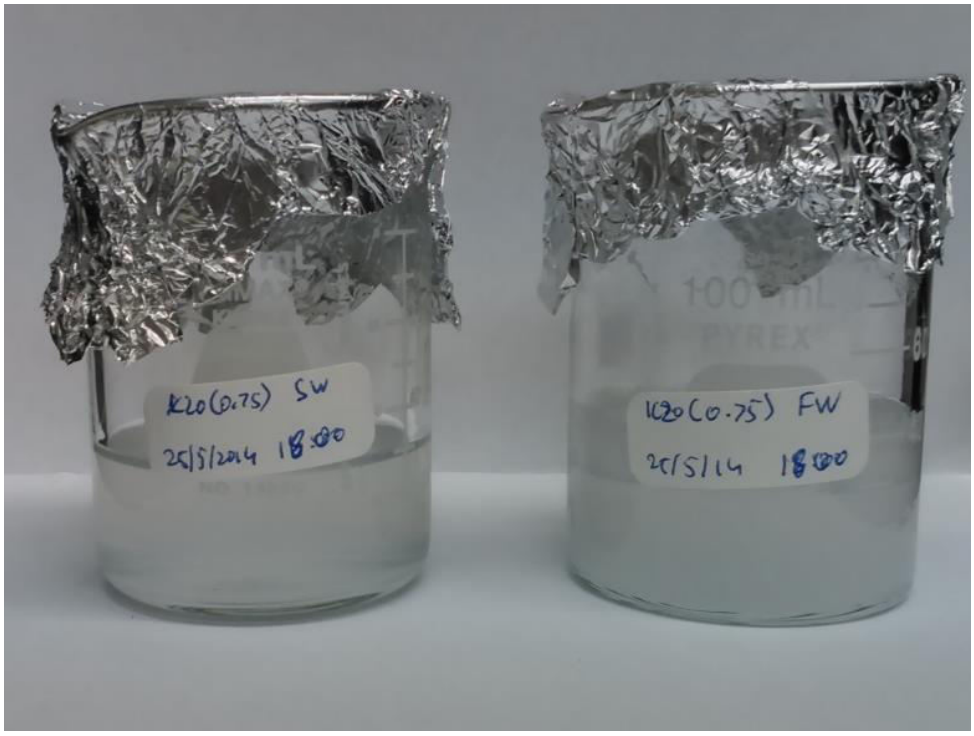

Figure 38 K20 (0.75 wt%) solution in sea water and formation water after preparation

Flow temperature ramp test over the range of 25-90^{o}C was conducted on these samples and compared. A heating rate of 2^{o}C/min and a fixed shear rate of 10(1/s) was used for this test.

Figure 39 shows the comparison of all the K20 (0.75 wt%) samples. At 25^{o}C the viscosity value of K20 (0.75 wt%) is 0.114 Pa.s (114cp) this gets reduced by almost 2.5 times for all the other saline solutions. It was observed that at 50% SW salinity the viscosity profile decreased greatly as compared to the 0% salinity case. The viscosity profile increased slightly at the 100% SW case. For the case of formation water the viscosity profile remained somewhat uniform till 52^{o}C. After this temperature the thermo-thickening effect came into play and the viscosity began to increase. Viscosity values of K20 (0.75 wt%) FW even surpassed that of the 0% salinity case after 72^{o}C. The sample reached the value of 0.067 Pa.s (67 cp) at 90^{o}C, 1.5 times more than its value at 25^{o}C and 1.3 times more than the viscosity reading of K20 (0.75 wt%) at 90^{o}C.

The effect of polymer concentrations on the thermo-thickening behavior is illustrated in Figure 40. Viscosity profiles of both K20 (0.2 wt%) SW and K20 (0.2 wt%) decreased with temperature and no thermo-thickening effect was observed. From these tests it can be concluded that for this TVP, the thermo-thickening property would come into effect only at highly saline conditions and moderately high polymer concentrations.

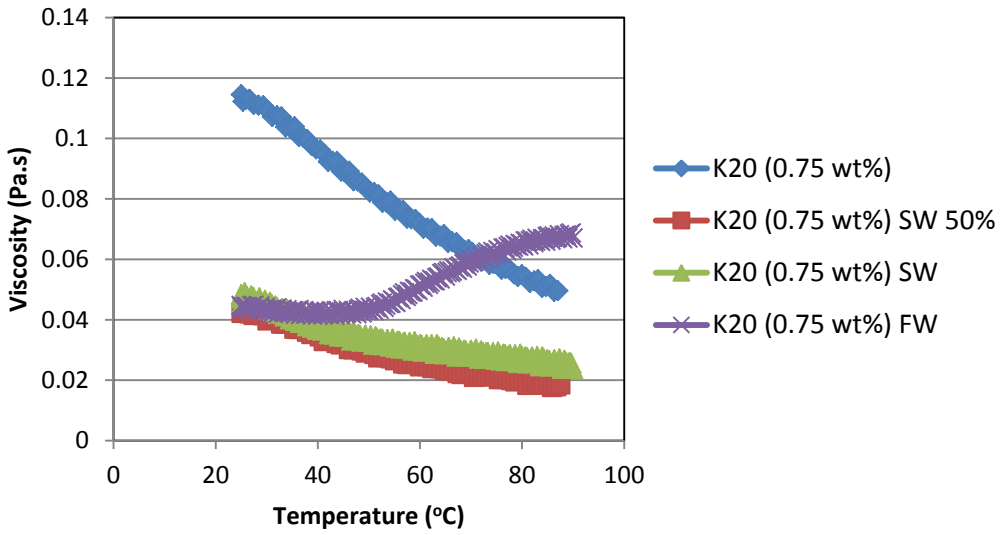

Figure 39 Flow temperature ramp test comparison of K20 (0.75wt %) at different salinity

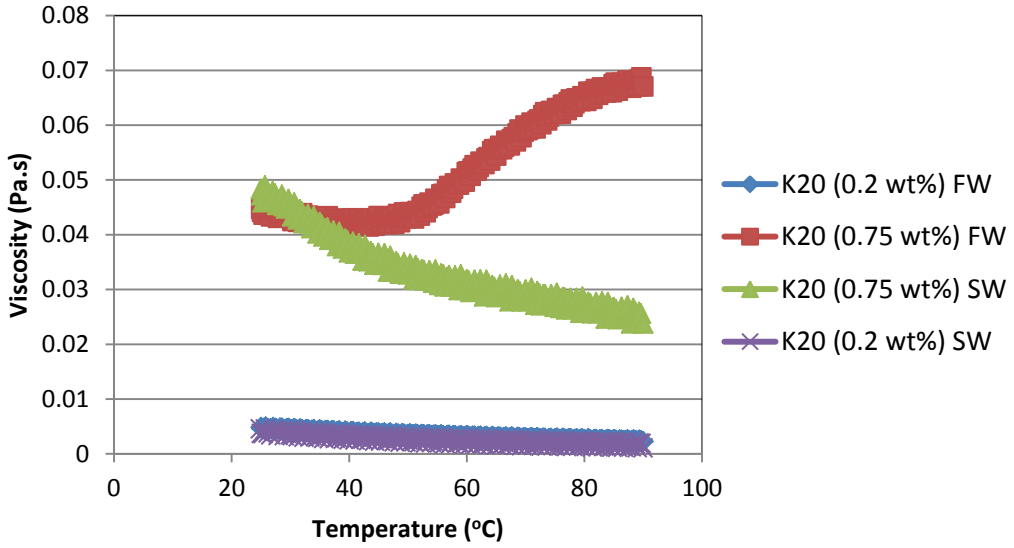

Figure 40 Flow temperature ramp comparison b/w K20 (0.2 wt%) and K20 (0.75 wt%)

4.3 Polymer Interaction with Clay

Attapulgite (ATP), 15A (a functionalized nano clay) and Calcium bentonite (Ca-bent) were tested to study their interaction with the polymer and to test them as an additive in an LCM system. Since both the polymers are anionic it was expected that the polymers would interact with the metals present inside the clay layers and make coordination bonds.

4.3.1 Alcomer130/ATP system

Sample preparation was carried out in two manners.

1. Attapulgite is a clay and a/c to API standards of WBM preparation, the clay content (bentonite, in the case of WBM) has to be mixed first in water followed by other components. Here the clay content to be used will not be of the same scale; in fact it would be quite less than that. However, mixing clay first followed by the polymer could be worth investigating.

2. While preparing a PAM solution, PAM has to be the first component that has to be added to the water while the water is being stirred; once a homogenous PAM solution is obtained only then can a cross-linker such as PEI be added to it. Otherwise problems occur in PAM dissolution. Since Alcomer130 is a copolymer of PAM, same rules would apply to it.

As attapulgite and PAM have not been used is this manner before, there were two possibilities:

1. Mixing ATP in water first then adding PAM to it.

2. Mixing PAM in water first then adding ATP to it once a homogenous solution is obtained.

Therefore two solutions for Alcomer130/ATP were prepared in the wt% ratio of 0.75:0.1.

The one in which ATP was added first is labeled ATP/A130 (0.1/0.75). The one in which Alcomer130 was added first is labeled A130/ATP (0.75/0.1).

A homogenous solution of ATP/A130 (0.1/0.75) was obtained after 1 day of stirring, Figure 41. For the A130/ATP (0.75/0.1) system, ATP formed aggregates and did not dispersed uniformly for 3 days. Figure 42 shows the ATP aggregates in the A130/ATP (0.75/0.1) system after 1 day of stirring. On the fourth day of stirring the aggregates in the A130/ATP (0.75/0.1) system subsided as shown in Figure 43.

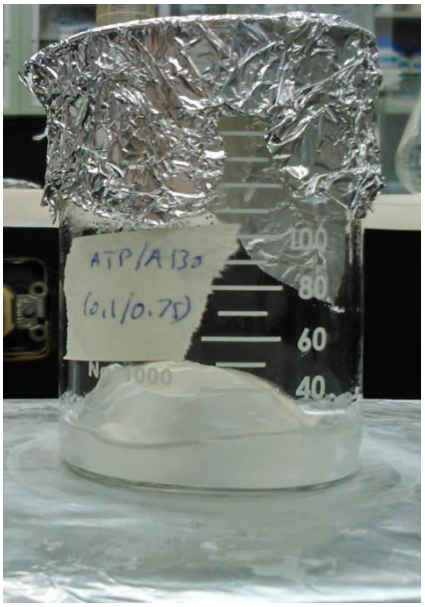

Figure 41 ATP/A130 (0.1/0.75) homogenous solution obtained after one day stirring

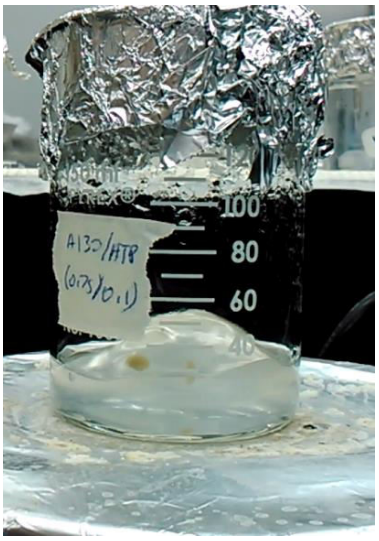

Figure 42 A130/ ATP (0.75/0.1) after one day of stirring. ATP aggregates are visible in the system.

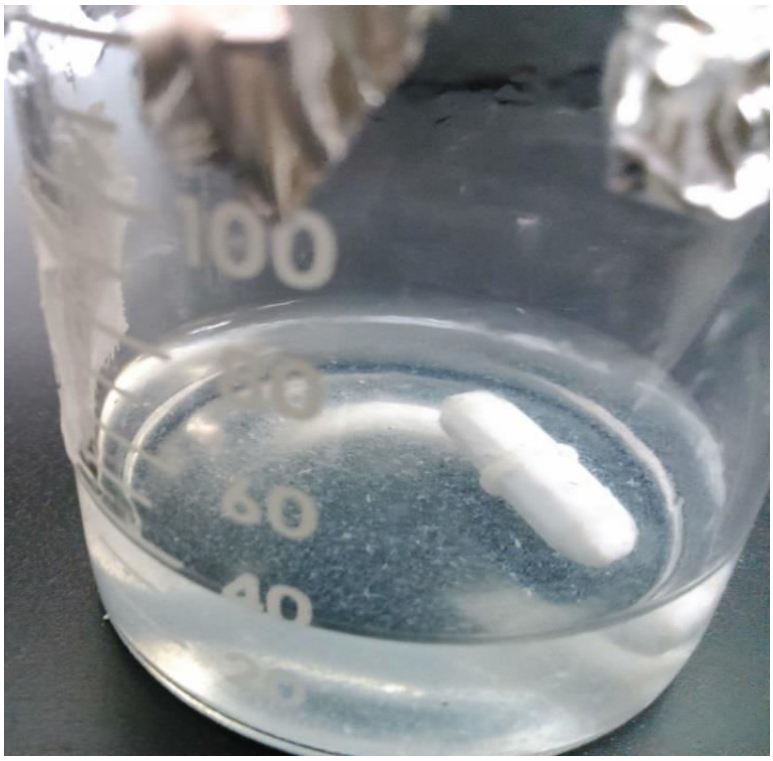

Figure 43 A130/ATP (0.75/0.1) system after 4 days of stirring

Figure 44 shows the flow sweep profile comparison of Alcomer130 (0.75 wt%), ATP/A130 (0.1/0.75) and A130/ATP (0.75/0.1) at 25^{o}C. ATP/A130 (0.1/0.75) gave a slightly higher viscosity profile than Alcomer130 (0.75 wt%) at low shear rates. While the viscosity profile A130/ATP (0.75/0.1) was the least than all the three.

Figure 45 shows the frequency sweep comparison of all the three systems. In the complex moduli comparison the G' of ATP/A130 (0.1/0.75) slightly surpassed that of Alcomer130 (0.75 wt%) but its G" trend is also higher than that of Alcomer130 (0.75 wt%). This improvement is not significant because the increase in energy loss capacity of ATP/A130 (0.1/0.75) is more than the increase in the energy storage capacity of ATP/A130 (0.1/0.75).

G" of the A130/ATP (0.75/0.1) system began to follow the same trend as the other two systems after 10 rad/s. Before this angular frequency the trend is different. G' trend of the A130/ATP (0.75/0.1) is the least of all three. At 0.1 rad/s it is about 2 times less than the G' values of the other two systems and 1 Pa less than the G" value of the ATP/A130 (0.1/0.75) system. At 100 rad/s it does manage to catch up to the G' trend of Alcomer130 (0.75 wt%). A130/ATP (0.75/0.1) offers poor complex moduli alteration than the other two systems. This indicates that a different mixing method, could result in a different material interaction and the systems would thus exhibit different properties.

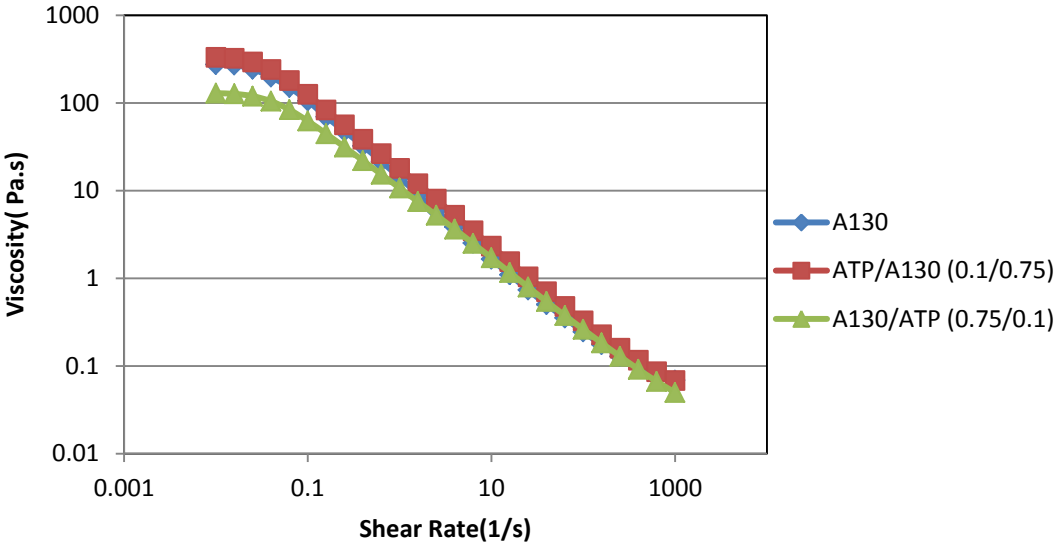

Figure 44 Flow sweep profile comparison

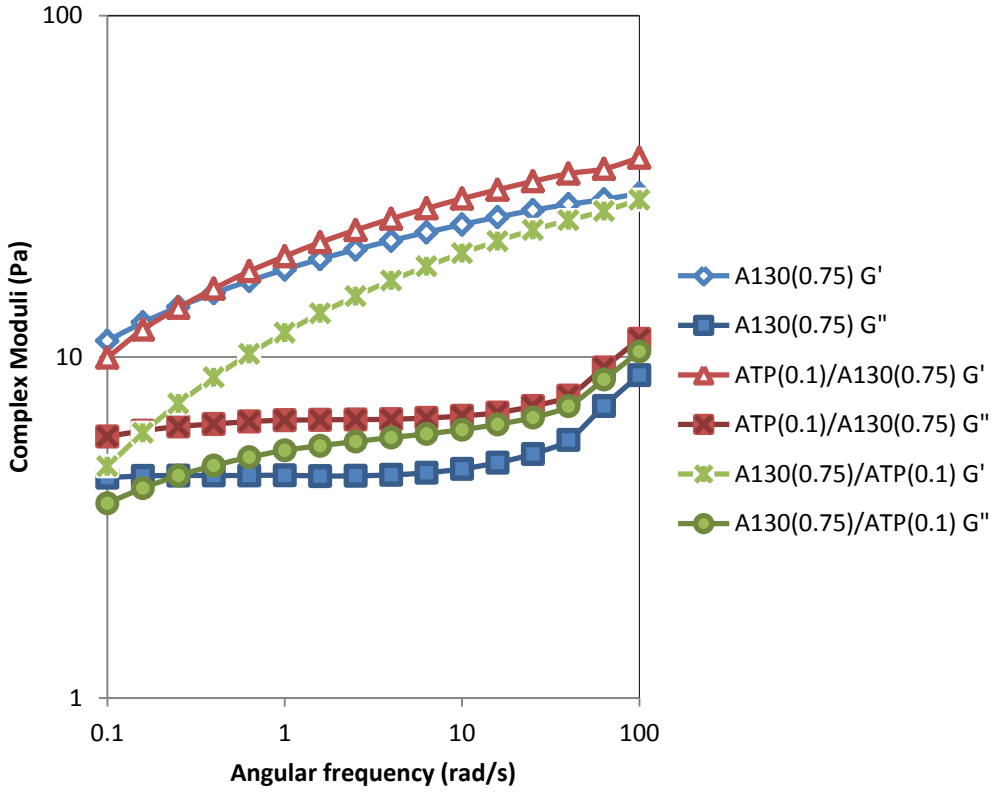

Figure 45 Frequency sweep profile comparison

Flow temperature ramp comparison indicated that the viscosity profile of the ATP/A130 (0.1/0.75) system is almost stable with the temperature ramp just like the profile of Alcomer130 (0.75 wt%). A130/ATP (0.75/0.1) system experienced a drop in its viscosity profile with rising temperature. As can be observed from the graph in Figure 46, the A130/ATP (0.75/0.1) system has the steepest slope of the viscosity curve.

Oscillation temperature ramp comparison shows that the storage modulus of all the three systems decreased with temperature while the loss modulus rose. A130/ATP (0.75/0.1) system was affected by temperature to a greater degree than the other two systems, Figure 47.

From these results it can be concluded that the ATP/A130 (0.1/0.75) system gave better rheology results as compared to the A130/ATP (0.75/0.1) system with a shorter mixing time.

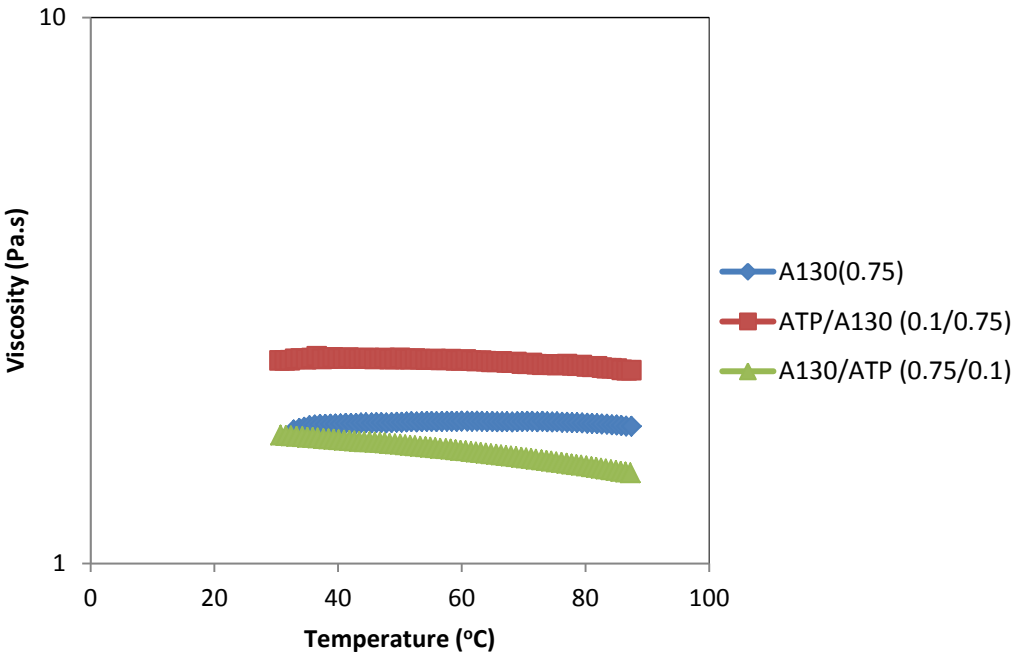

Figure 46 Flow temperature ramp comparison

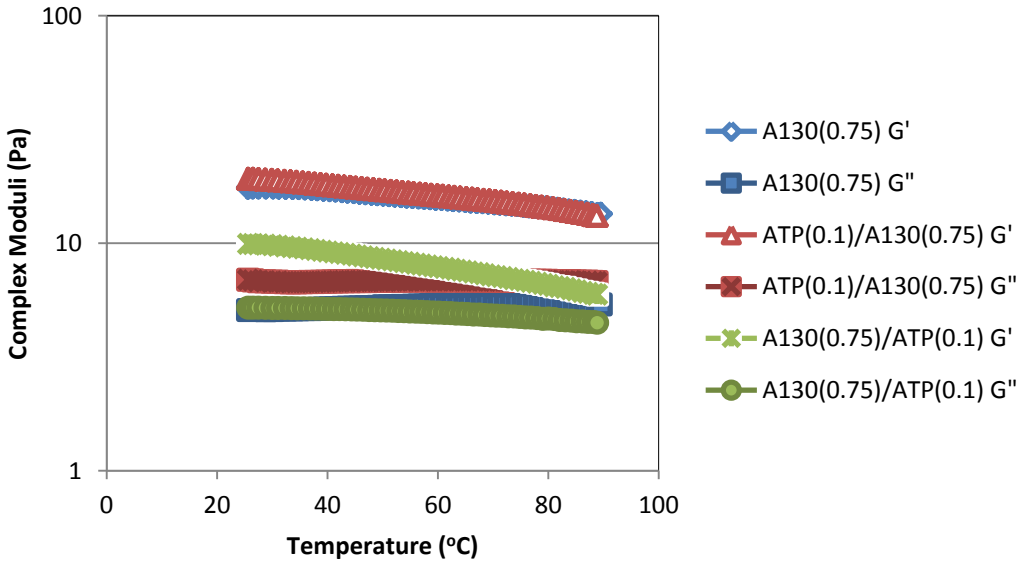

Figure 47 Oscillation temperature ramp profile comparison

4.3.1.1 ATP/Alcomer130 (0.3/0.75)

To further study the findings in the previous results, the effect of concentration was sought to be studied for the mixing pattern that gave the better rheology. In this new system the concentration of ATP was increased 3 times while that of Alcomer130 was kept the same.

Figure 48 shows the ATP/A130 (0.3/0.75) system after the sample had been stirred for 3 days, brown ATP aggregates were visible in the solution. Figure 49 presents the state of the system after it had been stirred for 5 days at 25^{o}C. After the fifth day the system was transferred to the rheometer for testing. A lot of ATP content was found to have been settled on the stir bar. This meant that the amount of ATP added to the Alcomer130 solution might have not in its entirety interacted with the polymer.

The viscosity profile against shear rate for the ATP/A130 (0.3/0.75) system did not show any improvement in comparison to the viscosity profile of Alcomer130 (0.75 wt%) at 25^{o}C, Figure 50.

Just like the ATP/A130 (0.1/0.75) system, this system had low G' value at 0.1 rad/s. The profile then rose with increasing frequency matching the G' profile of Alcomer130 (0.75 wt%) but never surpassed it like the ATP/A130 (0.1/0.75) system did.

Since all the ATP did not interact with Alcomer130 in the ATP/A130 (0.3/0.75) system. The system was stirred and heated for 5 days at 50^{o}C to study if temperature has a role to play in the ATP and Alcomer130 interaction.

As is evident from Figure 51 the G' curve of ATP/A130 (0.3/0.75) system at 50^{o}C surpassed the 25^{o}C curve after 19 rad/s angular frequency. After 25 rad/s it even

exceeded the G' of the base polymer. G" of this system was also higher than the rest. This showed that temperature slightly affected the properties of the ATP/A130 (0.3/0.75) system.

What was concluded from this study was that mixing sequence, concentration and temperature are the limiting factors between the ATP and Alcomer 130 interaction.

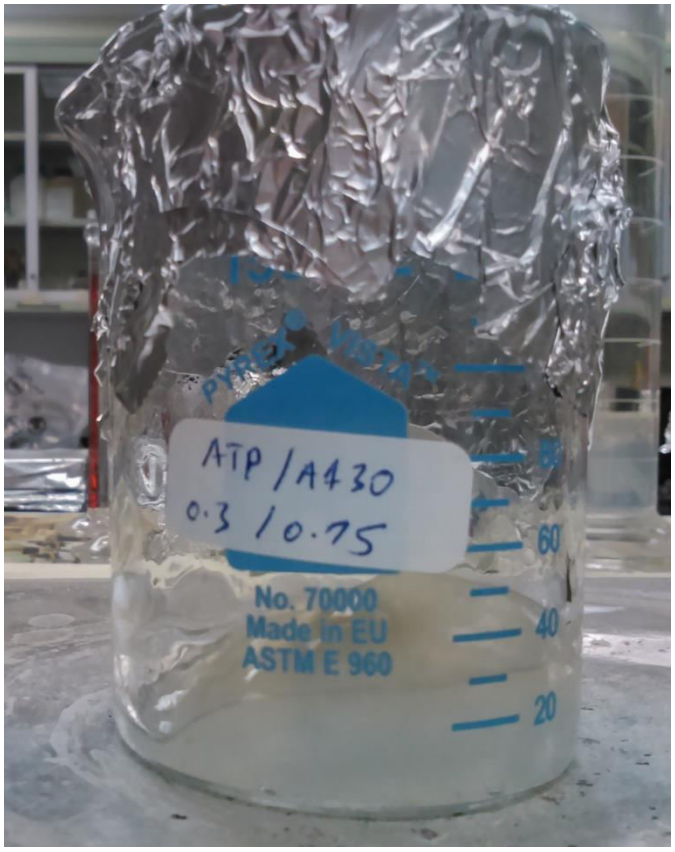

Figure 48 ATP/A130 (0.3/0.75) after 3 days

Figure 49 ATP/A130 (0.3/0.75) after 5 days (left) ATP deposits are visible on the stir bar (right)

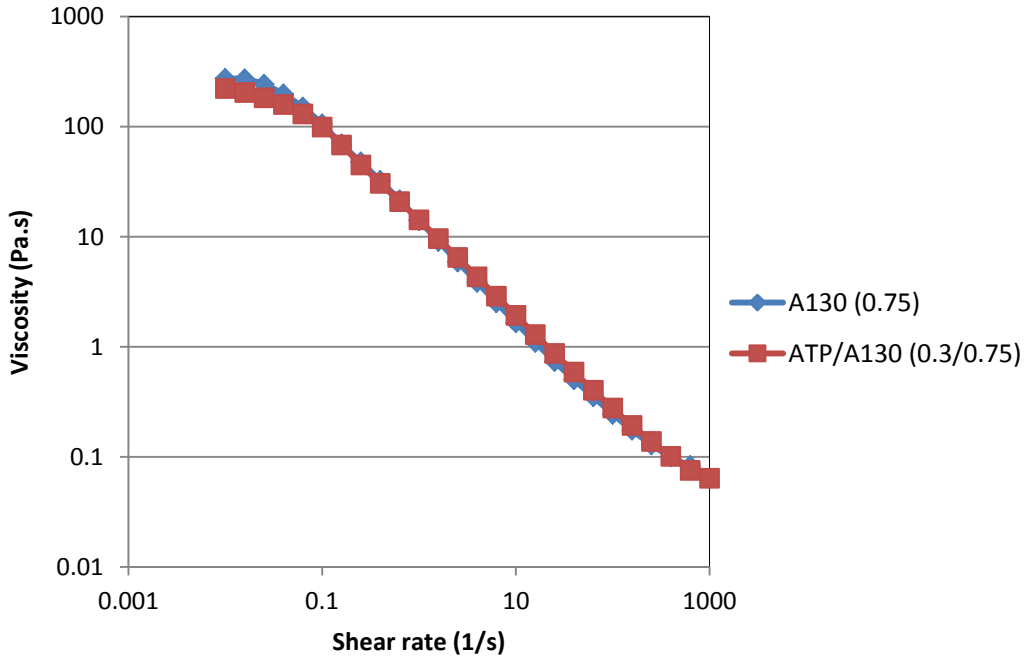

Figure 50 Flow sweep profile comparison

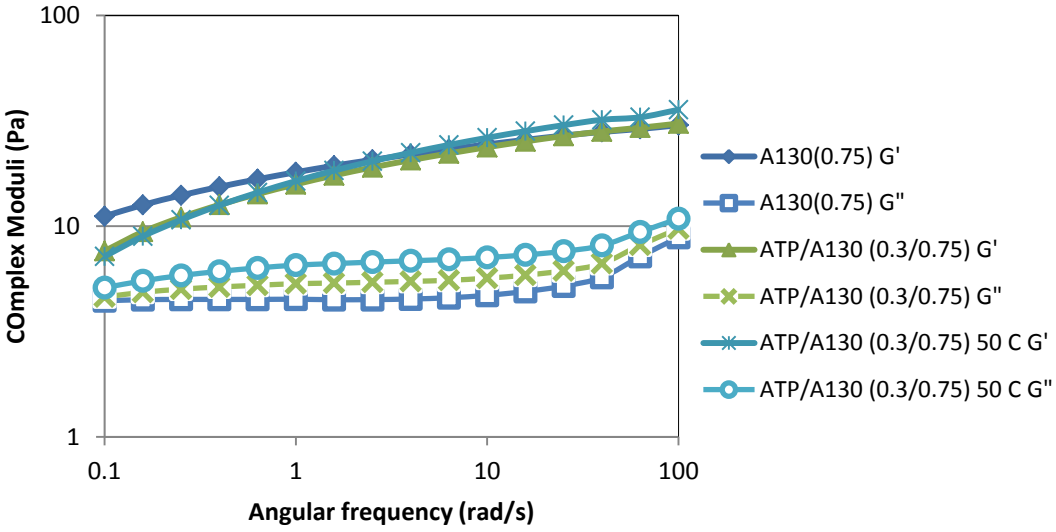

Figure 51 Frequency sweep profile comparison

4.3.2 Alcomer130/15A system

Alcomer130 was also tested with 15A, in the concentration ratio of 0.75:0.1 wt%. As 15A is a functionalized nano-clay it is added in the Alcomer130 as a potential cross-linker. After a homogenous solution of Alcomer130 was obtained, 15A was gradually added to the Alcomer130 solution while the solution was being stirred by a magnetic stirrer. The system was left in the stirring condition for 2 days at 25^{o}C. Figure 52 shows the system after preparation, the solution had visibly changed from transparent to milky.

To study whether temperature would have an effect on the interaction of 15A with Alcomer130 the sample was heated to 50^{o}C and tested at the same temperature. Figure 53 shows the complex moduli comparison of the A130/15A (0.75/0.1) at 25^{o}C and 50^{o}C along with the base polymer's moduli. The G' trend of this system over the entire frequency range is less than that of Alcomer130 (0.75 wt%) and the G" trend matches the G" trend of Alcomer130 (0.75 wt%). This specifies that the complex moduli have slightly waned due to 15A addition. Moduli trend of 50^{o}C overlaps the results of the same system at 25^{o}C. It can be inferred that the interaction of 15A with Alcomer130 offers no improvement in rheology even at moderate temperature.

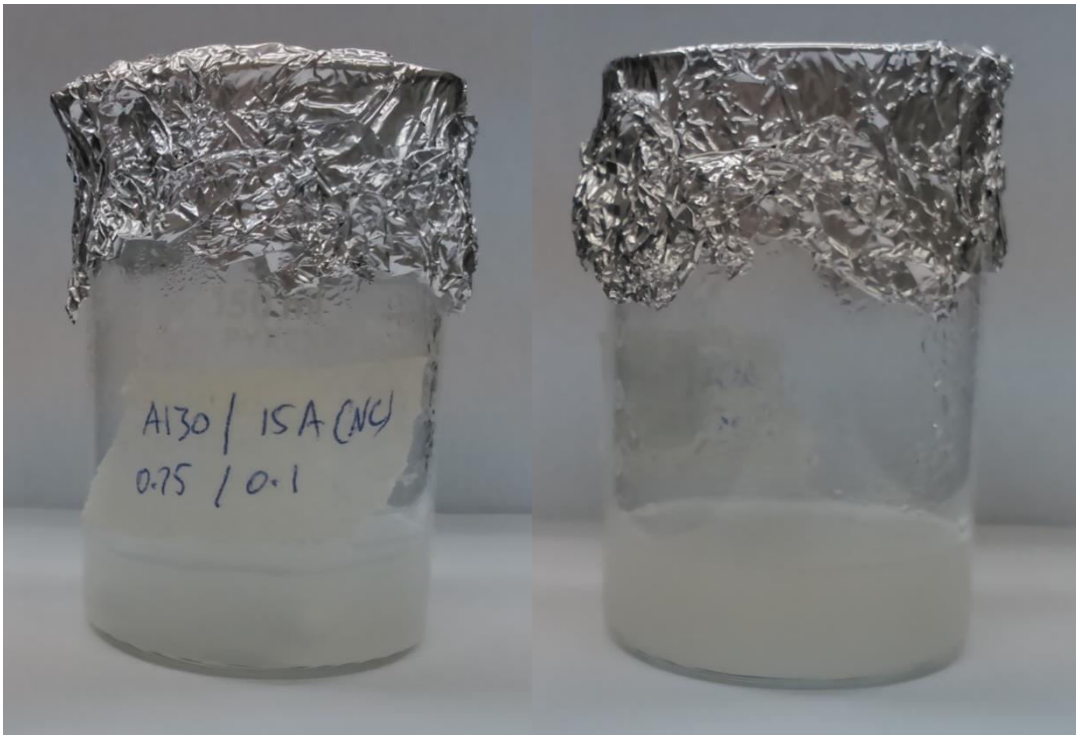

Figure 52 A130/15A (0.75/0.1) system after 2 days

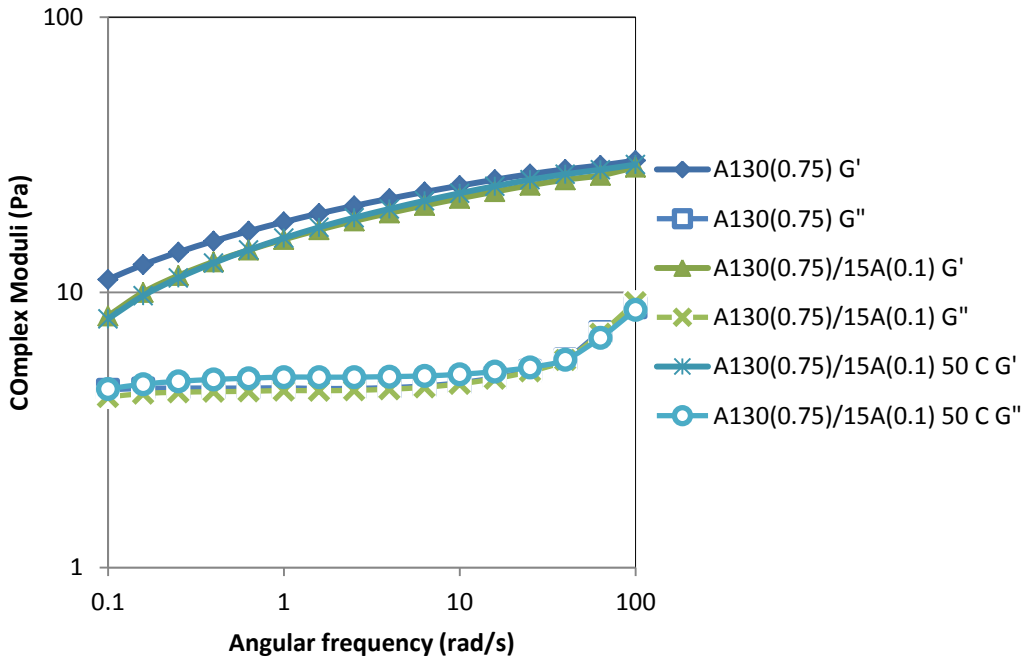

Figure 53 Frequency sweep profile comparison of A130/15A

4.3.3 Interaction with Calcium bentonite

To further study the interaction of clay with the polymers a locally produced clay Calcium-bentonite (Ca-bent) was added to Alcomer130. Using the same mixing sequence as that of ATP the wt% used was Ca-bent/HPAM (0.1/0.75). First Ca-bent was added into distilled water and stirred for about two days. A130 was then added to the system and the system was stirred for another two days, before studying its rheological properties. Figure 54 shows the system after preparation. Rheology results of this system when compared with the base polymer showed that interaction had taken place between this local bentonite and the PAM copolymer.

Flow sweep comparison in Figure 55 shows that the system gave low viscosity values than the base polymer at low shear rates. From the complex moduli comparison in Figure 56 it can be observed that Ca-bentonite had adversely affected the complex moduli of the system. The clay containing system experienced a G' and G" intersection at 0.1 rad/s which is non-existent in the case of the base polymer. Furthermore at 0.1 rad/s both the values are less than the value of G" of the base polymer. For the higher frequency range its energy storage capacity got decreased and the energy dissipation ability increased, which is not an improvement but a converse of that.

The temperature ramp results comparison, Figure 57, showed that the presence of Ca-bentonite shifted the apparent uniform viscosity profile of Alcomer130 to that of a thermo-thinning profile at the shear rate of 10 1/s.

In short, Ca-bentonite as a component to the Alcomer130/clay system did not prove to be a rheology enhancing additive.

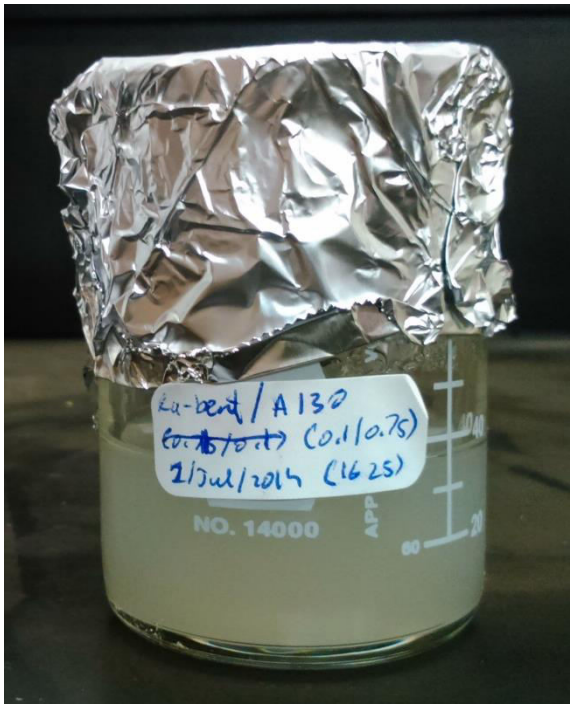

Figure 54 Ca-bent/A130 (0.1/0.75) system

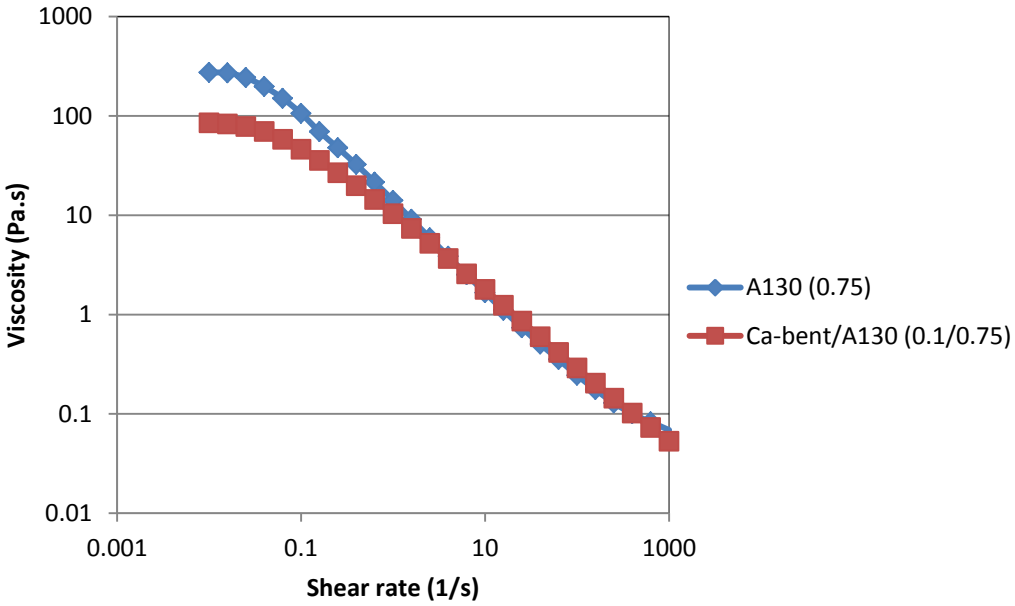

Figure 55 Flow sweep profile of Ca-bent/A130 (0.1/0.75) vs Alcomer130 (0.75)

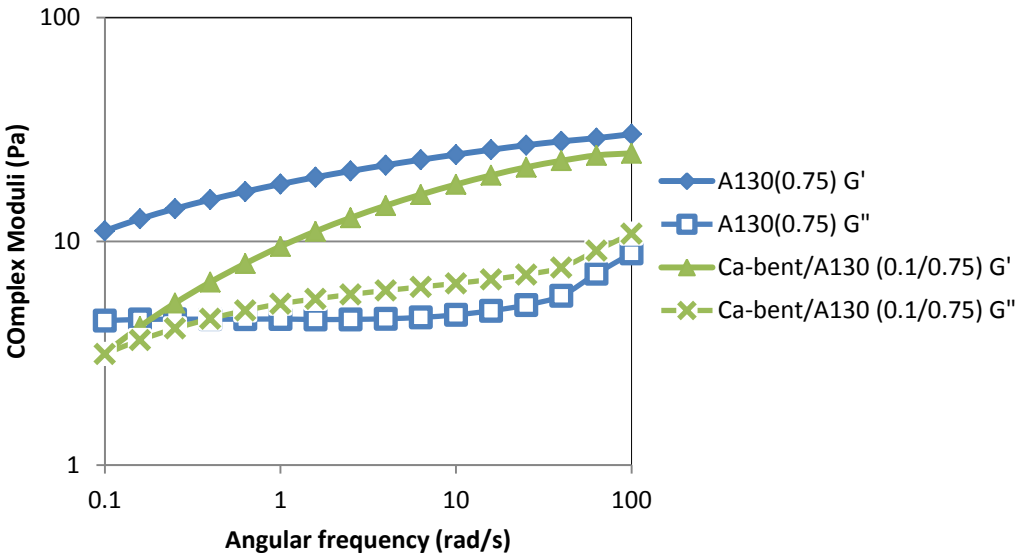

Figure 56 Frequency sweep profile of Ca-bent/A130 (0.1/0.75) vs Alcomer130 (0.75)

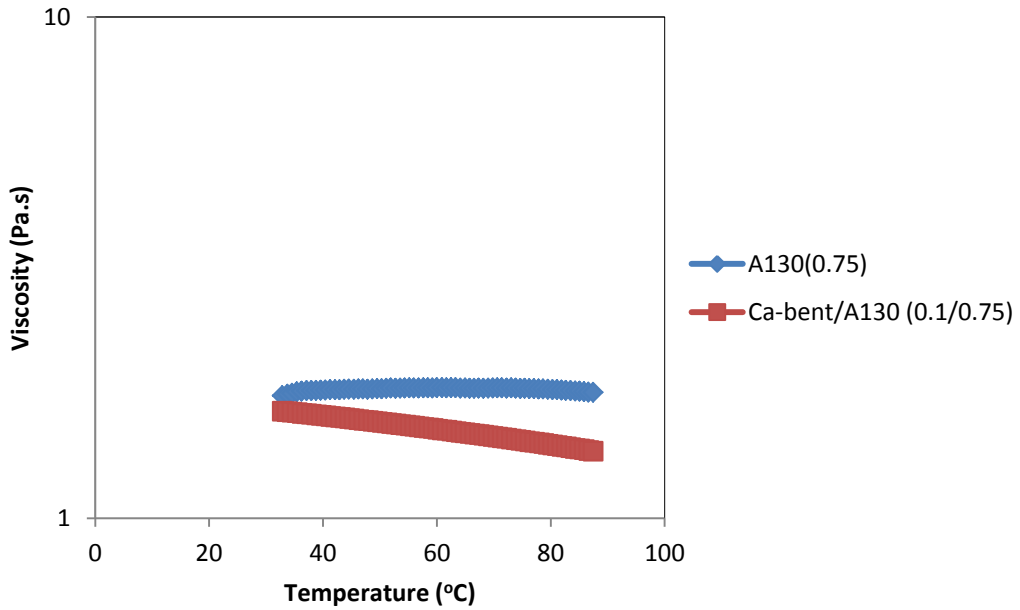

Figure 57 Flow Temperature Ramp profile of Ca-bent/A130 (0.1/0.75) vs Alcomer130 (0.75).

Clays were mixed with HPAM in the similar manner as that with Alcomer130 but no interaction between them was observed. Figure 58 shows the images of the Ca-bent/HPAM (0.1/0.75) system before and after the addition of HPAM to it. After the sample was removed from the beaker for testing clay deposits were observed on the stir bar.

Figure 59 presents the frequency sweep comparison of Ca-bent/HPAM (0.1/0.75) with HPAM (0.75 wt%). The modulus curves of the clay containing system exactly overlays on the complex moduli curves of HPAM; same was the case with ATP. Since HPAM did not interact with the clays, this meant that the anionic ends of the HPAM and the metallic ends of the clays were not able to form coordination bonds. As the clays have complex layered structures it would not have been possible for the ends to come in contact. Interactions with Alcomer130 suggested that under certain conditions clays do affect the properties of the polymer. The most probable reason would be that some elements in the clay interact with the different type of monomer present in the Alcomer130 copolymer.

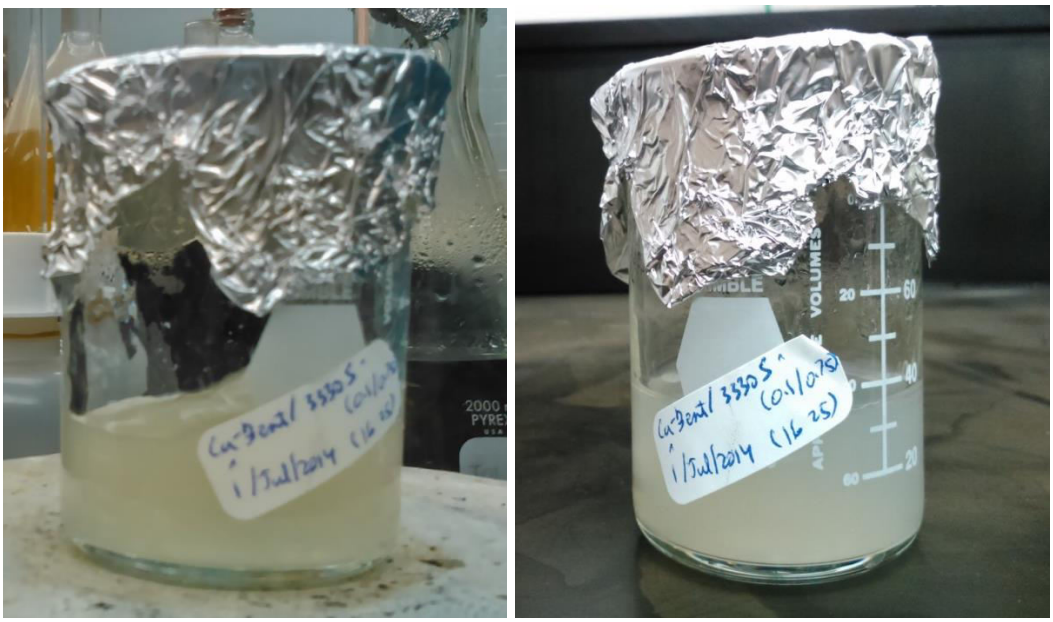

Figure 58 Ca-bent/HPAM (0.1/0.75) before (left) and after (right) HPAM addition

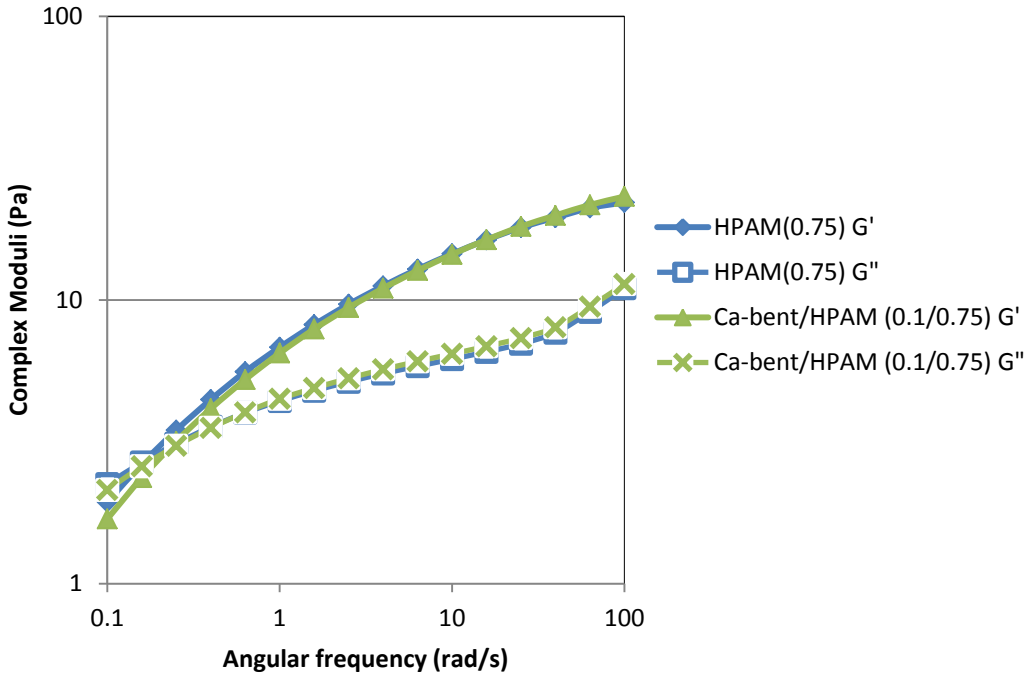

Figure 59 Frequency sweep profile of Ca-bent/HPAM (0.1/0.75) vs HPAM (0.75 wt%)

CHAPTER 5

DIFFERENTIAL SCANNING CALORIMETRY

Differential scanning calorimetry (DSC) is a thermo-analytical technique. DSC has mostly been used to study crystallization kinetics. In principle the physics behind crystallization and gelation is the same. In crystallization heat is released due to the formation of solid crystals while in gelation it is because of the crosslinking reactions that lead towards the formation of 3D gels. Most recently DSC has been used to study the gelation kinetics of a gelling solution of PAM and PEI in distilled water for water shutoff application over the temperature range of 80 – 120^{o}C (El-Karsani et al., 2014). By relating fractional gelation with time the gelation kinetics was modeled and the gelation process was modeled using the Avrami model. The effect of presence of salts was also studied in that research paper and it was found that the salt presence reduced the rate constant by 60-80% but do not affect the gelation reaction order.

DSC experiments were performed on the HPAM/PEI and A130/PEI samples to study the effect of crosslinker concentration on the fractional gelation of the systems. The data was also fit on the Avrami model to obtain the reaction rate constant and order of reaction of the gelling solutions. The Avrami equation used for studying the gelation kinetics is given (El-Karsani et al., 2014):

$$ln[-ln(1 - x_t)] = \ln k_t + m\, lnt$$

x_t = fractional gelation, $\left[x_t = \frac{Total\ heat\ released\ upto\ time\ t}{Total\ heat\ released\ for\ the\ non-isothermal+isothermal\ regime}\right]$

m = exponent related to the order,

t = time during gelation,

k_t = rate constant.

Plotting a straight line plot of $\ln[-\ln(1-x_t)]$ vs lnt can be used to obtain the slope m and the intercept k_t.

5.1 Experiment Procedure

The DSC experiments were performed in the TA Q1000 instrument manufactured by TA Instruments; running integral analysis of the data was performed on the accompanying Universal Analysis software. The instrument is connected to a refrigerating cooling system and a N_2 cylinder. The purge gas is kept at a flowrate of 50 cm^3/min.

The gelant to be tested is stirred for 20 minutes in order to ensure proper mixing. Then an amount less than 1 ml is carefully placed inside an aluminum hermetic pan using a syringe. The pan is then sealed with a lid using a compression tool. An empty pan is used as a reference pan. The mass of the pan containing the sample is measured before and after the experiment to ensure that there is no loss of mass during the experiment. If there is a significant difference between the sample pan mass before and after the experiment, then it implies that the sealing was not proper and the experiment needs to be repeated.

According to the testing scheme the sample was kept at equilibration at 30^{o}C for 5 minutes. Then the sample was ramped at a rate of 1.5^{o}C/min till 100^{o}C. At 100^{o}C it was left at isothermal condition for 5 hours.

5.2 Results

Figure 60 shows the fractional gelation vs time comparison for the HPAM/PEI samples. A clear pattern is observed in these gelling solutions. In the non-isothermal region of the curve the fractional gelation increases with increasing crosslinker concentration. After 30 minutes, 10% of the solution for all the samples had been converted to gel. 100% solution to gel formation was obtained after about 3 hours and 20 minutes for all the three samples. This is the instance where all of the PEI immine groups have attacked and crosslinked with the available crosslinking sites on HPAM.

Figure 61 shows the Avrami model plot for all the HPAM/PEI samples. All the three curves overlap each other; this indicates that the reaction order is the same for this system irrespective of the tested crosslinker concentration. The reaction order for all the HPAM/PEI samples was 2. Table 5 summarizes the reaction rate constant and reaction order for each HPAM/PEI sample.

Figure 62 shows the fractional gelation comparison of the A130/PEI samples. In the non-isothermal section the fractional gelation variation follows no pattern with respect to the crosslinker concentration. At 10 minutes of gelation time both A130/PEI (2/0.6) and A130/PEI (2/1) experienced less than 0.5% gelation while A130/PEI (2/1.2) underwent 1% gelation. At 30 minutes gelation time all the A130/PEI variants had experienced 10% gelation. Just like the HPAM/PEI gelants, A130/PEI underwent 100% gelation at about 3.4 hours. The Avrami plot, as shown in Figure 63, shows that for the 0.6 and 1wt% PEI, the reaction order for the A130/PEI samples are the same. For the A130/PEI (3/1.2) however the reaction order is different. Table 6 summarizes the reaction rate constant

and reaction order for each A130/PEI sample. This is because of the structural difference of A130 from HPAM.

From the results it can be concluded that the gelation kinetics information obtained from the DSC tests can be used for designing the injection process. Tests could be designed in accordance to the subsurface temperature and salinity conditions to simulate the injection process and study how the gelant would behave under those conditions. Based on the results the gelant composition could be modified e.g. If reaching the target depth takes more time than the 100% fractional gelation time of the gels, then a suitable retarder could be added to delay the reaction time.

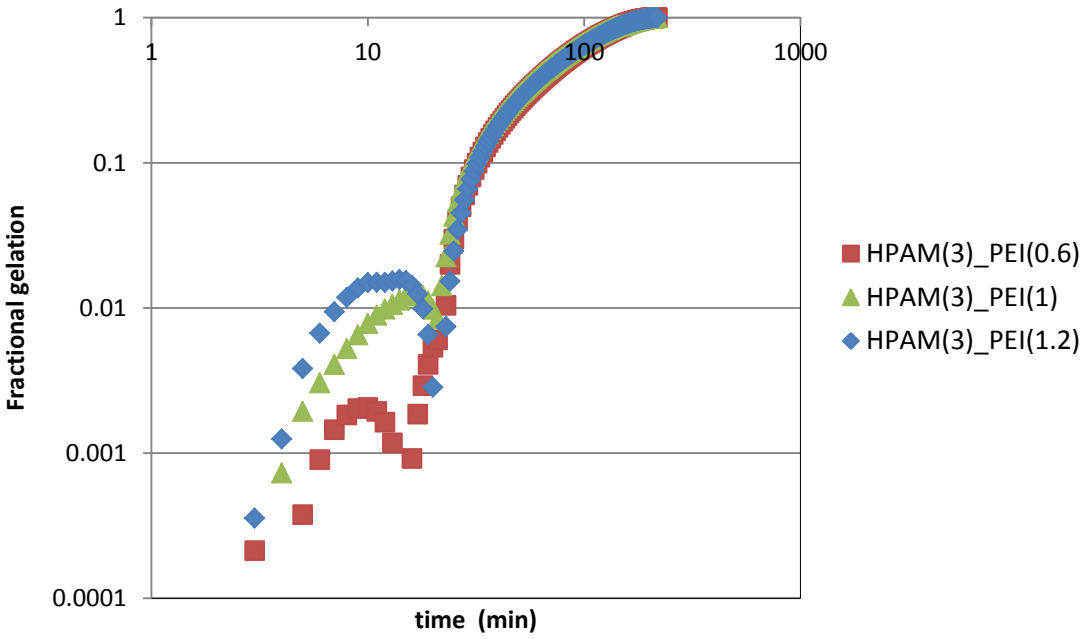

Figure 60 Fractional gelation profiles for HPAM/PEI

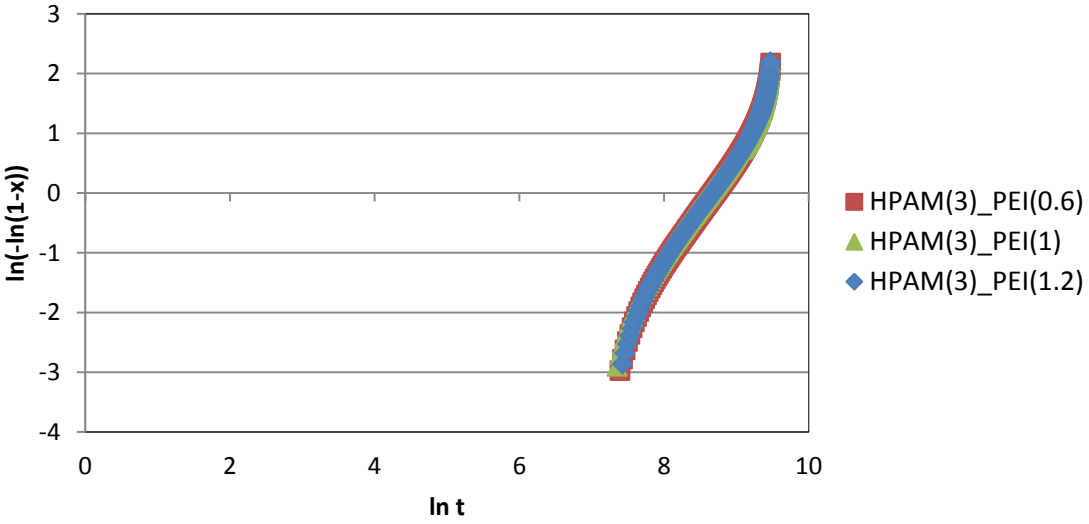

Figure 61 Avrami plot HPAM/PEI

Table 5 Avrami parameters for HPAM/PEI

HPAM/PEI	Reaction rate constant (min^{-1})	Reaction order
3/0.6	3.16034E-08	2
3/1	3.1953E-08	2
3/1.2	3.93803E-08	2

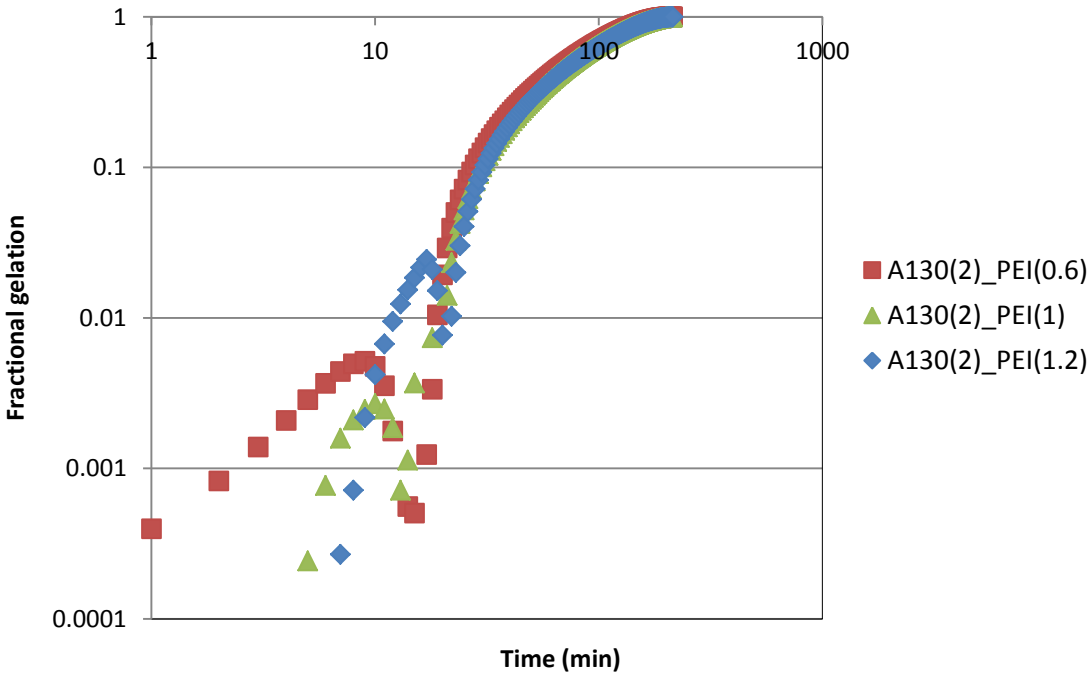

Figure 62 Fractional gelation profiles for A130/PEI

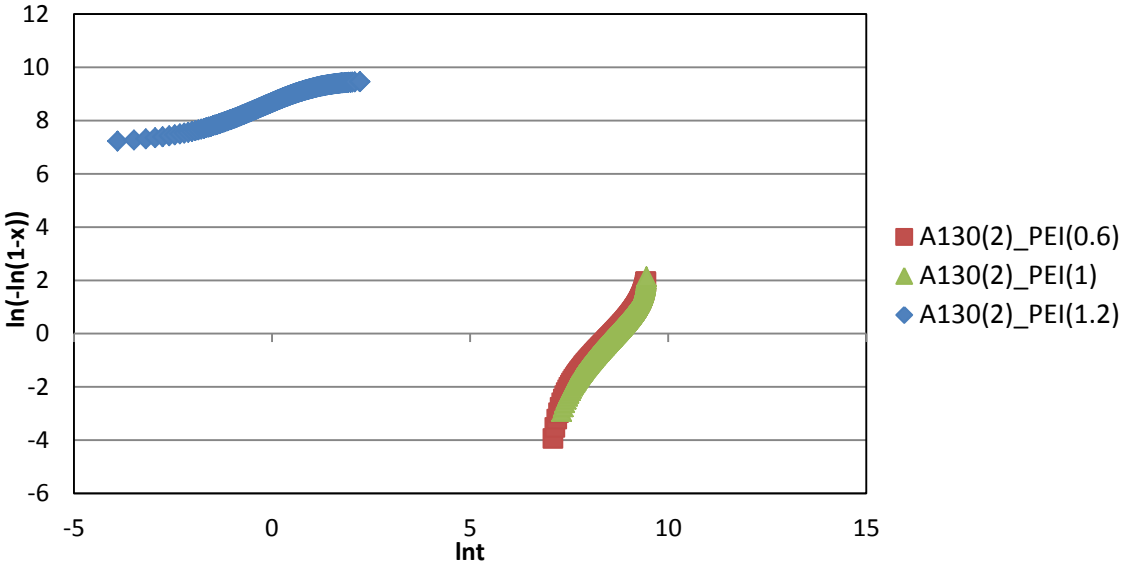

Figure 63 Avrami plot A130/PEI

Table 6 Avrami parameters for A130/PEI

A130/PEI	Reaction rate constant (min^{-1})	Reaction order
3/0.6	8.33681E-08	1.891
3/1	5.47768E-08	1.930
3/1.2	5750.258	0.485

CHAPTER 6

SEE THROUGH SETUP

Performance of polymer solutions and Polymer/crosslinker systems has been tested in the laboratory scale by subjecting them to flow in a porous media and studying their properties. A flow setup comprising of a synthetic core, core-holder and constant flow pump was used in a study conducted by Jia et al. (2012) to investigate the effect of shear on gelation. Reddy et al. (2003) in their work had tested a cross-linker system for water shut off application on Brea sandstone core. This was a high pressure and high temperature flow setup consisting of a Hassler sleeve apparatus and multiple flow taps in the flow cell for recording pressure readings at each segment.

For this study a see through flow setup had been set up. The purpose of which is to visually observe the effectiveness of an LCM system. The flow setup comprises of a see through synthetic core, transfer cells, pressure gauges and a pressure source. The test involves the injection of the LCM into the porous media followed by the drilling mud. Figure 64 and Figure 65 illustrates the schematic diagram and picture of the see through setup respectively. There are separate transfer cells for Mud and LCM. Pressure gauges are connected to the upstream and downstream ends of the see through core for recording the pressure difference across the core. Since the synthetic core is transparent the visual movement and the depth of penetration of the fluid entering the core can be recorded as a function of pressure. The pressure readings and the transition of the LCM and Mud across the see through setup will determine the quality of the LCM.

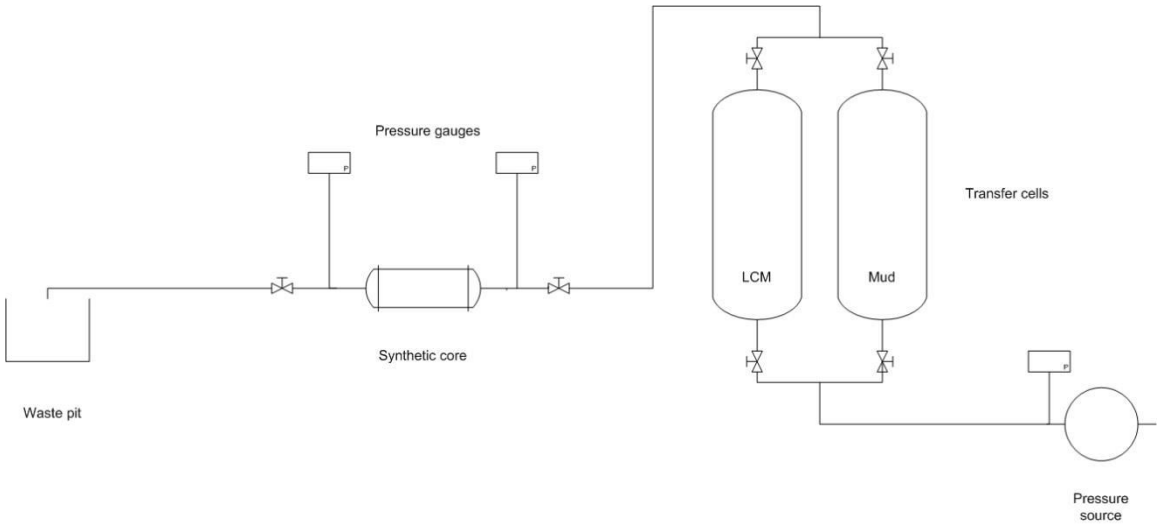

Figure 64 Schematic Diagram of the see through setup

Figure 65 See through setup

6.1 Core Characterization

Before the see through setup could be used for LCM system studies, core preparation and characterization was essential. The outer body of the core is basically a plexi glass tube. This transparent cylindrical container is then filled and packed with glass beads to make a porous media, once the core is prepared it can then be used to imitate a thief zone. Figure 66 illustrates the pre-test see through core. Depending on the glass bead size and its mixing sequence the core characteristics would change. Three different glass beads sequence were used to obtain three different core types. Figure 67 shows the available glass beads.

Core characterization involves first of all saturating the core with a fluid of known viscosity. This is then followed by porosity and permeability determination.

6.1.1 Porosity Determination

For porosity determination the core was saturated with a commercially available engine oil (viscosity =147 cp). Its density and viscosity was determined using a pycnometer and Ostwald viscometer respectively.

The porosity determination setup is composed of the synthetic core, fluid source and a vacuum pump. The Schematic diagram and the picture of the setup itself can be seen in Figure 68 and Figure 69. The vacuum pump is used to create a vacuum inside the core while the inlet valve between the core and the fluid source is kept closed. It is left in this condition for a sufficient amount of time in order to ensure proper vacuum. Once the vacuum condition is achieved, the vacuum valve is closed and the inlet valve is opened.

In this manner the saturating fluid, due to pressure difference, would move into the core and effectively saturate it. Saturation was carried out this way to prevent the presence of air bubbles. Presence of air bubbles not only affects the porosity readings but they create a nuisance when it comes to permeability determination because they cause fluctuations in the transducer readings.

For porosity calculations the dimensions of the empty glass tube were measured to calculate the bulk volume (V_b) of the core. The dimensions of the synthetic core are as follows:

Core Length: 20.45 cm

Core cross sectional area: 4.85 cm^2

Bulk volume: 4.85 x 20.45 = 99.1827 cm^3

For the pore volume (V_p) calculation the packed core was weighed before and after saturation. V_p was calculate by using the equation below.

$$V_p = \frac{m_1 - m_2}{\rho}$$

m_1 = mass of synthetic core + glass beads + saturated fluid, g

m_2 = mass of synthetic core + glass beads, g

ρ = density of the fluid, g/cm^3

After the bulk and pore volumes were determined, porosity was calculated. Porosity is the ratio of the pore and bulk volume or in other words it is the percentage of the pore volume that contains fluid. Mathematically it is represented as,

$$\emptyset = \frac{V_p}{V_b}$$

$\emptyset =$ porosity of the media

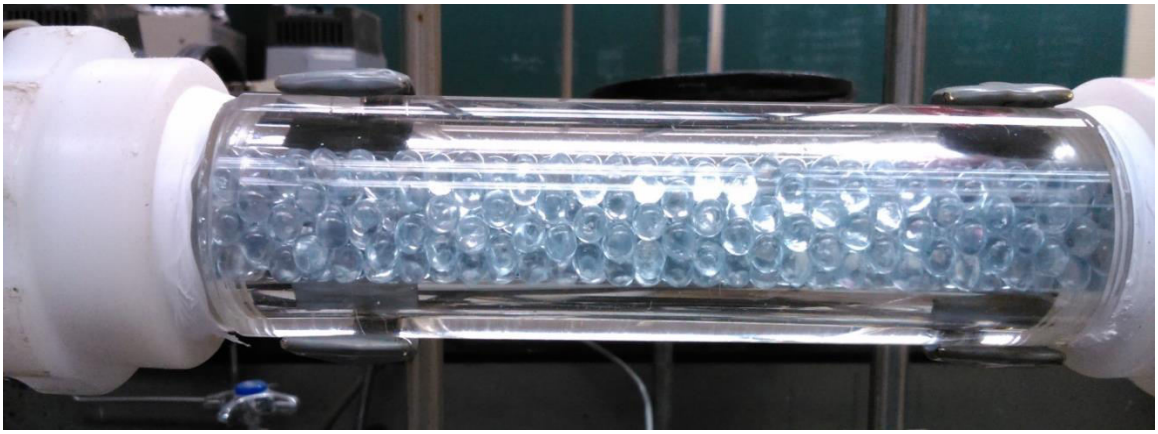

Figure 66 the synthetic see through core

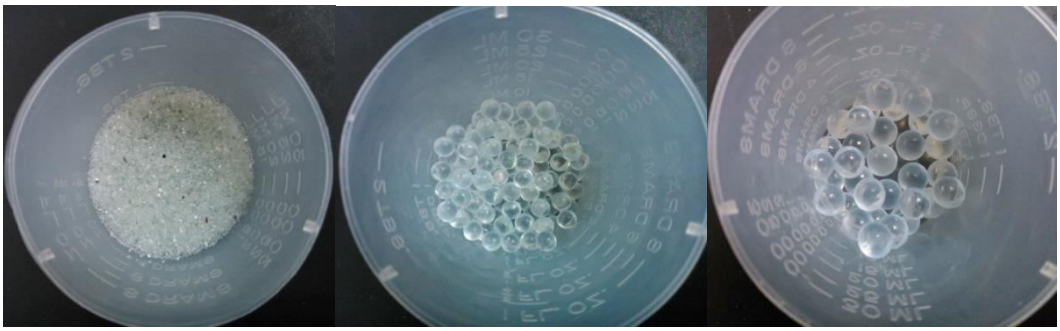

Figure 67 Different glass beads sizes (sizes from left to right: 0.5 mm, 3 mm and 6 mm)

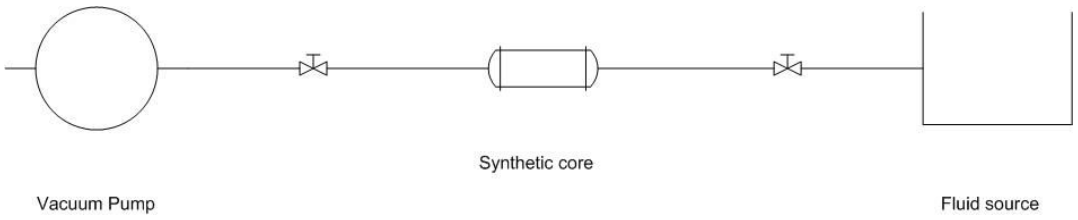

Figure 68 Schematic diagram of the porosity determination setup

Figure 69 Porosity determination setup

6.1.2 Permeability Determination

Once the porosity of a particular sequence has been determined the saturated core was connected to the permeability determination setup for permeability calculation. The saturated synthetic core was connected to a displacement cell containing the saturated fluid. A positive displacement pump was used to pump the fluid inside the core. Across the synthetic core a transducer was connected to record the pressure difference across the core. Schematic illustration of the setup and the setup itself can be seen in Figure 70 and Figure 71 respectively.

Initially distilled water (viscosity=1 cp) was used to saturate the core. Since the media is very permeable the pressure drop encountered were so low that the transducer was not able to record it and give a stable reading. Water was replaced with engine oil (viscosity=147 cp) as the saturating fluid and a back pressure valve was added to the setup to counter this problem. Flowrates were recorded at the outlet once a stable transducer reading was obtained.

An important precursor of this experiment is the calibration of the transducer. It has to be calibrated in order to associate the pressure value to the subsequent transducer reading.

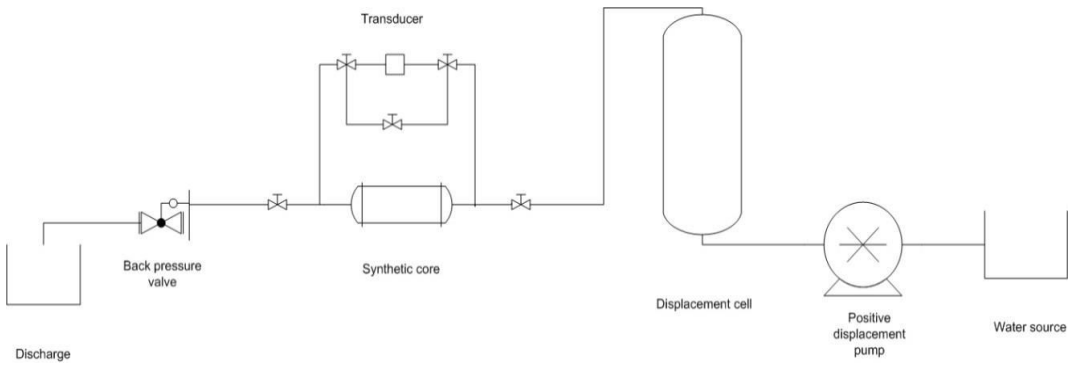

Figure 70 Schematic diagram of the permeability determination setup

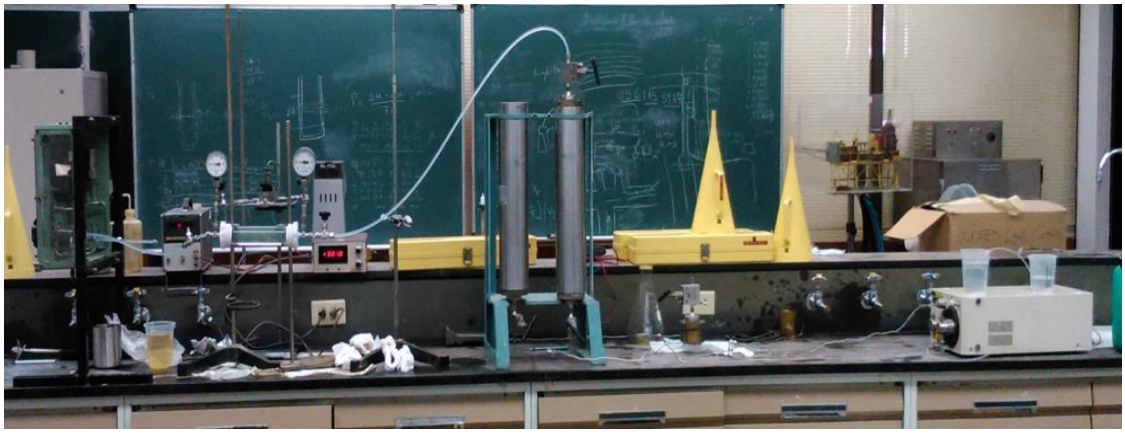

Figure 71 Permeability determination setup

6.1.2.1 Transducer Calibration

A 2 psi transducer was connected to a mercury barometer. Pressure was varied and the corresponding transducer readings were recorded. The straight line equation involving these two data sets was used to translate the transducer readings into pressure readings. Figure 72 shows the transducer calibration chart.

After the permeability determination experiment has been conducted, the permeability value of the core can be calculated using the Darcy law.

6.1.2.2 Darcy's Law

Darcy's law at constant elevation is a simple proportional relationship between the instantaneous discharge rate through a porous medium, the viscosity of the fluid and the pressure drop over a given distance.

Figure 73 shows the schematic representation of the Darcy Law. Mathematically it is defined as;

$$q = \frac{kA\Delta P}{\mu L}$$

where,

q = flow rate, ml/s

A = cross-sectional area of the core, cm_2

L = Length of the core, cm

ΔP = pressure difference b/w the upstream and the downstream end of the media, atm

k = permeability, D

6.2 Core Properties

Different beads sequence and characterization resulted in three different core types. The properties of which are listed in Table 7. The least permeable core had about 306 D permeability value with about 36% porosity and the most permeable had the permeability value of 2965 D and 44% porosity. This would be helpful in observing the performance of different LCM systems under different permeability and porosity conditions. For ease of reference the three core types have been given reference codes.

Table 7 Core properties

Core type code	Permeability (D)	Porosity (%)	Sequence (mm dia.)
k1	306	36	0.5
k2	432	38	0.5 (25g), 3 (5g)
k3	2965	44	6

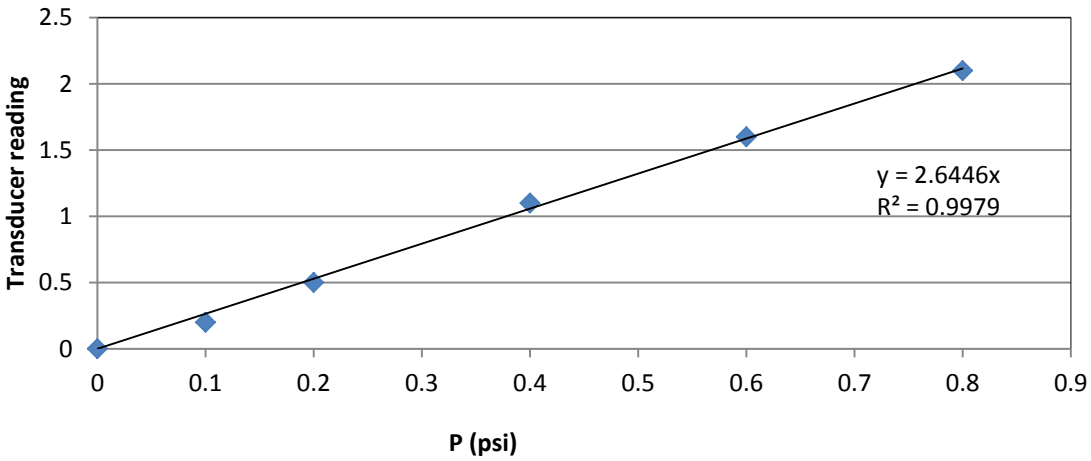

Figure 72 Transducer calibration

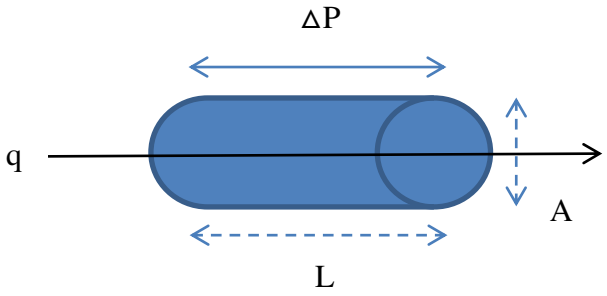

Figure 73 Representation of Darcy law

6.3 Experiment Procedure

The flow experiment is conducted in the following manner. Fluid is injected inside the synthetic core at fixed pressure intervals (10 psi) and its penetration is recorded. The LCM system is injected first inside the synthetic core at a particular pressure and its movement is recorded inside the core. If there is no observed increment in the depth of penetration for a period of 30 minutes then the pump pressure is raised to a higher value. Once the LCM system completely saturates and breakthroughs the core at a certain pressure or the maximum pump pressure is reached, this phase of the experiment is stopped. Mud is then injected inside the LCM saturated synthetic core and the same procedure is followed. The experiment ends when either the mud breakthroughs the system or when the system prevents mud loss until the maximum pump pressure is reached.

6.4 Commercial LCM

Three commercial grade LCMs products of DrilChem were used to study their performance in a porous media. The idea was to set the commercial LCMs as benchmark for the polymer based LCMs. In the absence of these products' field formulation, different compositions of the Mud/LCM system were tested. The products bear the commercial names as DrilEzy, SoluSeal and Stoploss. These commercial LCMs are a blend of different organic and inorganic materials, the main component being cellulose. DrilEzy is in the form of fine blended powder, SoluSeal is a mixture of flakes and fibers

while Stoploss is a mixture of fibers, granules and small pieces of wood; as can be seen in Figure 74.

Four different compositions were prepared for all the three Mud/LCM systems. In an 8.6 ppg Sodium-bentonite mud one LCM product would be in 1, 3, 5 and 8wt%s, thus making four Mud/LCM systems for each product. Rheology of all these compositions was performed on the 5550 HPHT viscometer manufactured by Chandler and the accompanying software titled Rheo. The Mud/LCM systems were tested over a temperature range of 90-170^{o}F (32-77^{o}C) to study and compare their profile and select the composition with the best rheology for flow experiments.

All three basic rheology tests for non-Newtonian fluids were conducted on the Mud/LCM systems. The tests performed were plastic viscosity (PV) measurement, yield point (YP) measurement and 10s/10min gel strength. PV is a parameter of the Bingham plastic model. It is the slope of the shear stress/shear rate line above the yield point. PV represents the viscosity of a mud when extrapolated to infinite shear rate on the basis of the mathematics of the Bingham model. YP is another parameter of the Bingham plastic model. It is the yield stress extrapolated to a shear rate of zero. For a drilling fluid YP is used to evaluate its ability to lift cuttings out of the annulus. Gel strength is the shear stress measured at low shear rate (3rpm) after a mud has set quiescently for a period of time (10 seconds and 10 minutes) in the standard API procedure. For a drilling fluid the gel strength is one of the important properties because it demonstrates the ability of the drilling mud to suspend drill solid and weighting material when circulation is ceased.

To calculate the plastic viscosity and yield point a testing schedule is made in the Rheo software as per the API standards for testing a drilling fluid; the viscometer then automatically performs the test and fits the data using Bingham Plastic model and generates the plastic viscosity and yield point of the fluid. Unlike the FANN viscometer, in the Chandler 5550 viscometer there is no direct way of measuring the 10 s and 10 min gel values. In order to do this one has to make a schedule and read the maximum shear stress reading after 10 second and 10 minutes of stoppage at low rpm.

On the basis of rheology tests, one composition from each Mud/LCM system was selected for testing in the see through flow setup; this was the composition that demonstrated the best rheology profile.

Figure 75 and Figure 76 represent the PV and YP profiles of the Mud/DrilEzy system. It is clear from the graphs that 3wt% profile gives the highest values over the temperature range followed closely by 1wt%. 3wt% was selected from this composition.

For the case of SoluSeal 8wt% gave the highest PV trend followed by 1wt%, as apparent from Figure 76. Figure 77 shows the YP comparison where the highest trend is generated by 1 wt% SoluSeal. Gel strength profile comparison of 1 and 8wt% SoluSeal was done to select the best candidate for this Mud/LCM system. Figure 79 shows that for all the tested temperature ranges 1wt% SoluSeal gave the better results and thus it was selected.

The PV profile comparison of Stoploss showed close match between 1 and 3 wt%, Figure 80. The YP comparison was the deciding factor in the case of Stoploss as the 1wt% curve was an average of 1.4 times higher than the 3wt% curve, as evident from Figure 81. So from the Mud/Stoploss system 1wt% composition was selected.

8.6 ppg Na-bentonite water based mud (WBM), 3wt% DrilEzy, 1wt% SoluSeal and 1wt% Stoploss were flown in the see through setup. For the k1 core all four systems flushed through the core in less than 20 seconds at the ΔP of 3.7 psi as can be seen from the depth of penetration vs ΔP in Figure 82.

The permeability tested was very high and such Mud/LCM compositions failed to act as a bridging material. Information regarding the field formulation used by the product owner is necessary to design a lab scale test in order to set a performance benchmark. Another limitation in this experiment was with the testing of Stoploss. Stoploss is a mixture of various sized components. The large particles had to be removed through a sieve after the Mud/Stoploss system had been blended. It is because they would have plugged the tubings of the current system. Thus Stoploss was not tested in its entirety.

Figure 74 DrilEzy (left), SoluSeal (middle) and Stoploss (right)

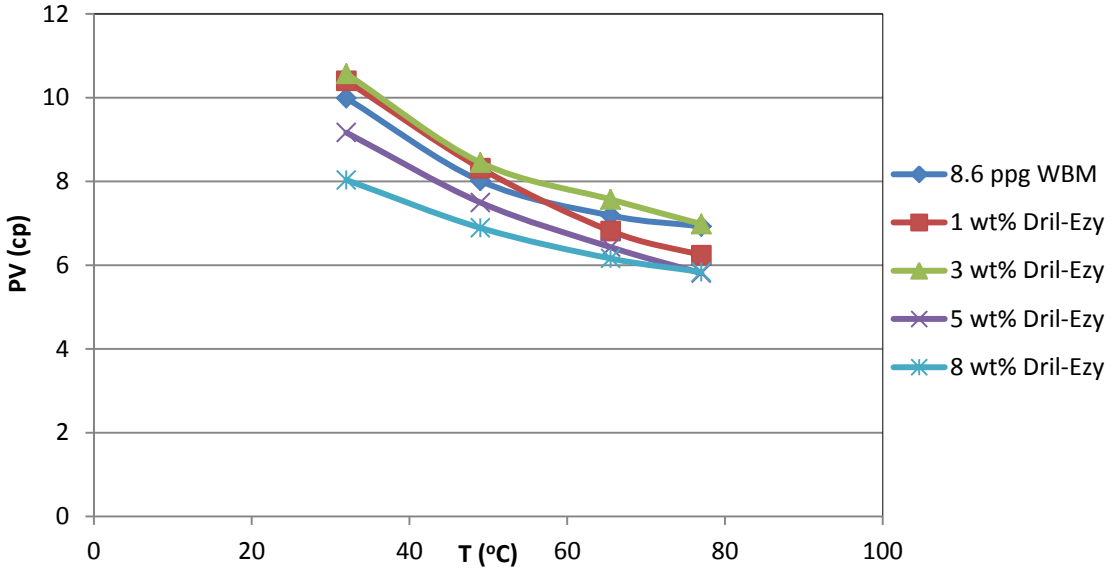

Figure 75 PV profile of DrilEzy

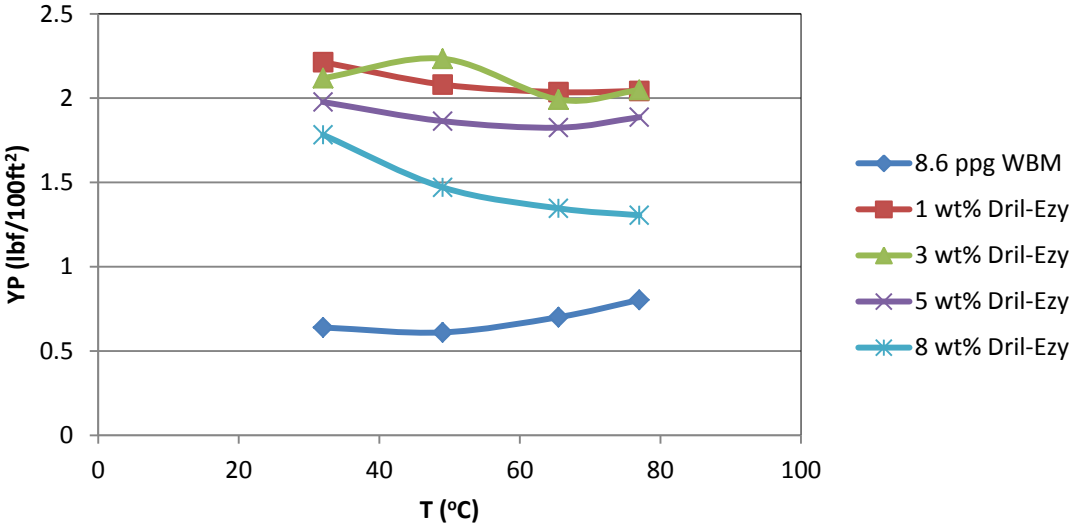

Figure 76 YP profile of DrilEzy

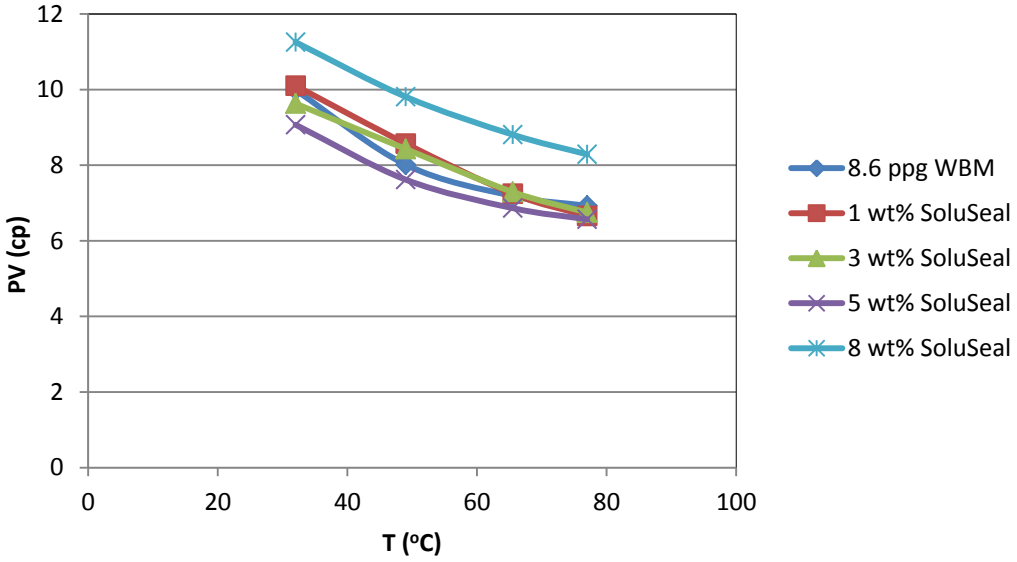

Figure 77 PV profile of SoluSeal

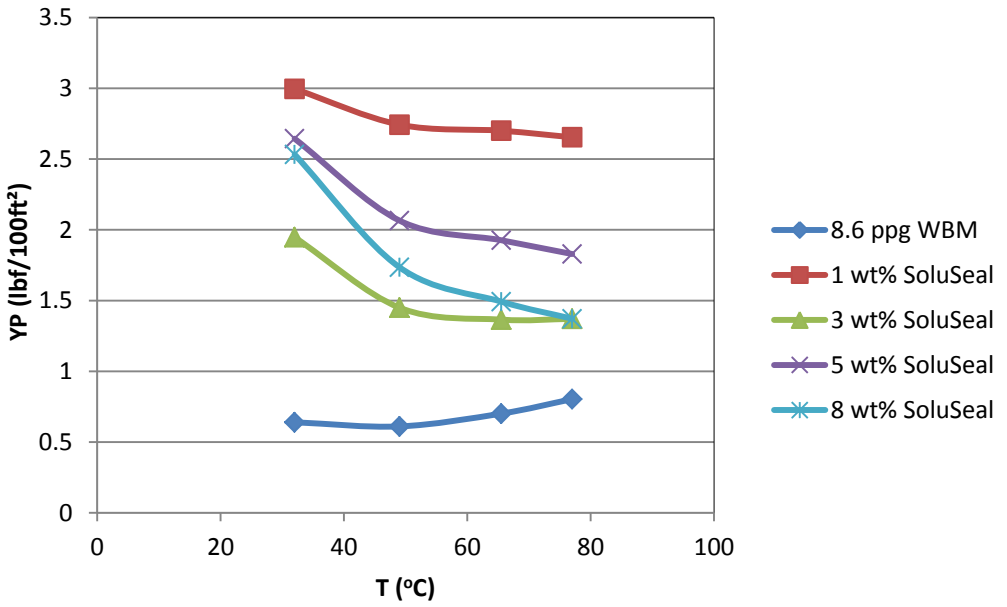

Figure 78 YP profile of SoluSeal

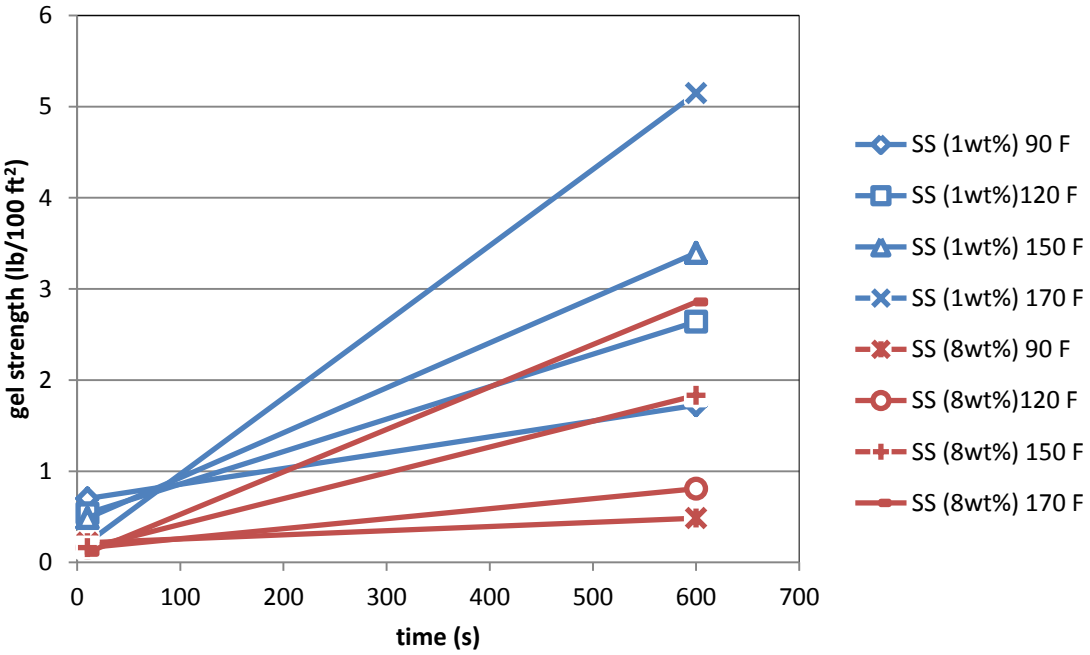

Figure 79 Gel strength profile comparison of SoluSeal 1wt% and 8wt% Mud/LCM system

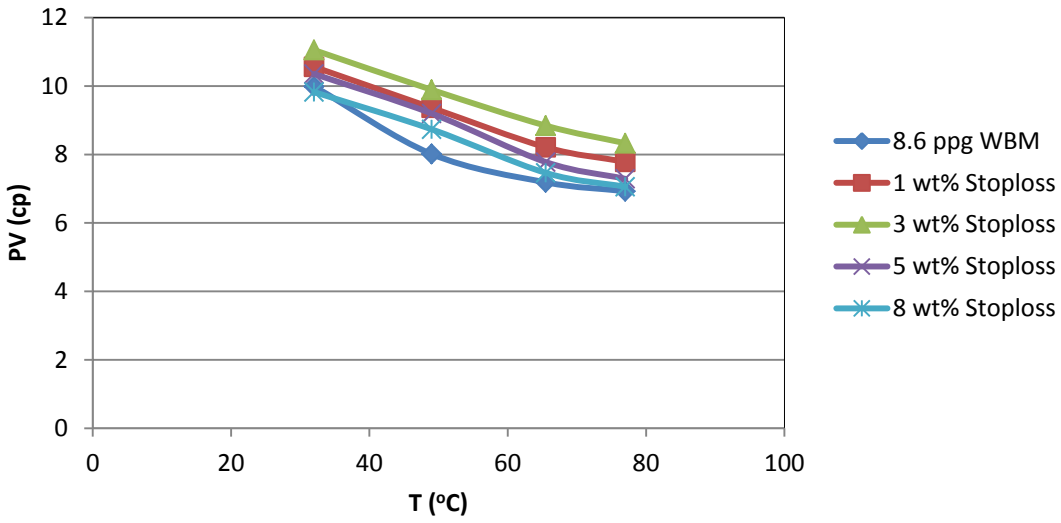

Figure 80 PV profile of Stoploss

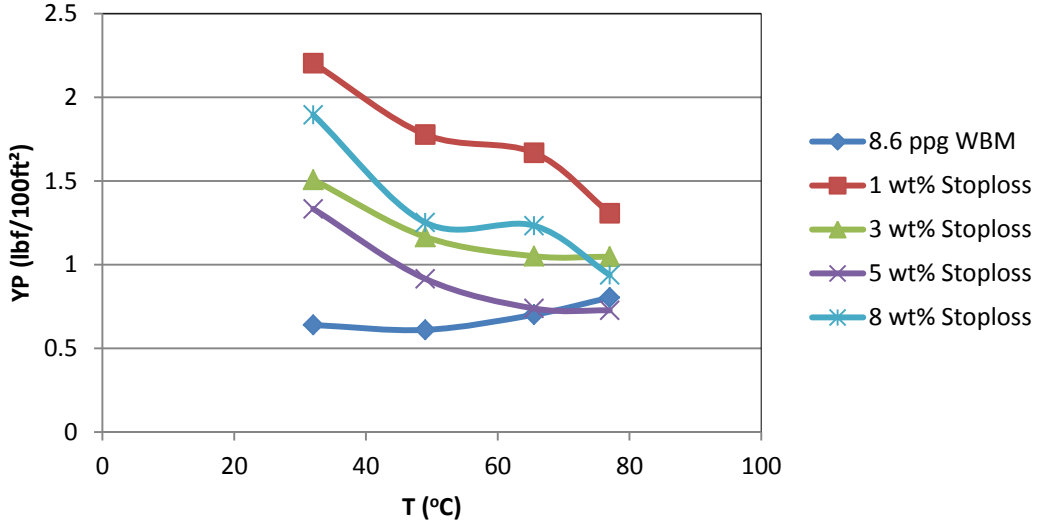

Figure 81 YP profile of Stoploss

Table 8 Rheological properties of the Mud/LCM systems at r.t.p

Mud/LCM Systems	YP (lbf/100ft²)	PV (cP)
Na-bentonite based WBM	0.995024	10.2773
3wt% DRIL-EZY/Mud system	2.659053803	11.8783445
1wt% STOPLOSS/Mud system	1.69692564	10.6587925
1wt% SOLU-SEAL/Mud system	1.766811729	10.7042542

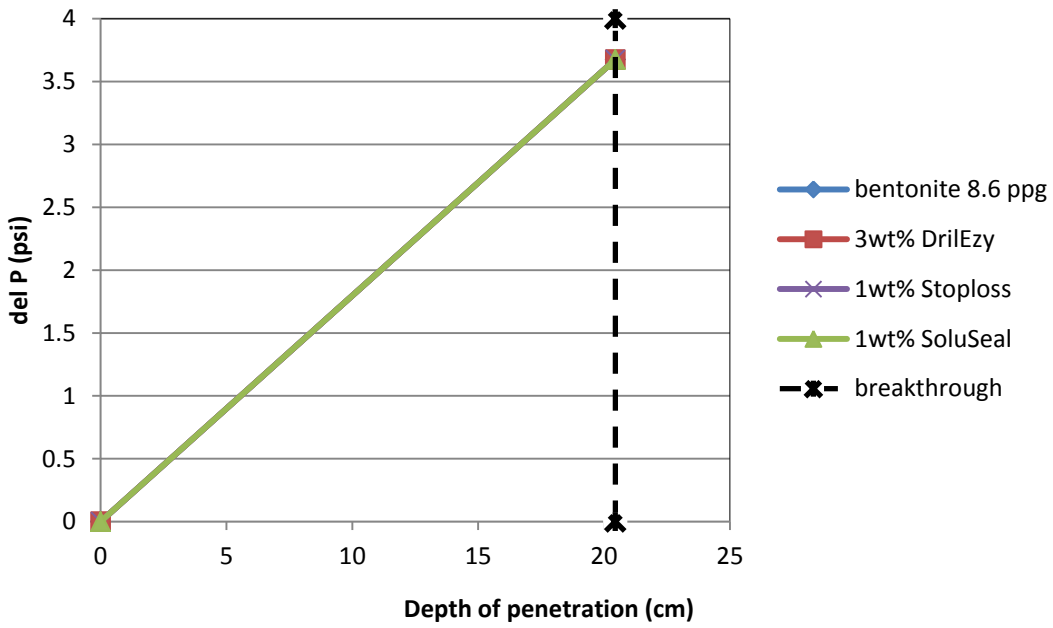

Figure 82 Flow performance of the LCMs

6.5 Polyacrylamide/Phenol Formaldehyde (PAM/PF)

A polyacrylamide and phenol-formaldehyde gel (PAM/PF) was prepared and tested on the see through setup. Following the patented procedure (David, 1984); solid phenol (0.4 g) and resorcinol (0.1 g) were dissolved in 50 ml of 0.5% polyacrylamide using a magnetic stirring bar. Paraformaldehyde (0.37 g) was added to the system followed by 0.35 ml of a 10% NaOH solution. The solution thus contained approximate concentrations of 0.8% phenol, 0.2% resorcinol, 0.75% formaldehyde, 0.5% polyacrylamide. The stirring solution was maintained at 75°C for 3 days and a gel was obtained. Figure 83 shows the bulk sample of the gel.

The PAM/PF gel obtained was a stable flowing gel that underwent some shrinkage with time. When this gel was injected in the k1 core, signs of penetration appeared when the water associated with the gel started to migrate inside the core at 100 psi pump pressure. Till the maximum pump pressure it had migrated to 5.1 cm inside the core. After mud was injected this distance kept on increasing. At the ΔP of 96 psi this became 5.6 cm, which went to 9.9 cm at the ΔP of 150 psi. This migration of water was because the injected mud was not able to displace or break through the gel in the zone and the exerted pressure on the gel pushed the water associated with it further inside the core. No mud loss happened in this experiment as the gel had successfully restricted mud movement. Figure 84 shows the condition of the core before and after mud injection, the front movement is dominant towards the base of the core. Figure 85 shows how the upstream end of the core looked after the experiment was finished. The gel had migrated 1.6 cm inside the core and held its ground against the mud.

When injected in the k2 core the gel migration was uneven. About 3.8 cm of the core was completely saturated with the gel, the top part of the core had a further 1.9 cm gel penetration and the bottom had the associated water presence till an additional distance of 4 cm, as can be seen in Figure 86. This saturation level remained unchanged for the entire experiment as the gel was able to completely ward off the mud advancement.

In the case of the k3 core the gel began to flow at the pump pressure of 50 psi and broke through the core at 80 psi pump pressure. At the ΔP of 33 psi, mud was able to make a channel through the gel in turn resulting in a total fluid loss. Figure 87 shows the picture of the core after the breakthrough.

Figure 88 shows the comparison of the PAM/PF gel performance with respect to different permeabilities. The dotted line in the k1 curve represents the presence of fluid within the core before mud injection. That part had to be included in order to present the complete picture because mud injection had resulted in the increase in the depth of penetration. The curve did not touch the breakthrough because the gel had prevented the fluid loss. For the case of k2 mud was not allowed to enter the zone by the gel and there was no increase in the depth of penetration inside the core, the k2 line falls exactly on the y-axis. This performance is different from k1 because here the depth of penetration of the gel is greater than that in k1. The k3 curve shows that till 27 psi ΔP the gel was able to hold back the mud. At the ΔP of 33 psi it gave way and allowed the mud to flow.

Because the gel showed signs of shrinkage with time the gel performance was tested at different time periods to study its effect on its performance. Figure 89 shows the comparison of the tests performed at different time periods on the k1 core type. It

includes the first test conducted on this core type, followed by a test after about 1 month and then one done after 3 months from the previous test. The dotted lines denote the maximum penetration of the gel system which includes the water associated with the gel. The legend on the curves shows the depth of the core that was completely and uniformly saturated by the gel. For the first test it was 1.6 cm and no mud breakthrough happened. For the 1 month test case it was 1.2 cm and the mud broke through at the ΔP of 132 psi. Depth of effective gel penetration was 0.7 cm for the test conducted after 4 months and the gel gave way to the mud at ΔP of 125 psi. Thus with time the performance of the gel decreased. This happened because with time the gel got denatured and it shrank giving off water. That was why the effective penetration of gel decreased. This allowed the mud to exploit the weak region in the gel barrier and broke through it at the pressure above its bearing capacity.

For practical purposes a gel cannot be pumped via the drill string to seal the loss zone. To use a mature gel for this application would require a separate pumping pathway. That would be possible if the drilling site is being operated by a hybrid rig where the drill string and coil tubing can be operated from the same unit. This option would be very expensive and not economically viable specifically for this purpose alone. If on a drilling site a hybrid rig is used and there a loss circulation problem is encountered then this option could be considered only if it is feasible to do so.

Figure 83 PAM/PF gel

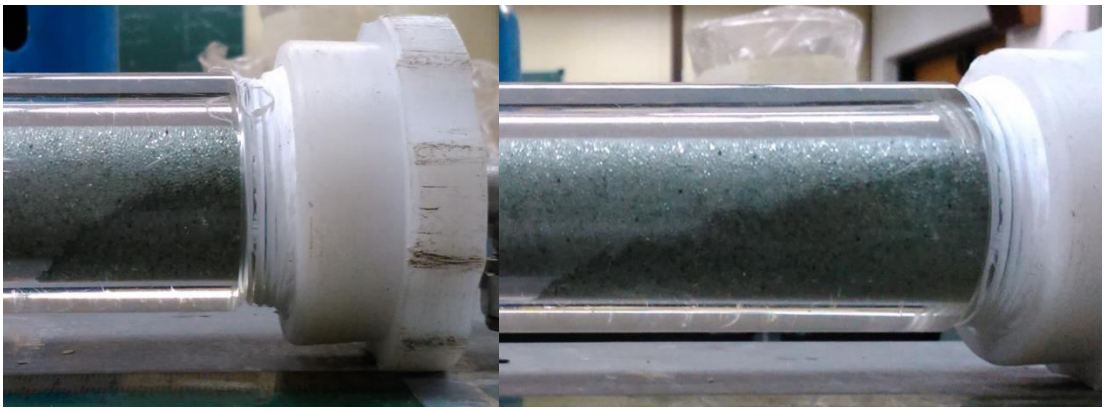

Figure 84 k1 after PAM/PF gel injection (left) and after mud injection (right)

Figure 85 Upstream end of the core after unpacking (left), depth of penetration of the gel [1.6 cm] (right)

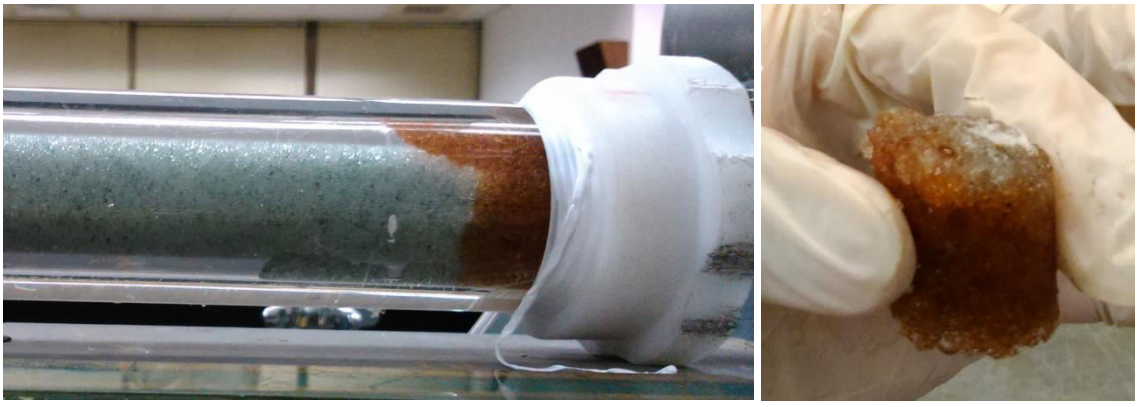

Figure 86 PAM/PF migration in k2 (left) PAM/PF gel encased in glass beads after unpacking (right)

Figure 87 PAM/PF saturated k3 core compromised by mud flow at 33psi ΔP

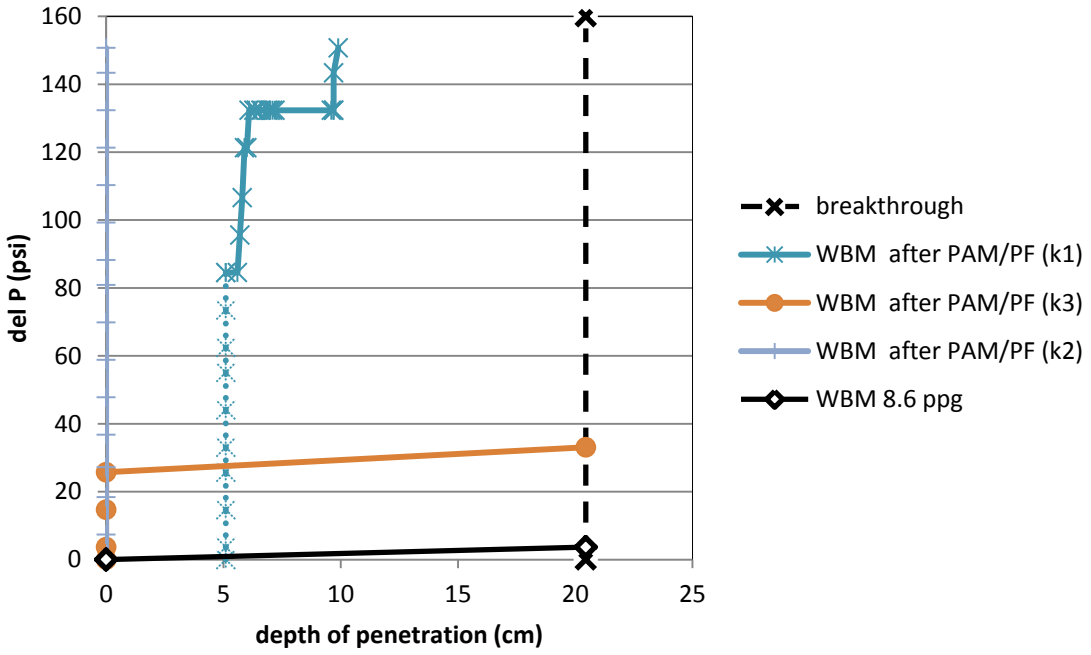

Figure 88 PAM/PF performance w.r.t to core type

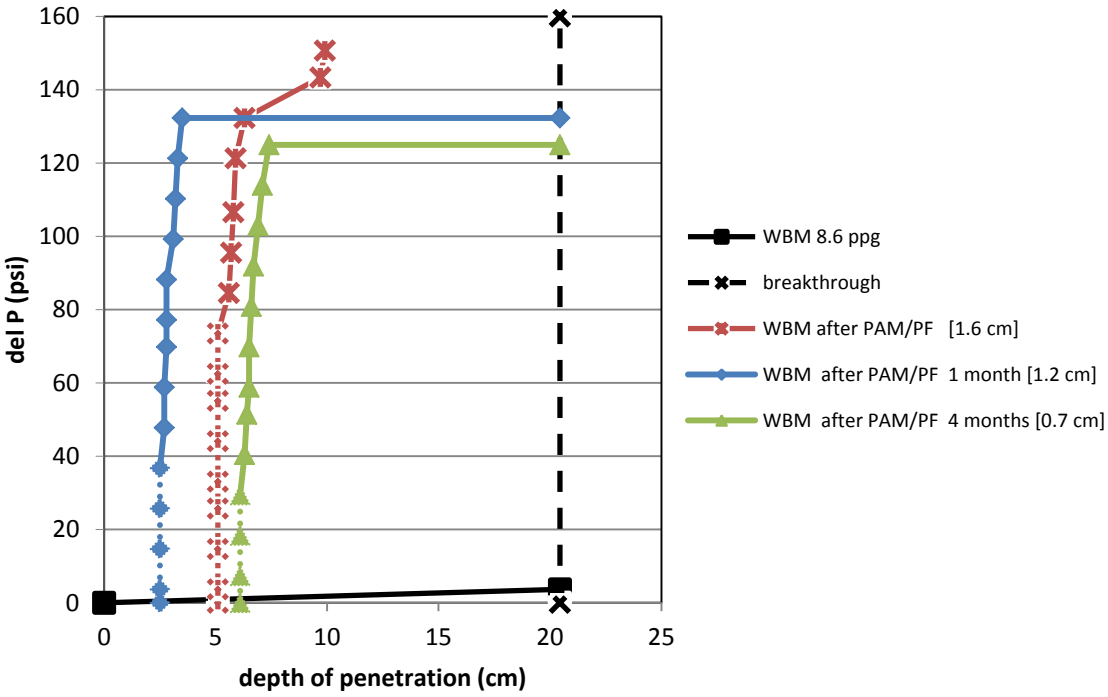

Figure 89 PAM/PF performance in relation to time and effective penetration in k1

6.6 HPAM/PEI (3/1.2) and A130/PEI (2/1.2) see through results

Bulk volumes of HPAM/PEI (3/1.2) and A130/PEI (2/1.2) were prepared at room temperature and tested on the see through setup to study the effectiveness of the system. Though gelation is a strong function of time and temperature, the gelation process starts immediately after the reactants are mixed. At room temperature condition the rate of reaction is very slow and not much property enhancement is obtained.

The limitations of the current system is that that it cannot be used for high temperature testing i.e. injection of the flowing gelant at room temperature and then heating up of the synthetic core to encourage in-situ gelation. Since the synthetic core is not a single piece component nor a metallic pressure cell this is not possible. The synthetic core is composed of separate glass, plastic and metallic parts each having a different coefficient of volumetric expansion. Heating the gelant saturated core in an oven will cause it to crack and create leaks. Injection of rigid gels on the other hand is a pumping issue. The setup however can be used to study the performance of a partially gelled flowing gelant.

Following the procedure described before, HPAM/PEI (3/1.2) and A130/PEI (2/1.2) were mixed at room temperature for 1.5 hours to ensure proper mixing of the bulk sample. HPAM/PEI (3/1.2) was injected in the k1 core. At 40 psi pump pressure did the gelant start to move inside the core. The penetration of the gelant was very minimal with respect to time. At 60 psi pump pressure the gelant had penetrated a distance of 3.5 cm inside the core and by this time the movement was almost piston like. At 130 psi pump pressure the gelant took 5 hours to reach the end of the core and till the maximum pressure did not broke through the core. The whole experiment took about 12.5 hours.

Mud was injected after the potential LCM and the same procedure was followed. Till the maximum pump pressure and a pressure difference of 150 psi across the core, the mud was not able to break through the core. HPAM/PEI (3/1.2) though still not a rigid gel had successfully blocked the zone under the tested conditions.

HPAM/PEI (3/1.2) was then flowed in the k3 core; the gelant completely saturated the core at 50 psi pump pressure. Figure 90 shows the k3 core saturated with HPAM/PEI (3/1.2). Thereafter, mud was injected in the core and at the pressure difference of 26 psi it started displacing the gel. After 11 minutes the mud broke through the gel and partial losses began to occur. This mud and gel flow continued for about 50 minutes after which enough gel had been displaced that the mud faced no resistance in flow and total fluid loss occurred. Figure 91 shows the k3 core condition after incurring complete fluid loss.

When A130/PEI (2/1.2) gelant was injected in the k1 core its migration, just like HPAM/PEI (3/1.2), was very slow. The A130/PEI (2/1.2) gelant was able to penetrate a distance of 7.1 cm inside the core till the maximum pump pressure was reached. This phase of the experiment took 12 hours to complete. A130/PEI (2/1.2) also proved successful in preventing losses when mud was injected into the core saturated by it. Mud was not able to break through the core till the maximum pump pressure. Figure 92 shows the A130/PEI (2/1.2) saturated k1 core.

For the k3 core, A130/PEI (2/1.2) fully saturated it in a few hours at 40 psi pumping pressure. Mud was then injected after it and at a pressure difference of 26 psi it began to displace the gel. This was then followed by partial losses and then a complete loss after 18 minutes from breakthrough.

Figure 93 summarizes the HPAM/PEI and A130/PEI see through results. The comparison shows that in both the core conditions they behave in a similar manner, preventing losses in k1till the del. P of 150 psi and experiencing losses at 26 psi del. P in k3.

Figure 90 k3 core saturated with HPAM/PEI (3/1.2)

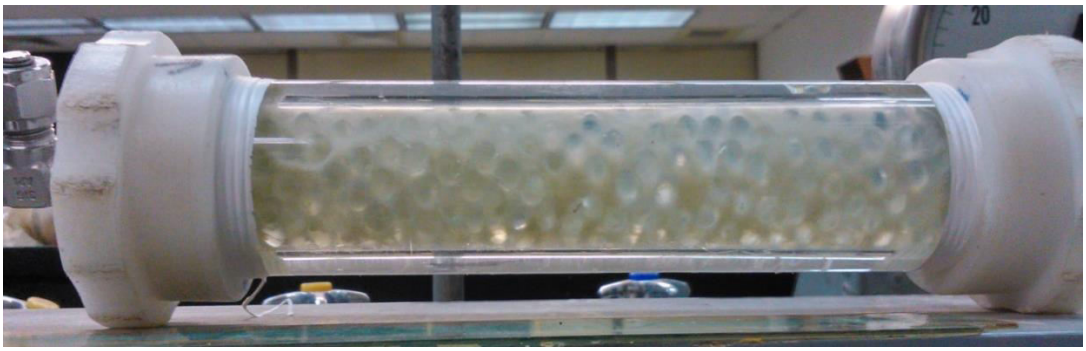

Figure 91 Mud breakthrough in the HPAM/PEI (3/1.2) saturated k3 core

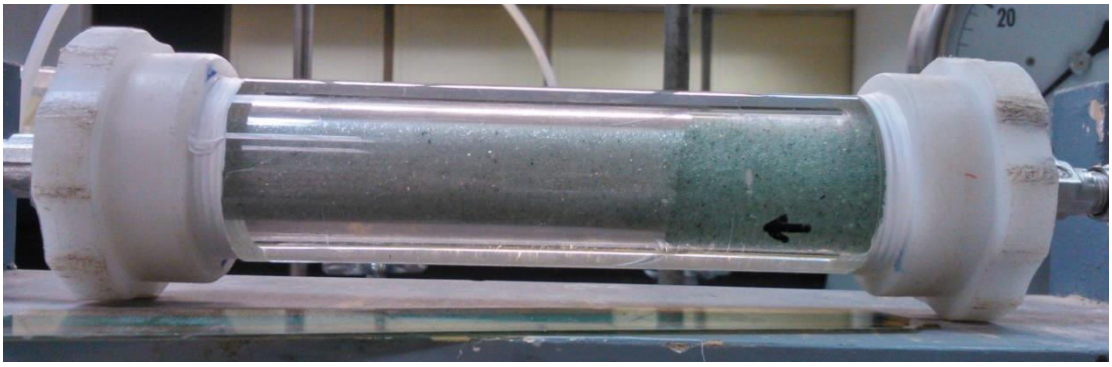

Figure 92 A130/PEI (2/1.2) saturated k1 core, maximum penetration of 7.1 cm

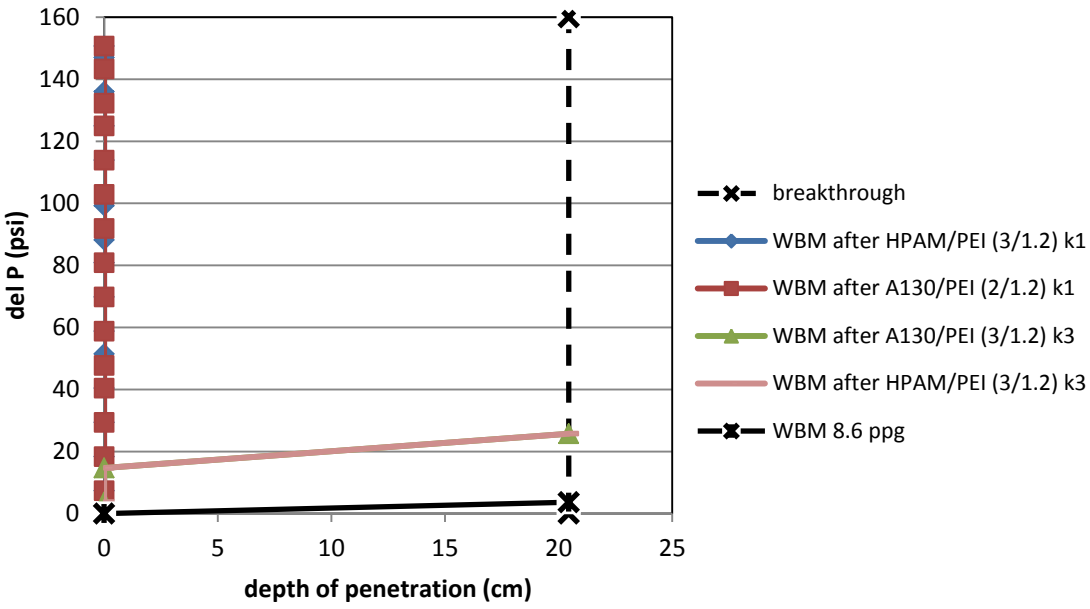

Figure 93 HPAM/PEI (3/1.2) and A130/PEI (2/1.2) performance w.r.t permeability

CHAPTER 7

CONCLUSION and RECOMMENDATION

Findings from this study include:

1. Optimum polymer/crosslinker identification is an essential first step towards attaining a rigid and stable gel. Strong gels were obtained by using the maximum polymer concentration and this was reflected in the rheology results.
2. Gel strengths were greatly enhanced by temperature and aging time. For the HPAM/PEI gels the degree of property enhancement increased with increasing temperature and ageing time.
3. The thermo-associative temperature for the TVP is a function of its concentration and solvent salinity.
4. Clays do not interact with HPAM, their interaction with PAM based polymers do not cause an improvement in property. Mixing sequence plays an important role in this interaction but that window of interaction is very minimal.
5. The DSC experiments can be used to simulate the heat profile of the injection depth. Moreover the fractional gelation trend can be used to design/modify the placement process.
6. Flowing gels can be injected directly in the affected zone if economics allow but for a rigid gel like HPAM/PEI and A130/PEI the placement method involving in-situ gelation is the only option.

7. Both HPAM/PEI (3/1.2) and A130/PEI (2/1.2) gelants had successfully prevented mud loss in a zone having 36% porosity and 300 D permeability at room temperature and pressure conditions.

The next phase now would be to acquire field formulation of the commercial LCMs and testing them in the lab to establish a benchmark for comparison with non-conventional LCMs. Also acquisition and study of polymers and crosslinkers with known structures for possible usage as LCM should be carried out e.g. naturally occurring and environmental friendly polymers like chitosan and cellulose. Acquisition and further study of TVPs at higher concentrations is also needed.

There are some limitations with the current see through system. It cannot be used for high temperature applications and conventional LCMs with large sized components cannot be tested in it. Therefore, there is a need for an HPHT flow loop. The see through setup could serve the material screening purpose while the HPHT flow loop could be used to simulate the actual field problem and study the means to mitigate them.

Figure 94 shows the schematic diagram of the proposed HPHT flow loop. This flow loop would be equipped with a gear pump so that high pressure conditions could be created. The design is made to simulate the subsurface annulus conditions. The mud or the LCM would be pumped into the annulus via the drill string and could be flowed back or passed through the loss circulation zones connected to the vessel. These zones will be metallic components that could be opened or isolated via valves. The annulus and the zones would have heating elements and thermal jackets so that high temperature conditions could be achieved. In this way in-situ gelation of an LCM system could be tested. The zones

would be gravel filled and varying the gravel size and packing arrangement would result in different permeability and porosity conditions. This setup could also serve as a transition between lab and field application. Once a good LCM system has been developed to tackle a field condition then it could be tested on the HPHT flow loop first before finding its application in the field.

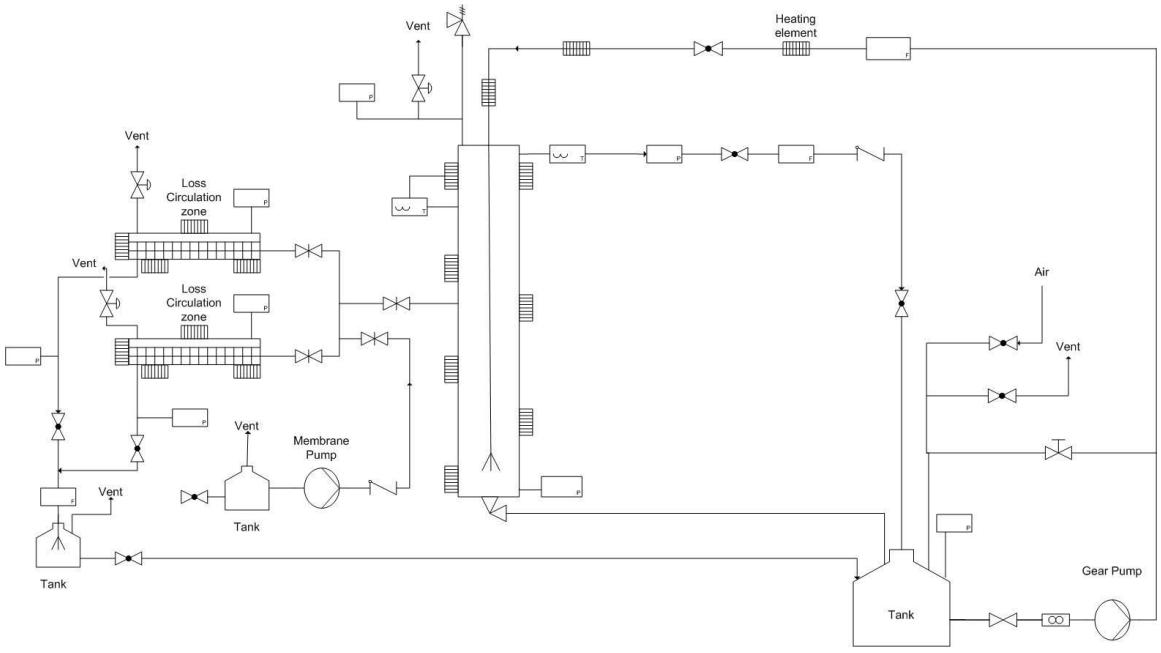

Figure 94 Schematic diagram of the proposed HPHT flow loop

References

1. J. M. Bugbee. 1953. Lost Circulation-A Major Problem in Exploration and Development. Paper API 53014 presented at Drilling and Production Practice.

2. Md. Amanullah and Richard Boyle. 2006. A Multifunctional Gel System To Mitigate Deepwater Drilling Challenges. Paper SPE 104080-MS presented at International Oil & Gas Conference and Exhibition, Beijing, China, 5-7 December. DOI: 10.2118/104080-MS

3. Pavel Marinescu, Reinhard Josef Oswald and Paulin Vlasceanu. 2007. Uniquely Characteristics Mixed-Metal Oxide (MMO) Fluid Cure Lost Circulation While Meeting European Environmental Regulations. Paper SPE 110341-MS presented at Asia Pacific Oil and Gas Conference and Exhibition, Jakarta, Indonesia, 30 October-1 November. DOI: 10.2118/110341-MS.

4. J. Ghassemzadeh. 2009. US Patent 7923413, Lost Circulation Material for Oil Field Use.

5. B. Zusatz. 2004. US Patent 7726400, Compositions and Methods for Treating Lost Circulation.

6. M.H. Alqam, H.A. Nasr-El-Din and J.D. Lynn. 2001. Treatment of Super K-Zones Using Gelling Polymers. Paper SPE 64989 presented at the International Symposium on Oilfield Chemistry, Houston, 13–16 February. DOI: 10.2118/64989-MS.

7. Julio Vasquez, Faruk Civan, Thomas M. Shaw, E. Dwyann Dalrymple, Larry Eoff, B.R. Reddy and David Brown. 2003. Laboratory Evaluation of High-Temperature Conformance Polymer Systems. Paper SPE 80904 presented at the Production and Operations Symposium, Oklahoma City, Oklahoma, USA, 22–25 March. DOI: 10.2118/80904-MS.

8. C. O. Ukachukwua, O. Ogbobea and S.A. Umorenb. 2010. Preparation and characterization of biodegradable polymer mud based on millet starch. London, England: Taylor and Francis Group, LLC. DOI: 10.1080/00986440903412902

9. Robert K. Prud'homme, Jonathan T. Uhl, John P. Poinsatte, and Frederick Halverson. 1983. Rheological Monitoring of the Formation of Polyacrylamide/Cr^{+3} Gels. SPE J. 23 (5): 804–808. SPE-10948-PA. DOI: 10.2118/10948-PA.

10. Thomas P. Lockhart. 1994. Chemical Properties of Chromium/Polyacrylamide Gels. SPE Advanced Technology Series 2 (2): 199–205. SPE-20998- PA. DOI: 10.2118/20998-PA.

11. Klaas te Nijenhuis, Annemiek Mensert and Pacelli L. J. Zitha. 2003. Viscoelastic behaviour of partly hydrolyzed polyacrylamide/chromium(III) gels. Rheologica Acta 42 (1–2): 132–141. DOI: 10.1007/s00397-002-0264-9

12. Robert D. Sydansk. 1990. A Newly Developed Chromium (III) Gel Technology. SPE Reservoir Engineering 5(3): 346–352. SPE-19308-PA. DOI: 10.2118/19308-PA

13. Carol L. Dona, Don W. Green and G. Paul Willhite. 1997. A Study of the Uptake and Gelation Reactions of Cr(III) Oligomers with Polyacrylamide. Journal of Applied Polymer Science (1997) 64, 1381. DOI: 10.1002/(SICI)1097-4628(19970516)64:7<1381::AID-APP18>3.0.CO;2-#

14. Ghaithan A. Al-Muntasheri, Hisham A. Nasr-El-Din and Ibnelwaleed A. Hussein. 2007. A rheological investigation of a high temperature organic gel used for water shut-off treatments. J. Pet. Sci. Eng. 59 (1–2): 73–83. DOI: 10.1016/ j.petrol.2007.02.010.

15. Robert D. Sydansk and Southwell G.P. 2000. More than 12 Years' Experience With a Successful Conformance-Control Polymer-Gel Technology. SPE Prod & Fac 15 (4): 270–278. SPE-66558-PA. DOI: 10.2118/66558-PA.

16. Robert D. Sydansk and Marathon Oil Company. 2003. Acrylamide-Polymer/ Chromium(III)-Carboxylate Gels for Near Wellbore Matrix Treatments. SPE Advanced Technology Series, Vol. 1, No.1, April 2003.

17. Ahmad Moradi-Araghi. 1991. U.S patent 4994194, Altering High Temperature Subterranean Formation Permeability.

18. Paola Albonico, Martin Bartosek, T.P. Lockhart and Emilio Causin. 1994. New Polymer Gels for Reducing Water Production in High-Temperature Reservoirs. Paper SPE 27609 presented at the 1994 European Production Operations Conference and Exhibition. DOI: 10.2118/27609-MS

19. Mary Hardy, Wouter Botermans, Aly Hamouda, Jarl and John Warren. 1999. The First Carbonate Field Application of a New Organically Cross-Linked Water Shutoff Polymer System. Paper SPE 50738 presented at the 1999 SPE International Symposium on Oilfield Chemistry held in Houston, TX, February 16-19. DOI: 10.2118/50738-MS

20. Ahmad Moradi-Araghi. 1993. US Patent 5179136, Gelation of acrylamide-containing polymers with aminobenzoic acid compounds and water dispersible aldehydes.

21. Ahmad Moradi-Araghi, G. Bjornson and P.H. 1993. Thermally Stable Gels for Near-Wellbore Permeability Contrast Modifications. Paper SPE 18500, Advanced Technical Series, Vol. 1, No. 1, p. 140-145, 1993. DOI: 10.2118/18500-PA

22. Ahmad Moradi-Araghi. 1994. Application of Low-Toxicity Cross-Linking Systems in Production of Thermally Stable Gels. Paper SPE 27826 presented at the 1994 SPE/DOE Symposium on Improved Oil Recovery held in Tulsa, OK, April 17-20. DOI: 10.2118/27826-MS

23. H.T. Dovan, R.D Hutchins and B.B. Sandiford. 1997. Delaying Gelation of Aqueous Polymers at Elevated Temperatures Using Novel Organic Cross-Linkers. Paper SPE 37246 presented at the 1997 SPE International Symposium on Oilfield Chemistry, Houston, TX, February 18-21. DOI: 10.2118/37246-MS

24. Ahmad Moradi-Araghi. 2000. A review of thermally stable gels for fluid diversion in petroleum production. J. Pet. Sci. Eng. 26 (1–4): 1–10. DOI: 10.1016/S0920-4105(00)00015-2

25. Ahmad Moradi Araghi, and Peter H Doe. 1987. Hydrolysis and Precipitation of Polyacrylamides in Hard Brines at Elevated Temperatures. SPE Reservoir Engineering Journal 2 (02) May 1987. DOI: 10.2118/13033-PA

26. Mohammed Omer and Abdullah Sultan. 2013. Effect of Metal Ions on the Rheology and Thermal Properties of Polymeric Lost Circulation Material. Paper SPE 164433 presented at Middle East Oil and Gas Show and Conference, 10-13 March, Manama, Bahrain. DOI: 10.2118/164433-MS

27. B.R. Reddy, Larry Eoff, E. Dwyann Dalrymple, Kathy Black, David Brown and Marcel Rietjens. 2003. A Natural Polymer-Based Cross-Linker System for Conformance Gel Systems. SPE Journal Volume 8 Issue 02 2003, 13–17. DOI: 10.2118/84937-PA

28. J.C. Morgan, P.L. Smith and D.G Stevens. Chemical Adaptation and Deployment Strategies for Water and Gas Shut-off Gel Systems. Paper presented at the 1997 Royal Chemistry Society's Chemistry in the Oil Industry International Symposium, Ambleside, UK, April 14-17

29. J. Vasquez, E.D. Dalrymple, Larry Eoff, B.R. Reddy and F. Civan. 2005. Development and Evaluation of High-Temperature Conformance Polymer Systems. Paper SPE 93156 presented at the International Symposium on Oilfield

Chemistry, The Woodlands, Texas, USA, 2–4 February. DOI: 10.2118/93156-MS.

30. M.B. Hardy, C.W. Botermans and P. Smith. 1998. New Organically Cross-Linked Polymer System Provides Competent Propagation at High Temperatures in Conformance Treatments. Paper SPE 39690 presented at the SPE/DOE Symposium on Improved Oil Recovery, Tulsa, 19–22 April.

31. Pacelli L. J. Zitha, C. Wouter Botermans, Jeroen v. d. Hoek and Fred J. Vermolen. 2002. Control of flow through porous media using polymer gels. Journal of Applied Physics 92 (2): 1143–1153. DOI:10.1063/1.1487454.

33. J.D. Allison and J.D. Purkaple. 1988. Reducing permeability of highly permeable zones in underground formations. US Patent No. 4,773,481.

34. G.A. Al-Muntasheri, H.A. Nasr-El-Din and P.L.J. Zitha. 2008. Gelation Kinetics and Performance Evaluation of an Organically Crosslinked Gel at High Temperature and Pressure. SPE J. 13 (3): 337–345. SPE- 104071-PA. DOI: 10.2118/104071-PA

35. G.A Al-Muntasheri, H.A. Nasr-El-Din, J.A. Peters and P.L.J. Zitha. 2006. Investigation of a High-Temperature Organic Water-Shutoff Gel: Reaction Mechanisms. SPEJ 11 (4): 497–504. SPE-97530-PA. DOI: 10.2118/97530-PA.

36. Roger P. Ortiz Polo, Rafael Rodriguez Monroy, Nelson Toledo, E. Dwyann, Larry Eoff and Don Everett. 2004. Field Applications of Low Molecular-Weight Polymer Activated with an Organic Cross- Linker for Water Conformance in South Mexico. Paper SPE 90449 presented at the 2004 SPE Annual Technical Conference and Exhibition held in Houston, TX, September 26-29. DOI: 10.2118/90449-MS

37. K Gakhar, R H Lane and A. Texas. 2012. Low Extrusion Pressure Polymer Gel for Water Shutoff in Narrow Aperture Fractures in Tight and Shale Gas and Oil Reservoirs. Paper SPE 151645 presented at the International Symposium and Exhibition on Formation Damage Control, 15-17 February, Lafayette, Louisiana, USA, 2012. DOI: 10.2118/151645-MS

38. Ghaithan A. Al-Muntasheri , Hisham A. Nasr-El-Din and Pacelli Lidio Jose Zitha. 2009. A Study of Polyacrylamide-Based Gels Crosslinked with Polyethyleneimine. SPE Journal 14 (02), 2009, 245–251. DOI: 10.2118/105925-MS

39. Carmen Chelaru, I. Diaconu and C. I. Simionescu. 1998. Polyacrylamide obtained by plasma-induced polymerization for a possible application in enhanced oil recovery. Polymer Bulletin 40 (6):757–764. DOI: 10.1007/s002890050319

40. Chuanrong Zhong, Pingya Luo, Zhongbin Ye and Hong Chen. 2009. Characterization and solution properties of a novel water-soluble terpolymer for enhanced oil recovery. Polymer Bulletin 62(1):79–89. DOI: 10.1007/s00289-008-1007-6

41. J. Hou. 2007. Network modeling of residual oil displacement after polymer flooding. Journal of Petroleum Science and Engineering 59(4):321–332. DOI: 10.1016/j.petrol.2007.04.012

42. W.M. Kulicke, R. Kninewske and J. Klein. 1982. Preparation, characterization, solution properties and rheological behaviour of polyacrylamide. Progress in Polymer Sciences 8(4):373–468. DOI:10.1016/0079-6700(82)90004-1

43. Leung WM and Axelson DE. 1987. Thermal degradation of polyacrylamide and poly(acrylamide-co- acrylate). Journal of Polymer Science A 25(7):1852–1864. DOI: 10.1002/pola.1987.080250711

44. Yang MH. 1999. The rheological behavior of polyacrylamide solution. Journal of Polymer Engineering 19(5):371–381. DOI: 10.1515/POLYENG.1999.19.5.371

45. Sabhapondit A, Borthakur A and Haque I. 2003. Characterization of acrylamide polymers for enhanced oil recovery. Journal of Applied Polymer Science 87(12):1869–1878. DOI: 10.1002/app.11491

46. Kheradmand H, Francois J and Plazanet V. 1988. Hydrolysis of polyacrylamide and acrylic acid– acrylamide copolymers at neutral pH and high temperature. Polymer 29(5):860–870. DOI: 10.1016/0032-3861(88)90145-0

47. J. François, N.D. Truong, G. Medjahdi and M.M. Mestdagh. 1997. Aqueous Solutions of Acrylamide-Acrylic Acid Copolymers : Stability in the Presence Alkalinoearth Cations. Polymer 38 (1997), 6115–27. DOI:10.1016/S0032-3861(97)00165-1

48. Hourdet D, L'Alloret F and Audebert R. 1994. Reversible thermothickening of aqueous polymer solutions. Polymer 35(12):2624–2630. DOI: 10.1016/0032-3861(94)90390-5

49. Quansheng Chen, Yu Wang, Zhiyong Lu and Yujun Feng. 2012. Thermoviscosifying Polymer Used for Enhanced Oil Recovery: Rheological

Behaviors and Core Flooding Test. Polymer Bulletin, 70 (2012), 391–401 DOI: 10.1007/s00289-012-0798-7

50. Wang Y, Feng YJ, Wang BQ and Lu ZY. 2010. A novel thermoviscosifying water-soluble polymer: synthesis and aqueous solution properties. Journal of Applied Polymer Science 116(15):3516–3524. DOI: 10.1002/app.31884

51. Messersmith PB and Znidarsich F. 1997. Material Research Society Symposium Proceeding 1997; 457-507–12. DOI: 10.1557/PROC-457-507

52. Wu JH, Lin JM, Zhou M and Wei CR. 2000. Synthesis and properties of starch-graft polyacrylamide/clay superabsorbent composite. Macromolecular Rapid Communications 2000;21(15):1032–4.
DOI: 1022-1336/2000/1510-1032$17.50+.50/0

53. Lin, Jianming, Jihuai Wu, Zhengfang Yang, and Minli Pu. 2001. Synthesis and Properties of Poly(acrylic acid)/Mica Superabsorbent Nanocomposite. Macromolecular Rapid Communications, 22 (2001), 422–24 DOI: 10.1002/1521-3927(20010301)22:6<422::AID-MARC422>3.0.CO;2-R

54. Zhang Weian, Luo Wei and Fang Yue'e. 2005. Synthesis and Properties of a Novel Hydrogel Nanocomposites. Materials Letters, 59 (2005), 2876–80 DOI: 10.1016/j.matlet.2005.04.033

55. Baojun Bai, Liangxiong Li, Yuzhang Liu, He Liu, Zhongguo Wang and Chunmei You. 2007. Preformed Particle Gel for Conformance Control : Factors Affecting Its Properties and Applications, (April 2004), 17–21. DOI: 10.2118/89389-PA

56. Yuanqing Xiang, Zhiqin Peng and Dajun Chen. 2006. A New Polymer/clay Nano-Composite Hydrogel with Improved Response Rate and Tensile Mechanical Properties. European Polymer Journal, 42 (2006), 2125–32. DOI: 10.1016/j.eurpolymj.2006.04.003

57. Vincent A. Hackley and Chiara F. Ferraris. 2001. Guide to Rheological Nomenclature : Measurements in Ceramic Particulate Systems. NIST Special Publication 946.

58. Alain Zaitoun, Patrick Makakou, Nicolas Blin, Rashid S. Al-Maamari, Abdul-Aziz Rashid Al-Hashmi and Mahmoud Abdel-Goad. 2012. Shear Stability of EOR Polymers. SPE Journal 17 (02), June: 335–39. DOI: 10.2118/141113-PA

59. Khalid S. M. El-Karsani, Ghaithan A. Al-Muntasheri, Abdullah S. Sultan and Ibnelwaleed A. Hussein. 2014. Gelation kinetics of PAM/PEI system. Journal of

Thermal Analysis and Calorimetry, 116(3), 1409–1415. DOI:10.1007/s10973-014-3754-y

60. Hu Jia, Jin-Zhou Zhao, Fa-Yang Jin, Wan-Fen Pu, Yong-Ming Li, Ke-Xing Li, and Ji-Mao Li. 2012. New Insights into the Gelation Behavior of Polyethyleneimine Cross- Linking Partially Hydrolyzed Polyacrylamide Gels. Ind. Eng. Chem. Res., 2012, 51 (38), pp 12155–12166.DOI: 10.1021/ie301818f

61. David O. Falk 1984 US patent 4485875, Process for selectively plugging permeable zones in a subterranean formation.

Vitae

Name	:Mohammad Danish Hashmat
Nationality	:Pakistani
Date of Birth	:3/26/1987
Email	:the_01@msn.com
Address	:F.B.Area, Karachi, Pakistan
Academic Background	:MS PETE KFUPM and BE-Petroleum Engg., NEDUET